

Washington University in St. Louis

Washington University Open Scholarship

All Theses and Dissertations (ETDs)

Spring 4-17-2013

Intermediate Level Mechanisms Supporting Face Perception

Eric J. Feczko

Washington University in St. Louis

Follow this and additional works at: <https://openscholarship.wustl.edu/etd>



Part of the [Neuroscience and Neurobiology Commons](#)

Recommended Citation

Feczko, Eric J., "Intermediate Level Mechanisms Supporting Face Perception" (2013). *All Theses and Dissertations (ETDs)*. 1066.

<https://openscholarship.wustl.edu/etd/1066>

This Dissertation is brought to you for free and open access by Washington University Open Scholarship. It has been accepted for inclusion in All Theses and Dissertations (ETDs) by an authorized administrator of Washington University Open Scholarship. For more information, please contact digital@wumail.wustl.edu.

WASHINGTON UNIVERSITY IN ST. LOUIS

Division of Biology and Biomedical Sciences
Neurosciences

Dissertation Examination Committee:

John R. Pruett, Jr., Chair

Steven E. Petersen

Bradley L. Schlaggar

Larry Snyder

Gordon Shulman

David Van Essen

Intermediate Level Mechanisms Supporting Face Perception

by

Eric Feczko

A dissertation presented to the
Graduate School of Arts and Sciences
of Washington University in
partial fulfillment of the
requirements for the degree of
Doctor of Philosophy

May 2013

St. Louis, Missouri

Table of Contents

Acknowledgements	vii
ABSTRACT OF THE DISSERTATION	viii
Chapter 1: Background and Significance	1
Face processing	1
Introduction	1
Studying mechanisms involved in face processing may provide important insights into object recognition and relevant clinical disorders.....	2
Face perception involves processing the arrangements of face features.....	3
Form-from-structure perception	9
Concentric and radial form-from-structure perception may involve processing the arrangements of features	9
Face and concentric form-from-structure perception may share a common processing mechanism	13
Neurophysiological evidence.....	13
Visual adaptation can be used to test this hypothesis directly	15
Visual masking experiments may provide evidence for interaction between concentric Glass pattern and face perception.....	21
References	27
Chapter 2: Preliminary Studies	33
Experiment 1: Effects of Glass pattern adaptation on Glass pattern discrimination	33
Introduction	33
Methods	33
Results	35

Discussion.....	37
Experiment 2: Effects of face and Glass pattern adaptation on upright/inverted face discrimination: 8 subject pilot.....	38
Introduction	38
Methods	38
Results	40
Discussion.....	43
Experiment 3: Effects of upright and inverted face adaptation on upright/inverted face discrimination: 16 subject pilot.....	45
Introduction	45
Methods	45
Results	45
Discussion.....	51
Summary.....	52
References.....	53
Chapter 3: Concentric Glass pattern masking, but not adaptation, impairs upright/inverted face discrimination	55
Introduction.....	55
General Methods	56
Participants	56
Experimental procedures	56
Experimental setup.....	56
Stimulus design.....	57
Staircasing procedure	59
Analysis.....	60

Experiment 4: face adaptation	61
Methods	61
Results: Adaptation to faces does not impair concentric Glass pattern discrimination	62
Discussion.....	66
Experiment 5: Glass pattern adaptation.....	67
Introduction	67
Methods	68
Results: Concentric Glass pattern masking, but not adaptation, impairs	
upright/inverted face discrimination.....	71
Discussion.....	74
General Discussion.....	74
References.....	75
Chapter 4: Sandwich masking experiments reveal pattern-specific masking for	
upright/inverted and gender face discrimination	77
Introduction	77
General Methods.....	77
Experiment 6: upright inverted face discrimination	78
Methods	78
Results: Concentric Glass pattern sandwich masking impairs upright/inverted face	
discrimination	79
Discussion.....	82
Experiment 7: Gender Discrimination	84
Methods	84
Results: Concentric Glass pattern sandwich masking impairs gender discrimination .	84
Discussion.....	86

General Discussion.....	86
Differences between concentric, radial, and translational Glass pattern masking effects on face discrimination	87
References.....	88
Chapter 5: Conclusions and Future Directions	90
Conclusions	90
Effects of visual masking suggest that concentric Glass pattern, radial Glass pattern, and face perception share a common processing mechanism	90
Findings from the visual masking and adaptation experiments suggest that the shared mechanism may only be affected by a stimulus for a short period of time	92
Implications for clinical disorders, such as autism or prosopagnosia	93
Implications for object recognition	93
Summary.....	94
Future fMRI masking studies may help characterize the neural mechanism for these interactions.....	95
Introduction	95
Methods	96
Preliminary Results	106
Expected Results	108
Additional pilots	112
Discussion.....	114
Pitfalls	116
Conclusion	117
References.....	117
Appendix: The hemodynamic response in simplex autism	122

Abstract.....	122
1. Introduction	123
2. Materials and Methods.....	125
2.1 Participants.....	125
2.2 MRI protocols	126
2.3 Behavioral paradigm	127
2.4 fMRI data analysis	127
3. Results	129
3.1 Primary analysis: two runs per subject matched for differences in motion between Simplex Autism and typical cohorts	130
3.2. Examination of group by time interactions found in the primary analysis at a liberal threshold.....	132
3.3. Secondary analyses: All four runs combined per subject, and each run per subject	133
4. Discussion	134
Acknowledgements.....	138
Financial Disclosures	138
References.....	139
Table and Figure Legends.....	141

Acknowledgements

This work was supported by a grant from the McDonnell Center for Systems Neuroscience. Eric Feczko's effort was supported by the Ophthalmology and Visual Sciences Training Grant (T32 EY013360), and the Systems and Molecular Neurobiology Training Grant (T32 GM0085151). John Pruett's effort was supported by K12 EY16336. I thank Sridhar Kandala for coordinating recruitment, scheduling, and assessments of the subjects. We would like to thank Gagan Wig and Mital Neta for contributing face stimulus sets. I would like to my thesis committee for providing excellent advice on experimental design. I would like to thank Fran Miezen for technical support and help with quality control for the experimental design. I would like to thank Richard Mulligan, Sridhar Kandala, and Sarah Hoertel, for helping to proofread the thesis. I would like to thank the Washington University School of Medicine Volunteers for Health for providing sources for recruitment.

ABSTRACT OF THE DISSERTATION

Intermediate Level Mechanisms Supporting Face Perception

by

Eric Feczko

Doctor of Philosophy in Neurosciences

Washington University in St. Louis, 2013

Dr. John R. Pruett, Jr., Chair

I propose that the intermediate neural mechanisms involved in face processing may be better understood by studying concentric form-from-structure integration. This dissertation involves behavioral adaptation and masking experiments that provide evidence regarding whether face perception and concentric form-from-structure perception engage a common processing mechanism.

Despite faces being complex visual stimuli, humans are able to perceive and identify faces rapidly. Studies of face perception strongly suggest that this ability involves processing the arrangement of the face features. Although high-level aspects of face perception have been studied extensively, less is known about the intermediate mechanisms involved in face processing. Converging evidence has shown that concentric form-from-structure perception involves processing the arrangement of the features and that face-sensitive mid- and high-level visual regions may be involved.

I used visual adaptation and visual masking experiments to test this hypothesis. My data show that masking with, but not adaptation to, concentric form-from-structure stimuli impairs face discrimination. The results of this thesis provide evidence that

concentric form-from-structure and face perception may share a common processing mechanism.

Chapter 1: Background and Significance

Despite faces being complex visual stimuli, humans are able to perceive and identify faces rapidly (for a review see: [1]). Studies of face perception strongly suggest that the ability to perceive faces relates to processing the arrangements of face features [2-18]. Although high-level aspects of face perception have been studied extensively, less is known about the intermediate mechanisms involved in face processing. Converging evidence has shown that humans perceive concentric and radial form-from-structure stimuli by processing the arrangements of features [19, 20] and that face-sensitive mid- and high-level visual regions may be involved [21-24]. This thesis describes visual adaptation and visual masking experiments that test the hypothesis that face, concentric, and radial form-from-structure perception engage a common processing mechanism.

Face processing

Introduction

Visual processing occurs in a distributed hierarchy, where neurons at successively higher levels are sensitive to increasingly more complex stimulus properties (for a classic comprehensive review see: [25], for a more recent review see: [26]). Low-level visual regions, such as V1 and V2, respond to local elements: some neurons in V1 are tuned to line orientations, and some neurons in V2 are tuned to arcs. Mid-level visual regions, such as ventral V4, respond to forms and patterns, such as non-Cartesian gratings [27]. High-level visual regions, such as the fusiform face area

(FFA), show sensitivity to objects such as faces [28]. A putative arrangement of these areas is illustrated in figure 1.1.

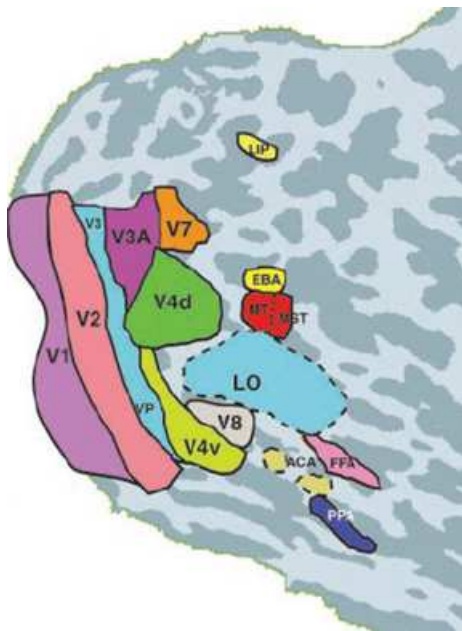


Figure 1.1. Crude depiction of putative human visual

areas on a flattened cortical surface. Adapted from Tootell et al [29]

Studying mechanisms involved in face processing may provide important insights into object recognition and relevant clinical disorders

Understanding face processing has great clinical relevance. Face processing deficits have been observed in disorders such as autism [30-37], a developmental disorder affecting approximately 1% of the human population [38, 39]. Studying the underlying mechanisms that support face processing may allow a better understanding of autism, which could lead to improvements in early diagnostic assessments and potential interventions [40]. Such research may also provide insights into the fundamentals of visual object recognition in general.

Face perception involves processing the arrangements of face features

Several critical paradigms have shed light on the involvement of holistic and configural processing mechanisms in face perception. Holistic processing refers to processing the face as a whole [5], while configural processing refers to processing the arrangement of face features [4]. Because processing the arrangement of face features is important for perceiving the face as a whole [11], the difference between holistic and configural processing lacks a precise experimental distinction. Therefore, the remainder of the thesis will use the term “processing the arrangements of face features” or “feature-arrangement processor” in order to avoid confusion. Many behavioral studies (e.g. the face inversion effect [41], Thatcher illusion [2, 6, 7, 15, 42-44], composite-face effect [4], part-whole effect [5, 6, 10, 45-47], and visual face search [48-50]) and electrophysiological studies [51, 52] provide convergent evidence that visual perception of human faces involves processing the arrangements of face features.

Face inversion effect

Face inversion has a pronounced effect on face recognition tasks. Whereas upright faces are rapidly recognized, inverted faces take longer and are harder to recognize [41]. Some have argued that the key difference between upright and inverted face processing is that upright face perception recruits an expertise pathway [3, 8, 9, 53, 54], because people generally develop high familiarity with upright faces. Perceiving an upright face may recruit a processor that responds to the arrangements of face features. Such a processor may be poorly utilized when perceiving an inverted face because the arrangement of inverted face features is unfamiliar. However, this expertise hypothesis is controversial. Others argue that, regardless of expertise, upright face perception

engages its own special neural pathway, and that inverted face perception engages a dedicated non-face visual pathway [55].

The Thatcher illusion

Because face perception involves processing the arrangements of features, distortions of these arrangements may be easier to perceive when the arrangements are more familiar (i.e. presented upright). Thompson et al [2] showed subjects pairs of the same face: one was normal, and the other was distorted by inverting the eyes and mouth. When the pair of faces was upright, subjects were rapidly able to indicate which face of the pair was distorted. When the pair was inverted, it became significantly harder for subjects to indicate the distorted face. This illusion was termed the “Thatcher illusion” (Figure 1.2). The Thatcher illusion has been reproduced and studied extensively [2, 6, 7, 15, 42-44]. The robustness of the illusion demonstrates that processing the arrangements of features is important for face perception.



Figure 1.2. The Thatcher illusion. When inverted, it is difficult to discriminate the normal from the distorted face (top). When upright, it becomes easy to discriminate the normal from the distorted face (bottom). Adapted from [1].

The composite face-effect

Young et al. tested the importance of processing arrangements of face features by using composite faces [4]. Subjects were presented with two face halves, a top half from one famous face and a bottom half from another famous face. Subjects were asked to identify the two halves for each trial. In some cases the halves were aligned to form a face, in others the halves were misaligned. Subjects were more accurate at recognizing the face halves when they were misaligned than when they were aligned, because when fused, the whole becomes represented in a way that makes it difficult to identify or say if the halves are different. Similar to the Thatcher Illusion, inverting the composite face reduces the effect (figure 1.3) [18], demonstrating the importance of processing the arrangements of face features in visual face perception.

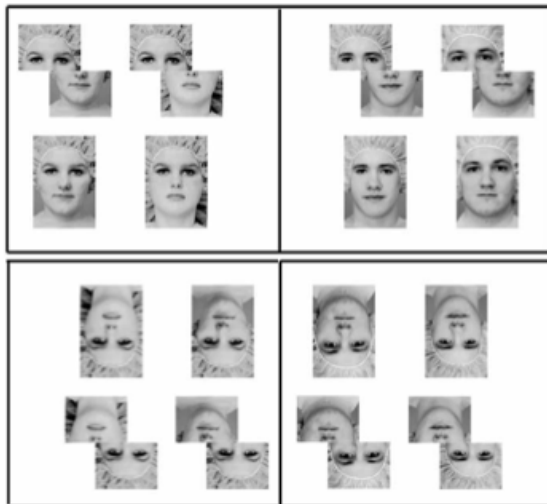


Figure 1.3. The composite-face effect, as

adapted from Mondloch et al. [18] Pairs of upright (top) and inverted (bottom) faces are shown in each of the two columns. The left column represents all conditions where the top-half of the face is identical for the pair. The right column represents all conditions where the top-half of the face is different for the pair.

The part-whole effect

Rhodes et al. tested whether face inversion impairs face recognition when a feature was swapped (i.e. dark eyes for light eyes) or the spacing between features was altered [6]. In the encoding phase, subjects viewed a series of faces. In the testing phase, subjects were presented with a pair of faces and asked which one of the pair they had seen before. Relative to upright face presentations, subjects were impaired when presented with a normal inverted face and an inverted face with swapped features or an inverted face with differently spaced features. Interestingly, subjects were not impaired when the inverted eyes or mouth were presented in isolation from the face. The lack of a face-inversion effect for presenting isolated face parts suggests that presenting the context of a whole face recruits feature-arrangement processing.

This effect was termed by Tanaka as the “part-whole effect” [5]. As in Rhodes et al., Tanaka et al. found that the face-inversion effect was eliminated when face parts were presented in isolation. Other studies have replicated the inversion effect that occurs when discriminating between a face and the same face with differently spaced features (figure 1.4) [10, 45-47]. Furthermore, this part-whole effect was not found for the perception of houses [5], indicating that processing the arrangements of features may be more important for perceiving faces than perceiving non-face objects.

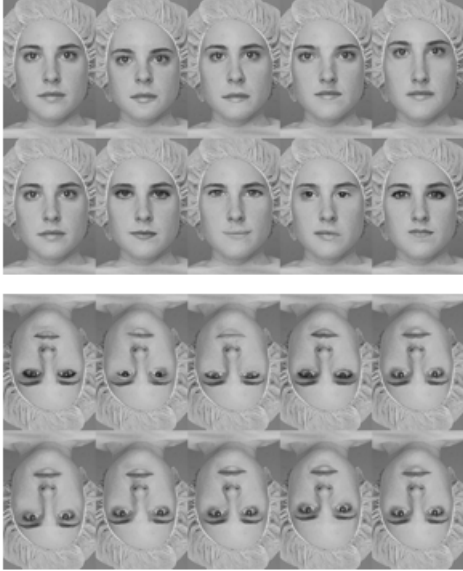


Figure 1.4. The part-whole effect, as adapted from

Mondloch, et al. [10] The top row of upright faces differ in the spacing of features, the bottom row of upright faces have different face features. The top row of inverted faces has different face features, while the inverted faces in the bottom row differ in the spacing of face features.

Visual face search

In a typical visual search task, a subject is shown arrays of objects and is asked to indicate whether a target object is present or absent. The number of items in an array varies throughout the experiment. The relationship between reaction time and the number of items in an array varies from task to task. For example, when searching for a blue square amidst green squares, the reaction time remains constant as the number of items increases, but when searching for a blue square amidst blue circles and green squares, reaction time increases as the number of items per array increases [56].

In visual face search experiments, where adults indicate whether a face is present amidst an array of common non-face objects (e.g., chairs [49, 50] or scrambled

scenes [48], the reaction time when a target is present remains constant as the number of items increases, but when the target is absent, reaction time increases as the number of items per array increases. Adults do not show such search patterns for a non-face object (e.g., cars) amidst other categorically different objects [49]. Adults do not show such search patterns for scrambled faces amidst scrambled non-face objects, suggesting that feature-arrangement processing may drive this effect [49]. At least 3 different labs have published empirical evidence supporting this in typical adults. The Pruett lab has unpublished evidence showing such patterns for face search in adults (Feczko, Povinelli, Petersen, and Pruett, unpublished) and typical and autistic 9-12 year olds (Pruett et al, in press in PLOS ONE). Although some have argued that these face search results are driven by a unique low-level property of faces [57], an intriguing alternative is that the arrangement of the face features enables face search [49, 58].

Electrophysiological studies

Electrophysiological studies of face perception in non-human primates have shown that some neurons in infero-temporal cortex are specifically tuned to whole faces. The initial electrophysiological study, conducted by Desimone et al, showed that these neurons were tuned to the arrangement of the face features [51]. Scrambling or removing the features of the presented face, such as the eyes or mouth, reduced the firing rates of these face-sensitive neurons.

Kobatake and Tanaka tested whether tuning for faces resulted from the combination of individual features by determining which features maximized the firing rates of face-sensitive, macaque, infero-temporal cortical neurons [52]. They found that the stimulus that maximized the firing rates of these cells was a schematic face

configuration. The configuration consisted of two black spots displaced horizontally and a horizontal black bar below the two black spots, embedded in a circular contour. If the spots, bar, or contour were absent, then the cell did not fire, indicating that face-sensitive neurons were not simply linearly summing the features of the configuration. Taken together with previous findings of face tuning in infero-temporal cortex, it appears that neurons in infero-temporal cortex are involved in processing arrangements of face features.

Summary

Numerous behavioral phenomena suggest that processing the arrangements of features is important for visual face perception. The existence of a feature-arrangement processor is supported by convergent electrophysiological data. Studying simpler stimuli that also engage such a processor may provide insights into face perception. Psychophysical, neurophysiological, and lesion data suggest that other kinds of form-from-structure stimulus perception also involve processing the arrangement of its features. The following section will discuss this literature.

Form-from-structure perception

Concentric and radial form-from-structure perception may involve processing the arrangements of features

Form-from-structure stimuli, such as Glass patterns, are defined by a set of rules that arranges meaningless, local elements [59]. A Glass pattern is constructed by a set of dot pairs, called dipoles. Each dipole has one dot randomly placed within the pattern and a member dot, whose displacement from the random dot is determined by a geometric rule. Although the local elements are meaningless, the arrangement of the

dipoles produces a global form. A rotational rule produces a concentric pattern.

Calculating the displacement from the tangent of an imaginary ellipse produces a radial pattern. Shifting the member dot vertically or horizontally produces a translational pattern. The visual processing mechanisms necessary for perceiving translational, radial, and concentric Glass patterns have been studied extensively.

Psychophysical studies

Because Glass patterns consist of arrangements of dot pairs, the coherence of these patterns can be expressed as the percentage of dot pairs following the geometric rule. Wilson and Wilkinson studied the salience of different types of Glass patterns by examining the coherence necessary to detect whether a Glass pattern has a global form or no global form [19, 20]. They found that concentric Glass patterns were the most salient, requiring only 12% coherence in order to be accurately detected. Radial Glass patterns were less salient; subjects could accurately detect them when the coherence was 24%. Translational Glass patterns were the most difficult to detect, requiring 56% coherence.

To test whether perception of the concentric Glass pattern involves feature-arrangement processing, Wilson and Wilkinson divided the stimuli into pie wedges. Some pie wedges contained signal dipoles, which were arranged in a concentric pattern, the others contained noise dipoles. The percentage of stimulus extent covered by signal wedges varied parametrically. They found that as the percentage of area containing signal wedges increased, the coherence necessary for accurate detection decreased [19]. Interestingly, this was not found for the translational Glass patterns, suggesting that concentric but not translational Glass pattern perception involves

processing the arrangements of features. When the same experiment was conducted on radial Glass patterns, Wilson and Wilkinson found a similar effect: as the percentage of area reflecting signal dipoles increased, detecting radial patterns became easier [20].

By examining the relationship between stimulus extent and critical duration, the minimal time necessary to discriminate a presented stimulus, Aspell et al. provided more (indirect) evidence that concentric form-from-structure patterns utilize feature-arrangement processing [60]. Subjects performed a two-alternative, two-interval, forced-choice task, where one interval contained a global form-from-structure stimulus and the other contained random noise. In each trial, subjects would indicate which interval contained a global form. By parametrically varying the stimuli, the authors could determine the critical duration for a given global form at a particular stimulus extent.

The authors found that the integration time for concentric forms decreased as the stimulus extent increased from 3 to 10.9 visual degrees. The opposite effect was found for translational forms. From these results, the authors argued that concentric forms are optimally processed by neurons with receptive field sizes greater than 3 visual degrees. Such neurons are classically found in infero-temporal cortex and possibly in V4 [52].

These psychophysical data suggest that concentric and radial, but not translational, form-from-structure perception involves processing the arrangements of features.

Electrophysiological studies show low-level tuning for concentric forms, but not concentric Glass patterns

Many electrophysiological studies have examined V4 tuning for complex shapes [27, 52, 61-66]. In particular, these studies have shown that some V4 neurons are tuned

to non-Cartesian concentric and radial forms (e.g., [27, 65]). However, Kobatake and Tanaka found that some V2 neurons are also tuned to non-Cartesian concentric and radial forms [52]. Hedge et al, examining changes in tuning specificity from V1 to V4, found that even some V1 neurons have tuning to concentric and radial forms [61]. Unlike forms, tuning for concentric Glass patterns is not found in V1 or V2 [67], but V4 tuning for concentric Glass patterns has not been studied. Unfortunately, to my knowledge, no such studies examining radial Glass pattern tuning exist. One key difference between form and form-from-structure processing is that form-from-structure perception may require global pooling of information (form-from-structure), whereas simple form perception does not.

A patient with a V4 lesion and impaired concentric pattern perception

By studying a patient with a putative V4 lesion, Gallant tested whether *human* V4 is necessary for complex object perception [68]. This patient had a focal lesion near the temporal-occipital junction in the right hemisphere. This lesion affected the lower-left quadrant of the patient's visual field. The patient showed no impairment in perceiving simple stimuli, such as oriented sinusoidal gratings, presented in the lower-left quadrant. When presented with concentric Glass patterns (and also other intermediate forms, such as non-Cartesian gratings) in the affected quadrant, the subject was unable to dissociate fully coherent concentric patterns from noise, demonstrating that V4 may be necessary for concentric Glass pattern perception. If a feature-arrangement processor is necessary for perception of concentric Glass patterns, then V4 may represent a component of this processor.

Summary

Psychophysical experiments suggest that concentric and radial, but not translational, form-from-structure integration engages a feature-arrangement processor. Evidence from lesion and electrophysiological studies is consistent with this hypothesis for concentric Glass patterns. Despite the psychophysical data, few neurophysiological studies have examined neuronal tuning or effects of lesions on radial Glass pattern perception.

Face and concentric form-from-structure perception may share a common processing mechanism

In the previous sections, it has been shown that face, concentric, and radial form-from-structure perception may involve processing the arrangements of features. The following sections present evidence hinting that this processing mechanism may be shared.

Neurophysiological evidence

Electrophysiological study

Kobatake and Tanaka showed that some neurons in macaque infero-temporal cortex were maximally tuned to whole faces [52], while other neurons in the same region of infero-temporal cortex showed maximal tuning to concentric rings, suggesting that aspects of concentric pattern and face perception are processed within the same neural regions. It is unfortunate that Kobatake and Tanaka did not test whether the same neurons show tuning to both faces and concentric rings.

fMRI studies

Using multi-voxel pattern classification, a recent fMRI study tested whether the BOLD activity from low- to high-level visual regions can be used to classify different Glass pattern types. The authors found that in successively higher-level visual regions BOLD activity better classified concentric and radial (but not translational) Glass patterns, suggesting that concentric and radial Glass pattern processing utilizes high-level visual regions [23]. Converging data from another fMRI study [22] suggest that high-level regions implicated in face processing are also implicated in concentric form processing. Using functional localizers, the authors identified a human homologue of V4 and also FFA, a human region engaged by faces more than non-face objects [28]. The authors tested whether V4 and FFA showed significant increases in activity for concentric, sinusoidal, and radial gratings. In V4, the BOLD signal significantly increased when concentric and radial gratings were presented. In FFA, the BOLD signal significantly increased when concentric, but not other, gratings were presented [22]. Another fMRI study showed that V1, V2, and V4 activity was sensitive to the global form of radial or concentric glass patterns [24]. Although this appears to contradict previous electrophysiological data [67], the authors suggested that the tuning observed in V1 and V2 may reflect feedback signals from V4 [24]. Taken together with electrophysiological data, this suggests that the same brain regions process faces, concentric, and radial forms. Concentric Glass pattern perception may be most similar to face perception, but these studies do not establish whether concentric form-from-structure and face perception share a processing mechanism at the level of individual neurons.

Prosopagnosia lesion study

Rentschler et al. tested whether impairments in face perception are accompanied by impairments in concentric form-from-structure perception [21]. Two patients with high-level visual lesions took part in the study. One patient showed strong impairments in face recognition (prosopagnosia), and the other showed strong impairments in reading (alexia). The authors found that the prosopagnosiac patient was impaired in concentric Glass pattern perception, while the alexic patient was unimpaired. He further tested the patients on local and global visual perception of textures, and found that the prosopagnosiac was only impaired at perceiving textures requiring global processing, while the alexic showed both local and global visual deficits for texture perception. Taken together, it appears that some global processing (i.e. feature-arrangement processing) mechanism involved in face perception may also be involved in concentric Glass pattern perception.

Summary

While the evidence above hints at a shared processor for face, radial, and concentric form-from-structure perception, none of the studies directly test this hypothesis. Visual adaptation and visual masking studies could be used to test whether face, concentric, and radial form-from-structure perception share a common processing mechanism.

Visual adaptation can be used to test this hypothesis directly

Behavioral effects of adaptation

When a subject views a stimulus for a long period of time, the subject perceives subsequently viewed stimuli as possessing attributes opposite those of the initial

stimulus. For example, viewing a blue square for a long period of time will cause subsequently viewed squares to appear more yellow. The prolonged exposure is referred to as adaptation, and the effect observed afterwards is termed the aftereffect. This aftereffect may result because the responses of individual neurons habituate to the attributes of the adapted stimulus [69-71]. Presumably, visual adaptation to blue causes the neurons' tuning curves to shift away from blue [70]. In terms of perception, the altered tuning curves cause a neutral color to be perceived as the color yellow [70]. Blue and yellow color adaptation may result because of a push-pull mechanism within retinal horizontal neurons [72].

Adaptation effects have been demonstrated from low to high levels of visual processing, using stimuli ranging from lines [73] to faces [17, 74-76]. Cross-adaptation has also been demonstrated across levels of visual processing, as adaptation to curves changes the subsequent perception of happy or sad faces [77].

Importantly, concentric [78-80], but not translational (see: Chapter 2), Glass pattern adaptation impairs concentric Glass pattern perception, suggesting that concentric patterns are processed differently from translational Glass patterns along the visual pathway. Similarly, radial Glass pattern adaptation impairs radial Glass pattern perception. Although one adaptation study suggested that concentric and radial Glass pattern perception may result from a push-pull mechanism [79], another more careful study showed that adaptation to radial Glass patterns may not affect concentric Glass pattern perception and vice versa [78]. The lack of Glass pattern cross-adaptation might suggest that, when processing the global form, concentric Glass pattern perception engages different neurons than radial Glass pattern perception.

Because face adaptation impairs subsequent face perception, concentric Glass pattern adaptation impairs subsequent concentric Glass pattern perception, and radial Glass pattern adaptation impairs subsequent radial Glass pattern perception, the hypothesis that face, concentric, and radial Glass patterns share a common processing mechanism could be tested by determining whether concentric or radial Glass pattern adaptation impairs subsequent face perception, and vice versa. The results from such behavioral adaptation experiments would inform an fMRI adaptation paradigm.

Neurophysiological mechanisms of adaptation

Functional MRI can be used to test where adaptation occurs along the visual hierarchy. fMRI visual adaptation studies can be divided into two types of studies: classic adaptation and within-session repetition suppression studies [69]¹. In classic adaptation, an adapting stimulus is presented for a long time (more than 20 seconds) before acquisition of functional MRI data. Within-session repetition suppression studies do not present the adapting stimulus prior to fMRI acquisition. In within-session repetition suppression, pairs of adapting and test stimuli are repeatedly presented in succession throughout fMRI data acquisition. Pairs of stimuli that show adaptation also show a reduction in the BOLD response. As above, the reduction in BOLD response indicates whether the visual presentation of two stimulus types (e.g. faces and concentric Glass patterns) activates the same neurons.

Classic fMRI adaptation has been used to explore adaptation of orientation-tuned neurons in low-level visual areas, such as V1. Tootell et al. presented subjects with

¹ Technically, repetition suppression can also occur between separate sessions. However, this form of repetition suppression may be a form of priming, not visual adaptation. Because priming is beyond the scope of this proposal, it will not be discussed here. For a review see [81].

sinusoidal gratings for 40s at a time [82]. After 40s, the grating would switch orientation. The BOLD response in V1 was greatest when the gratings switched to an orthogonal orientation. The BOLD response in V1 was smallest when the gratings changed orientation the least. Other studies replicated this result using a slightly different adaptation paradigm [83-85]. A grating at the adapting orientation was presented for more than 20 seconds prior to scanning. During scanning, test (gratings at varying orientations) and adapting gratings were presented in an interleaved fashion. The BOLD signal increased as the orientation of the test grating differed from the adapting orientation.

These results mirror findings from electrophysiological studies of orientation-tuning adaptation in macaque V1 [86, 87]. fMRI adaptation may occur because of effects of adaptation on individual neurons, fMRI adaptation can, therefore, be used to explore neural tuning for representations of visual stimuli. fMRI adaptation studies have explored neural mechanisms involved in face recognition.

Loffler et al. tested whether neurons in fusiform face area (FFA) were tuned to face identity, or face geometry [88]. Face geometry is a measure of the distance of a particular face configuration from a template face configuration (called the “mean face”). Each face is plotted in a multi-dimensional space (two dimensions are shown in figure 1.5). The vector (i.e. the direction and distance from the mean face) is unique for every face in the space. Faces that lie on a particular direction have the same set of features altered, and the distance from the mean determines how much the features are altered from the mean. Subjects were presented with blocks of faces in three conditions: identity, distance, and same. In the “same” condition, the same face was used

throughout the block (figure 1.5: blue circle). In the “distance” condition, the faces used varied in the distinctiveness from the mean face but not in which features were altered. This can be defined as the distance from the mean face along a single axis (figure 1.5: red oval). In this condition, for example, the mouth may become wider or thinner along a single line in the face space. In the “identity” condition, the faces presented varied in terms of the set of distinct features altered (i.e. the direction of the displacement from the mean face), but the level of distinctiveness from the mean face (i.e. the distance from the mean face) was kept constant (figure 1.5: green band). For example, a face with one identity may have a wider mouth than the mean face, while another face may have a shorter distance between the eyes than the mean face, but the degree to which each face differs from the mean face may be the same. For all conditions, subjects were presented pairs of faces in serial, rapid succession. Subjects indicated whether the second face had the same or different orientation from the first face.

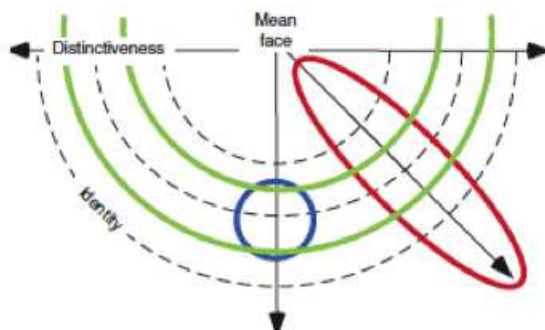


Figure 1.5. The plot of the face space defined

in Loffler et al [88]. Only half of the face space is shown in the diagram. The mean face is located at the center of the space. The arrows represent the distance from the mean face. The green band delineates the faces presented in the “identity” condition. The red ellipse delineates the faces presented in the “distance” condition. The blue circle delineates the faces presented in the “same condition”.

The authors found the BOLD signal was suppressed for the same and distance blocks, but not for the identity block. The BOLD signal suppression for the same block results because the adaptor and target were identical. The BOLD signal suppression for the distance block suggests that neurons in FFA are tuned to the same direction from a mean face. The BOLD signal was not suppressed for the identity block, which suggests that neurons in FFA are not tuned to specific distances from a mean face. Because varying distances from a mean face changes the face configuration, and varying direction alters the identity of the face, these results suggest that neurons in FFA are narrowly tuned to face identities, and broadly tuned to face configurations.

Gilaie-Dotan et al replicated this finding using a stimulus set of face morphs generated from a single face. Using adaptation to this face and its partially-morphed face set, they found that neurons in FFA are narrowly tuned to face identity [16], consistent with the findings from Loffler et al [88]. In a subsequent study, they extended this finding by testing whether neurons in FFA were tuned to representations of inverted faces [89]. Using an identical paradigm, they found that neurons in FFA were more broadly tuned to inverted faces than upright faces, and activity in FFA was not significantly different between inverted face and upright face conditions. Taken together, these face adaptation studies suggest that neurons in face-sensitive regions are differentially tuned to both upright and inverted faces. Some argue that increased expertise with upright faces causes FFA neurons to develop more narrow tuning curves [89].

Summary

Behavioral and imaging studies of visual adaptation may directly test whether face, concentric, and radial Glass pattern perception share a common processing mechanism. However the absence of any cross-adaptation effects does not rule out the possibility of a shared processing mechanism. Instead, it is possible that the mechanism is not sensitive to adaptation. Presentations of concentric and radial Glass patterns may suppress the activity of, but not alter the tuning curves of, neurons tuned to faces and vice versa. If so, then visual masking studies may reveal pattern-specific effects of masking on face perception.

Visual masking experiments may provide evidence for interaction between concentric Glass pattern and face perception.

Behavioral effects of visual masking

Visual masking is an effective tool used to study visual perception. Visual masking occurs when a stimulus (termed the “mask”) is presented either before (forward masking), after (backward masking), or both before and after (sandwich masking) another stimulus (termed the “target”). The presentation of the mask reduces the visibility of the target, and therefore limits the ability of the subject to perceive the target or discriminate it from other targets.

The literature on visual masking is vast (for two reviews see: [90, 91]). The visual mask can be presented surrounding the target (termed “paracontrast” for forward masks and “metacontrast” for backward masks), or the mask can be presented at an overlapping spatial location with the target. Visual masking effects can occur whether the mask is simply random noise, or is constructed to be similar to the target (termed

“pattern” masking). To simplify the discussion here, this thesis will focus on pattern masking of faces and Glass patterns, where the mask and target spatially overlap. Therefore, only two properties of pattern masking will be discussed here: the structure of the mask and the timing of its presentation.

Pattern-specific masking effects can be manipulated by the mask-target stimulus-onset-asynchrony (SOA), the duration between the onset of the mask and the onset of the target. Typically, effects of visual masking are strongest when the SOA is between 30 and 100 milliseconds [91], although this can vary depending on the mask and target (see below). In this range, a pattern-specific mask will generally reduce the visibility of the target. Although masking effects may be observed at either smaller or larger SOAs, the target generally increases in visibility as the SOA increases. Studies of pattern masking were performed to characterize the timing of face processing mechanisms (a summary of these studies can be found in [92]). The masking stimulus used in these studies comprised a series of overlapping alphabet letters (“N” and “O”, see figure 1.6) to ensure that the mask and the face did not utilize the same high-level processing mechanisms. Visual masking using the N-O mask revealed that the masking effects were strongest at 20 milliseconds after the onset of the face; subjects were impaired at determining face identity or whether the configuration of the face was altered.

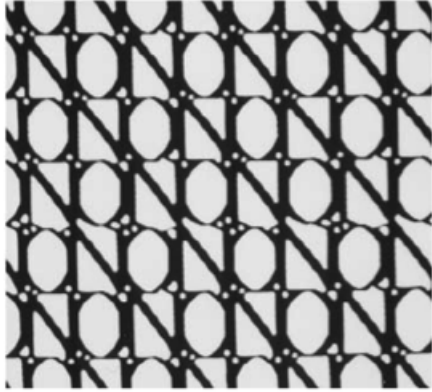


Figure 1.6. The N-O mask used in the behavioral and

electrophysiological studies conducted by Rolls et al. Adapted from [92].

The structure of the mask stimulus, as well as its luminance and contrast, can greatly affect its ability to change the discriminability of the target. A mask that better suppresses a target, compared to other masks of the same luminance and contrast, may be more likely to share a common processing mechanism with the target. In a study of Glass pattern masking, Chen et al. tested whether different Glass pattern (i.e. translational, radial, concentric, spiral) masks affected the discriminability of either concentric or radial Glass patterns from noise [93]. They found that spiral masks impaired concentric and radial Glass pattern discriminability greater than non-spiral masks. Surprisingly, radial masks did not affect concentric perception greater than noise masks, and concentric masks did not affect radial perception greater than noise. Such findings are consistent with a careful visual adaptation study that suggested independent mechanisms for radial and concentric Glass pattern detection [78].

A study of pattern masking was performed to investigate whether upright, scrambled, and inverted faces share a common processing mechanism [14]. Participants were presented with a mask (noise, house, scrambled face, upright face,

and inverted face) and a target upright face. The SOA of the target and the mask varied from trial to trial, so the mask may appear before (forward masking) or after (backward masking) the trial. After the presentation, subjects were presented with two faces and asked to select the face that matched the target. Observed pattern-masking effects were strongest when backward masking at an SOA of 80 milliseconds, where upright faces had the strongest effect of masking. However, relative to houses and noise masks, inverted face and scrambled masks impaired face discrimination as well, suggesting that inverted and scrambled face perception are more similar to upright face perception than house perception [1]. Therefore, if face, concentric, and radial Glass pattern perception share a common processing mechanism, then concentric and radial Glass pattern masking should impair face discrimination more than translational Glass pattern masking.

Neurophysiological mechanisms of visual masking

The neurophysiological mechanisms of paracontrast and metacontrast visual masking have been studied extensively [91], however, less is known about the neurophysiological effects of visual masking on face discrimination. Electrophysiological studies of masking face perception using the N-O mask suggest that pattern-specific masking reduces the firing responses of neurons tuned to faces 30 milliseconds after the onset of the face [92, 94]. These data are consistent with fMRI studies of backward masking of faces, which show a reduction in the BOLD response for some face sensitive visual regions when the masking effect was maximized [95-97].

Although it is not known why effective masks suppress neuronal responses to faces specifically, a review of the visual masking literature suggests two possibilities

[90, 91]. First, an effective mask (e.g. another face) may share a common processing mechanism with the target. Presenting the mask engages the shared processing mechanism and therefore interferes with the ability to perceive the target. Alternatively, an effective mask (e.g. the N-O mask) may simply engage one processing mechanism that communicates with a second mechanism engaged by perceiving the target. Presenting the mask affects this communication, which alters the ability to process and perceive the target.

Neurophysiological studies that can examine the neuronal responses to the mask and the target themselves may help dissociate the two possibilities. Regions affected by masking should show suppressed BOLD responses if the mask effectively suppresses target visibility. If the mask and the target utilize different processing mechanisms, then the presentation of the mask sans the target should not increase the BOLD response, relative to fixation, in the putative region. If the mask and the target utilize the same processing mechanism, then regions affected by masking should show increased BOLD responses when the mask is presented relative to fixation. An fMRI study of sandwich masking provides a paradigm for testing between these two possibilities [98]. The authors identified a region in primary visual cortex that showed reduced BOLD responses when the mask effectively suppressed the target., relative to when the mask did not effectively suppress the target. They then demonstrated that the same region of primary visual cortex responded to both the mask itself and the target itself, showing that the identified region is responsive to both the mask and the target. The fact that the region is responsive to both the mask and target suggests that the region instantiates a mechanism utilized when perceiving either of the two stimuli. Therefore, if concentric

and/or radial masking effects are observed in the behavioral experiments, this paradigm may provide a way to dissociate between these two possibilities (see: chapter 5 for a detailed discussion).

Differences between visual masking and visual adaptation

Behaviorally, visual masking and visual adaptation effects can be dissociated by examining the length of the aftereffect. Adaptation can affect the perception of the target for seconds [69], while visual masking effects dissipate after 500 milliseconds (and often, long before) [91]. Therefore, manipulating the time between the offset of the adaptor/mask and the onset of the target may reveal whether the effect of the adaptor/mask is due to adaptation or visual masking.

Visual adaptation may affect the tuning curves of individual neurons because the same neurons are responsive to both the target and the adaptor [72], while visual masking may occur even when different neurons in the same region engage either the mask or the target [91]. Therefore, an adaptor that is also an effective mask indicates that the same neurons respond to both the adaptor and the target. However, a mask that is an ineffective adaptor suggests that different neurons respond to both the mask and the target, and hints that the mask and the target may share a common processing mechanism, but not at the level of a single neuron.

Summary

Visual masking is a second psychophysical tool that can be used to test the hypothesis. If concentric and radial masking impairs face discrimination more so than translational masking, then face, concentric, and radial Glass pattern perception might engage a common processing mechanism. Comparing the results of visual masking

studies with the visual adaptation studies may provide further insight into the putatively shared neural mechanism. A negative finding from visual adaptation experiments, coupled with a positive finding from visual masking experiments, would suggest the existence of a shared processing mechanism and hint that the mechanism is not shared at the level of single neurons. A future fMRI sandwich masking study may shed light on the nature and location of this shared mechanism.

References

1. Tsao, D.Y. and M.S. Livingstone, *Mechanisms of face perception*. Annual Review of Neuroscience, 2008. **31**: p. 411-37.
2. Thompson, P., *Margaret Thatcher: a new illusion*. Perception, 1980. **9**(4): p. 483-4.
3. Diamond, R. and S. Carey, *Why faces are and are not special: an effect of expertise*. J Exp Psychol Gen, 1986. **115**(2): p. 107-17.
4. Young, A.W., D. Hellawell, and D.C. Hay, *Configurational information in face perception*. Perception, 1987. **16**(6): p. 747-59.
5. Tanaka, J.W. and M.J. Farah, *Parts and wholes in face recognition*. Q J Exp Psychol A, 1993. **46**(2): p. 225-45.
6. Rhodes, G., S. Brake, and A.P. Atkinson, *What's lost in inverted faces?* Cognition, 1993. **47**(1): p. 25-57.
7. Lewis, M.B. and R.A. Johnston, *The Thatcher illusion as a test of configural disruption*. Perception, 1997. **26**(2): p. 225-7.
8. Gauthier, I. and M.J. Tarr, *Becoming a "Greeble" expert: exploring mechanisms for face recognition*. Vision Res, 1997. **37**(12): p. 1673-82.
9. Gauthier, I. and C.A. Nelson, *The development of face expertise*. Curr Opin Neurobiol, 2001. **11**(2): p. 219-24.
10. Mondloch, C.J., R. Le Grand, and D. Maurer, *Configural face processing develops more slowly than featural face processing*. Perception, 2002. **31**(5): p. 553-66.
11. Maurer, D., R.L. Grand, and C.J. Mondloch, *The many faces of configural processing*. Trends Cogn Sci, 2002. **6**(6): p. 255-260.
12. Joseph, R.M. and J. Tanaka, *Holistic and part-based face recognition in children with autism*. J Child Psychol Psychiatry, 2003. **44**(4): p. 529-42.
13. Rouse, H., et al., *Do children with autism perceive second-order relational features? The case of the Thatcher illusion*. J Child Psychol Psychiatry, 2004. **45**(7): p. 1246-57.
14. Loffler, G., et al., *Configural masking of faces: evidence for high-level interactions in face perception*. Vision Res, 2005. **45**(17): p. 2287-97.

15. Boutsen, L., et al., *Comparing neural correlates of configural processing in faces and objects: an ERP study of the Thatcher illusion*. *Neuroimage*, 2006. **32**(1): p. 352-67.
16. Gilaie-Dotan, S. and R. Malach, *Sub-exemplar shape tuning in human face-related areas*. *Cereb Cortex*, 2007. **17**(2): p. 325-38.
17. Benton, C.P. and E.C. Burgess, *The direction of measured face aftereffects*. *J Vis*, 2008. **8**(15): p. 1 1-6.
18. Mondloch, C.J. and D. Maurer, *The effect of face orientation on holistic processing*. *Perception*, 2008. **37**(8): p. 1175-86.
19. Wilson, H.R., F. Wilkinson, and W. Asaad, *Concentric orientation summation in human form vision*. *Vision Res*, 1997. **37**(17): p. 2325-30.
20. Wilson, H.R. and F. Wilkinson, *Detection of global structure in Glass patterns: implications for form vision*. *Vision Res*, 1998. **38**(19): p. 2933-47.
21. Rentschler, I., B. Treutwein, and T. Landis, *Dissociation of local and global processing in visual agnosia*. *Vision Res*, 1994. **34**(7): p. 963-71.
22. Wilkinson, F., et al., *An fMRI study of the selective activation of human extrastriate form vision areas by radial and concentric gratings*. *Curr Biol*, 2000. **10**(22): p. 1455-8.
23. Ostwald, D., et al., *Neural coding of global form in the human visual cortex*. *J Neurophysiol*, 2008. **99**(5): p. 2456-69.
24. Mannion, D.J., J.S. McDonald, and C.W. Clifford, *The influence of global form on local orientation anisotropies in human visual cortex*. *Neuroimage*, 2010. **52**(2): p. 600-5.
25. Felleman, D.J. and D.C. Van Essen, *Distributed hierarchical processing in the primate cerebral cortex*. *Cerebral Cortex*, 1991. **1**(1): p. 1-47.
26. Hegde, J., *Time course of visual perception: coarse-to-fine processing and beyond*. *Prog Neurobiol*, 2008. **84**(4): p. 405-39.
27. Gallant, J.L., J. Braun, and D.C. Van Essen, *Selectivity for polar, hyperbolic, and Cartesian gratings in macaque visual cortex*. *Science*, 1993. **259**(5091): p. 100-3.
28. Kanwisher, N., J. McDermott, and M.M. Chun, *The fusiform face area: a module in human extrastriate cortex specialized for face perception*. *J Neurosci*, 1997. **17**(11): p. 4302-11.
29. Tootell, R.B., D. Tsao, and W. Vanduffel, *Neuroimaging weighs in: humans meet macaques in "primate" visual cortex*. *J Neurosci*, 2003. **23**(10): p. 3981-9.
30. Pelphrey, K.A., et al., *Visual scanning of faces in autism*. *J Autism Dev Disord*, 2002. **32**(4): p. 249-61.
31. Behrmann, M., C. Thomas, and K. Humphreys, *Seeing it differently: visual processing in autism*. *Trends Cogn Sci*, 2006. **10**(6): p. 258-64.
32. Pellicano, E., et al., *Abnormal adaptive face-coding mechanisms in children with autism spectrum disorder*. *Curr Biol*, 2007. **17**(17): p. 1508-12.
33. Wallace, S., M. Coleman, and A. Bailey, *Face and object processing in autism spectrum disorders*. *Autism Res*, 2008. **1**(1): p. 43-51.
34. Wolf, J.M., et al., *Specific impairment of face-processing abilities in children with autism spectrum disorder using the Let's Face It! skills battery*. *Autism Res*, 2008. **1**(6): p. 329-40.

35. Scherf, K.S., et al., *Atypical development of face and greeble recognition in autism*. J Child Psychol Psychiatry, 2008. **49**(8): p. 838-47.
36. Annaz, D., et al., *A cross-syndrome study of the development of holistic face recognition in children with autism, Down syndrome, and Williams syndrome*. J Exp Child Psychol, 2009. **102**(4): p. 456-86.
37. Gauthier, I., C. Klaiman, and R.T. Schultz, *Face composite effects reveal abnormal face processing in Autism spectrum disorders*. Vision Res, 2009. **49**(4): p. 470-8.
38. Chakrabarti, S. and E. Fombonne, *Pervasive developmental disorders in preschool children: confirmation of high prevalence*. Am J Psychiatry, 2005. **162**(6): p. 1133-41.
39. Mulvihill, B., et al., *Prevalence of autism spectrum disorders - Autism and Developmental Disabilities Monitoring Network, United States, 2006*. MMWR Surveill Summ., 2009. **58**(10): p. 1-20.
40. Tanaka, J.W., et al., *Using computerized games to teach face recognition skills to children with autism spectrum disorder: the Let's Face It! program*. J Child Psychol Psychiatry, 2010. **51**(8): p. 944-52.
41. Yin, R.K., *Looking at upside-down faces*. Journal of Experimental Psychology, 1969. **81**(1): p. 141-145.
42. Sturzel, F. and L. Spillmann, *Thatcher illusion: dependence on angle of rotation*. Perception, 2000. **29**(8): p. 937-42.
43. Lewis, M.B., *The lady's not for turning: rotation of the Thatcher illusion*. Perception, 2001. **30**(6): p. 769-74.
44. Riby, D.M., L.M. Riby, and J.L. Reay, *Differential sensitivity to rotations of facial features in the Thatcher illusion*. Psychol Rep, 2009. **105**(3 Pt 1): p. 721-6.
45. Leder, H. and V. Bruce, *When inverted faces are recognized: the role of configural information in face recognition*. Q J Exp Psychol A, 2000. **53**(2): p. 513-36.
46. Murray, J.E., E. Yong, and G. Rhodes, *Revisiting the perception of upside-down faces*. Psychol Sci, 2000. **11**(6): p. 492-6.
47. Freire, A., K. Lee, and L.A. Symons, *The face-inversion effect as a deficit in the encoding of configural information: direct evidence*. Perception, 2000. **29**(2): p. 159-70.
48. Lewis, M. and A. Edmonds, *Searching for faces in scrambled scenes*. Visual Cognition, 2005. **12**(7): p. 1309-1336.
49. Hershler, O. and S. Hochstein, *At first sight: a high-level pop out effect for faces*. Vision Res, 2005. **45**(13): p. 1707-24.
50. Kuehn, S.M. and P. Jolicoeur, *Impact of quality of the image, orientation, and similarity of the stimuli on visual search for faces*. Perception, 1994. **23**(1): p. 95-122.
51. Desimone, R., et al., *Stimulus-selective properties of inferior temporal neurons in the macaque*. J Neurosci, 1984. **4**(8): p. 2051-62.
52. Kobatake, E. and K. Tanaka, *Neuronal selectivities to complex object features in the ventral visual pathway of the macaque cerebral cortex*. J Neurophysiol, 1994. **71**(3): p. 856-67.

53. Gauthier, I., et al., *Activation of the middle fusiform 'face area' increases with expertise in recognizing novel objects*. Nat Neurosci, 1999. **2**(6): p. 568-73.
54. Tarr, M.J. and I. Gauthier, *FFA: A flexible fusiform area for subordinate-level visual processing automatized by expertise*. Nature Neuroscience, 2000. **3**(8): p. 764-769.
55. Kanwisher, N., *Domain specificity in face perception*. Nature Neuroscience, 2000. **3**(8): p. 759-763.
56. Wolfe, J.M., *Guided search 2.0: a revised model of visual search*. Psychonomic Bulletin and Review, 1994. **1**: p. 202-238.
57. VanRullen, R., *On second glance: still no high-level pop-out effect for faces*. Vision Research, In Press.
58. Hershler, O. and S. Hochstein, *With a careful look: Still no low-level confound to face pop-out*. Vision Research, 2006.
59. Glass, L., *Moire effect from random dots*. Nature, 1969. **223**(5206): p. 578-80.
60. Aspell, J.E., J. Wattam-Bell, and O. Braddick, *Interaction of spatial and temporal integration in global form processing*. Vision Res, 2006. **46**(18): p. 2834-41.
61. Hegde, J. and D.C. Van Essen, *A comparative study of shape representation in macaque visual areas v2 and v4*. Cerebral Cortex, 2007. **17**(5): p. 1100-16.
62. David, S.V., B.Y. Hayden, and J.L. Gallant, *Spectral receptive field properties explain shape selectivity in area V4*. J Neurophysiol, 2006. **96**(6): p. 3492-505.
63. Zana, Y. and A.C. Cavalcanti, *Contrast sensitivity functions to stimuli defined in Cartesian, polar and hyperbolic coordinates*. Spat Vis, 2005. **18**(1): p. 85-98.
64. Merigan, W.H., *Basic visual capacities and shape discrimination after lesions of extrastriate area V4 in macaques*. Vis Neurosci, 1996. **13**(1): p. 51-60.
65. Gallant, J.L., et al., *Neural responses to polar, hyperbolic, and Cartesian gratings in area V4 of the macaque monkey*. Journal of Neurophysiology, 1996. **76**(4): p. 2718-39.
66. Desimone, R. and S.J. Schein, *Visual properties of neurons in area V4 of the macaque: sensitivity to stimulus form*. Journal of Neurophysiology, 1987. **57**: p. 835-868.
67. Smith, M.A., A. Kohn, and J.A. Movshon, *Glass pattern responses in macaque V2 neurons*. J Vis, 2007. **7**(3): p. 5.
68. Gallant, J.L., R.E. Shoup, and J.A. Mazer, *A human extrastriate area functionally homologous to macaque V4*. Neuron, 2000. **27**(2): p. 227-35.
69. Kregelberg, B., G.M. Boynton, and R.J. van Wezel, *Adaptation: from single cells to BOLD signals*. Trends Neurosci, 2006. **29**(5): p. 250-6.
70. Kohn, A., *Visual adaptation: physiology, mechanisms, and functional benefits*. J Neurophysiol, 2007. **97**(5): p. 3155-64.
71. Clifford, C.W., et al., *Visual adaptation: neural, psychological and computational aspects*. Vision Res, 2007. **47**(25): p. 3125-31.
72. Packer, O.S., et al., *Blue-yellow opponency in primate S cone photoreceptors*. J Neurosci, 2010. **30**(2): p. 568-72.
73. Nakayama, K. and D.J. Roberts, *Line length detectors in the human visual system: evidence from selective adaptation*. Vision Res, 1972. **12**(10): p. 1709-13.

74. Webster, M.A., et al., *Adaptation to natural facial categories*. Nature, 2004. **428**(6982): p. 557-61.
75. Leopold, D.A., et al., *The dynamics of visual adaptation to faces*. Proc Biol Sci, 2005. **272**(1566): p. 897-904.
76. Anderson, N.D. and H.R. Wilson, *The nature of synthetic face adaptation*. Vision Res, 2005. **45**(14): p. 1815-28.
77. Xu, H., et al., *Adaptation across the cortical hierarchy: low-level curve adaptation affects high-level facial-expression judgments*. J Neurosci, 2008. **28**(13): p. 3374-83.
78. Ross, J. and J. Edwin Dickinson, *Effects of adaptation to Glass pattern structure and to path of optic flow*. Vision Res, 2007. **47**(16): p. 2150-5.
79. Clifford, C.W. and E. Weston, *Aftereffect of adaptation to Glass patterns*. Vision Res, 2005. **45**(11): p. 1355-63.
80. Vreven, D. and J. Berge, *Detecting structure in glass patterns: an interocular transfer study*. Perception, 2007. **36**(12): p. 1769-78.
81. Henson, R.N., *Neuroimaging studies of priming*. Prog Neurobiol, 2003. **70**(1): p. 53-81.
82. Tootell, R.B., et al., *Functional analysis of primary visual cortex (V1) in humans*. Proc Natl Acad Sci U S A, 1998. **95**(3): p. 811-7.
83. Larsson, J., M.S. Landy, and D.J. Heeger, *Orientation-selective adaptation to first- and second-order patterns in human visual cortex*. Journal of Neurophysiology, 2006. **95**(2): p. 862-81.
84. Fang, F., et al., *Orientation-tuned fMRI adaptation in human visual cortex*. Journal of Neurophysiology, 2005. **94**(6): p. 4188-95.
85. Engel, S.A., *Adaptation of oriented and unoriented color-selective neurons in human visual areas*. Neuron, 2005. **45**(4): p. 613-23.
86. Dragoi, V., J. Sharma, and M. Sur, *Adaptation-induced plasticity of orientation tuning in adult visual cortex*. Neuron, 2000. **28**(1): p. 287-98.
87. Carandini, M., J.A. Movshon, and D. Ferster, *Pattern adaptation and cross-orientation interactions in the primary visual cortex*. Neuropharmacology, 1998. **37**(4-5): p. 501-11.
88. Loffler, G., et al., *fMRI evidence for the neural representation of faces*. Nature Neuroscience, 2005. **8**(10): p. 1386-90.
89. Gilaie-Dotan, S., H. Gelbard-Sagiv, and R. Malach, *Perceptual shape sensitivity to upright and inverted faces is reflected in neuronal adaptation*. Neuroimage, 2010. **50**(2): p. 383-95.
90. Breitmeyer, B.G. and H. Ogmen, *Recent models and findings in visual backward masking: a comparison, review, and update*. Percept Psychophys, 2000. **62**(8): p. 1572-95.
91. Breitmeyer, B.G., *Visual masking: past accomplishments, present status, future developments*. Adv Cogn Psychol, 2007. **3**(1-2): p. 9-20.
92. Rolls, E.T., *Consciousness absent and present: a neurophysiological exploration*. Prog Brain Res, 2004. **144**: p. 95-106.
93. Chen, C.C., *A masking analysis of glass pattern perception*. J Vis, 2009. **9**(12): p. 22 1-11.

94. Rolls, E.T. and M.J. Tovee, *Processing speed in the cerebral cortex and the neurophysiology of visual masking*. Proc Biol Sci, 1994. **257**(1348): p. 9-15.
95. Rodriguez, V., et al., *Absence of face-specific cortical activity in the complete absence of awareness: converging evidence from functional magnetic resonance imaging and event-related potentials*. J Cogn Neurosci, 2012. **24**(2): p. 396-415.
96. Kim, M.J., et al., *Behind the mask: the influence of mask-type on amygdala response to fearful faces*. Soc Cogn Affect Neurosci, 2010. **5**(4): p. 363-8.
97. Morris, J.P., K.A. Pelphrey, and G. McCarthy, *Face processing without awareness in the right fusiform gyrus*. Neuropsychologia, 2007. **45**(13): p. 3087-91.
98. Huang, J., M. Xiang, and Y. Cao, *Reduction in V1 activation associated with decreased visibility of a visual target*. Neuroimage, 2006. **31**(4): p. 1693-9.

Chapter 2: Preliminary Studies

In the preliminary studies section, it will be shown that upright face adaptation impairs upright face perception, concentric Glass pattern adaptation impairs concentric Glass pattern perception, and concentric Glass pattern adaptation impairs subsequent inverted face perception. Under certain circumstances, a trend exists for concentric pattern adaptation impairing upright face perception. Taken together, the preliminary studies will set the stage for testing whether concentric form-from-structure and face perception share a common processing mechanism.

Experiment 1: Effects of Glass pattern adaptation on Glass pattern discrimination

Introduction

The initial attempts to test cross-adaptation between faces and Glass patterns were unsuccessful. Therefore, experiment 1 attempted to replicate form-specific Glass pattern adaptation [1-3]. The study tested whether adaptation to concentric, but not translational, Glass patterns impairs subsequent concentric Glass pattern discrimination.

Methods

Stimuli: Glass patterns were constructed using MATLAB and the psychophysics toolbox. Patterns were presented as white dots on a black background. Dots measured 0.04 visual degrees (one pixel). Dipole separation was 0.12 visual degrees. Dot density was 88 dipoles/deg². Glass patterns were constructed by randomly placing a series of dots in the stimulus. Each dot was paired with a second dot. Every pair of dots is called a dipole. For

every dipole, the second dot is displaced from the first according to a geometric rule. For translational patterns, the displacement is vertical. For circular concentric patterns, the displacement is defined as a rotation. For random patterns the direction of displacement is randomly determined while the distance is kept constant. Vertical translational patterns are used because they are more salient than non-vertical translational patterns [4, 5]. Luminance and contrast matching were both approximate, because all dot patterns contained the same number of white and black pixels. As discussed in the summary, these preliminary studies served as pilots for future studies (see Chapters 3 and 4), which precisely controlled the luminance and contrast of the stimuli.

Glass patterns were presented foveally. The extent of each Glass pattern measured 7 visual degrees in diameter. Target concentric Glass patterns were 30% coherent: 70% of the dipoles were oriented randomly. These noisy concentric patterns were chosen because previous findings of form-specific Glass pattern adaptation suggest that adaptation effects would be optimal when the targets are 30% coherent [1].

Experimental design: Subjects were seated in a dark room and instructed to maintain fixation on a dot on the center of a monitor. Five subjects performed three adaptation conditions (concentric, translational, none). For each adaptation condition, the first trial began with an initial adaptation period of 20 seconds. The initial adaptation period was chosen based on previous Glass pattern adaptation studies [1, 2]. During the initial adaptation period, a different exemplar of the same adapting stimulus (concentric, translational, none) was presented every 1 second. After the initial adaptation, either a noisy concentric or random Glass pattern was presented for one second. Subsequent trials began with a follow-up adaptation period of 5 seconds. After the follow-up adaptation, a noisy concentric or random Glass pattern was

presented for 1 second. Subjects indicated whether the target was concentric or not. For each condition, 30 noisy concentric and 30 random Glass pattern targets were presented.

Data analysis: For each subject, accuracy and d-prime (d'), a measure of discriminability [6] was derived for each target type per condition. D-prime, a measure of discriminability independent of bias, was derived from the accuracy measures. This measure can be calculated with the following equation: $d' = Z(\text{group A targets called A/group A targets}) - Z(\text{group B targets called A/group B targets})$, where $Z(p)$ is the inverse of the cumulative Gaussian distribution. Concentric Glass patterns were labeled as group A, while random Glass patterns were labeled as group B. Accuracy was analyzed using an adaptation condition by target type repeated measures ANOVA (3x2), while d' was analyzed using an adaptation condition repeated measures ANOVA (3 levels). Post hoc comparisons of accuracy and d' were made using pairwise t-tests. All p values are reported as uncorrected.

Results

As shown in figure 2.1, adaptation to concentric, but not translational, Glass patterns impaired concentric Glass pattern discrimination. The repeated measures ANOVA showed a significant main effect of adaptation ($F(2,8) = 20.8, p < 0.001, \eta_p^2 = 0.838$). Post-hoc tests showed that concentric Glass pattern adaptation impaired d' more so than translational ($t(4) = 5.78, p = 0.004$) and no ($t(4) = 4.24, p = 0.013$) adaptation.

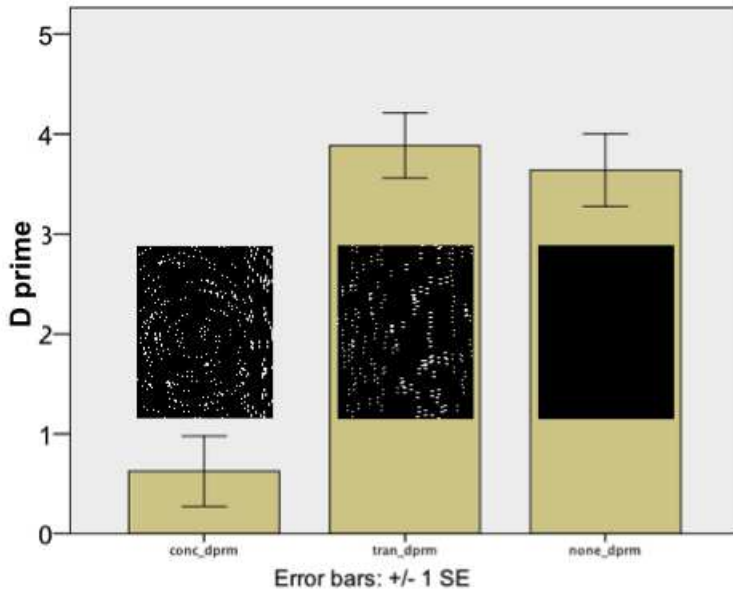


Figure 2.1 Graph of d' measures for experiment 1. Error bars represent one standard error of the mean and are corrected for repeated measures. Pictures on the columns represent the adaptation condition. From left to right, columns represent: concentric adaptation, translational adaptation, and no adaptation.

Accuracy data, presented in figure 2.2, show that Glass pattern adaptation impaired concentric, but not random, Glass pattern accuracy. A significant interaction between adaptation condition and target type was found ($F(1.04, 4.16) = 71.6, p < 0.001, \eta_p^2 = 0.947$). Post-hoc comparisons show that concentric Glass pattern adaptation impaired concentric Glass pattern accuracy relative to translational ($t(4) = 8.24, p = 0.001$) and no ($t(4) = 6.77, p = 0.002$) adaptation. No other post-hoc comparisons were significant ($p > 0.24$).

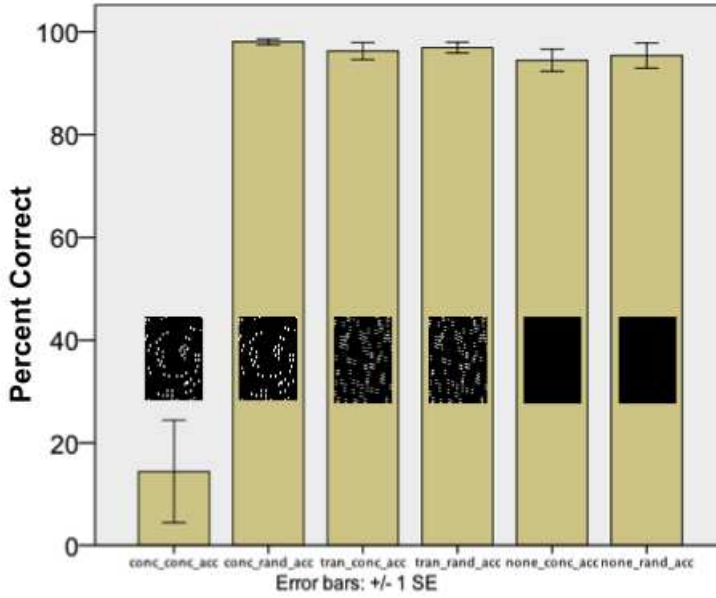


Figure 2.2 A graph of mean accuracy per condition per target type for experiment 1. Error bars represent one standard error of the mean and are corrected for repeated measures. Pictures on the columns represent the adaptation condition. From left to right, columns represent: concentric target accuracy for concentric adaptation, random target accuracy for concentric adaptation, concentric target accuracy for translational adaptation, random target accuracy for translational adaptation, concentric target accuracy for no adaptation, and random target accuracy for no adaptation.

Discussion

The data from experiment 1 show that adaptation to concentric Glass patterns impairs subsequent concentric Glass pattern perception. This is consistent with previous findings of Glass pattern visual adaptation, where concentric Glass pattern adaptation reduced subsequent perception of concentric Glass patterns [1-3]. Although this adaptation effect is robust, it is unclear whether the adapted mechanism is instantiated in low-level visual regions [1] or high-level visual regions [3].

Adaptation to translational Glass patterns does not impair concentric Glass pattern perception. This is consistent with psychophysical studies of translational and concentric Glass

pattern perception, which suggest that translational and concentric Glass patterns appear to utilize different processing mechanisms. Concentric Glass patterns become easier to discriminate as they become larger, while translational patterns become harder to discriminate [7]. Concentric, but not translational Glass patterns are more easily discriminated when the pattern is reflected in the entire stimulus as opposed to a piece of the stimulus [8]. Experiments 2 and 3 test whether faces, concentric, and radial Glass patterns show cross-adaptation effects.

Experiment 2: Effects of face and Glass pattern adaptation on upright/inverted face discrimination: 8 subject pilot

Introduction

Experiment 2 tested whether adaptation to concentric and radial Glass patterns impaired subsequent upright/face discrimination. The adaptation paradigm used in experiment 1 was modified for this study.

Methods

Equipment was identical to experiment 1, presented above. 8 subjects participated in this study

Stimuli: Faces in experiment 2 were either upright or inverted faces embedded in snow. The faces were provided from William Kelley's lab [9]. The snow consisted of white noise pixels with a Gaussian distribution centered on the relative luminance of a mid-gray background. The faces were embedded in snow to increase the difficulty of the task, as subjects were at ceiling when the faces were not embedded in snow. Glass patterns were constructed as described in experiment 1. The white dots were placed on a mid-level gray background. The stimulus extent was square to match the stimulus extent of the faces. The mean pixel intensity of the glass

patterns was approximated to the mean pixel intensity of the faces. Without these alterations, subjects were at floor when adapting to all Glass patterns because of differences in mean pixel intensity between Glass patterns and faces. Radial Glass patterns were also used in this study.

Experimental design: Subjects participated in seven adaptation conditions: upright faces, snow (the same snow used to embed the faces), no adaptor; and concentric, radial, translational, and random Glass patterns. The task sequence is shown in figure 2.3. Initial and follow-up adaptation periods were the same as described in experiment 1. After the adaptation periods, either an upright or inverted face was presented for 27 ms. The short target display was used to make the task harder. A backwards mask, consisting of snow, appeared at a stimulus onset asynchrony of 80ms in order to terminate processing of the stimulus. Without the backwards mask, subjects performed at ceiling for all adaptation conditions. Subjects indicated whether the target was an upright or inverted face.

Upright/inverted face adaptation paradigm

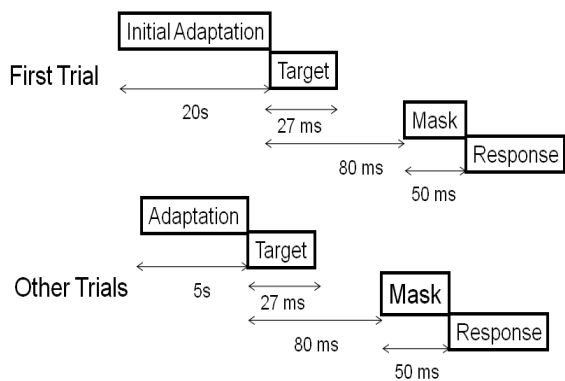


Figure 2.3 Schematic of face adaptation paradigm for experiment 2. The initial adaptation period (for the first trial) lasted 20 seconds. The adaptation period (for the other trials) lasted 5 seconds. During

adaptation periods, an adapting stimulus is presented every 1 second. The mask consists of snow, as described in stimuli.

Data analysis: For each subject, accuracy data per target type and d' were derived for each condition. As in experiment 1, repeated measures ANOVAs were used to test for significant differences in accuracy (7x2 repeated measures ANOVA) and d' (7-level repeated measures ANOVA). Although the Glass patterns were approximately the same in terms of luminance and contrast, the face and snow stimuli may differ from the Glass patterns. As a result, two sets of post-hoc comparisons were made. One set of post hoc tests compared face adaptation to snow and no adaptation to test whether adaptation to faces impaired upright/inverted face discrimination. The second set of post-hoc tests compared concentric Glass pattern adaptation to radial, translational, and random Glass pattern adaptation to test whether concentric adaptation impaired upright/inverted face discrimination more than translational, radial, or random Glass patterns. Glass pattern stimuli were luminance and contrast equated, the other post hoc tests compared concentric Glass pattern adaptation to radial, translational, and random Glass pattern adaptation. P values are all reported as uncorrected.

Results

Measures of d' (figure 2.4) show that concentric, compared to non-concentric, Glass pattern adaptation impairs upright/face discrimination. A main effect of condition was found in the repeated measures ANOVA ($F(6,42) = 4.92$, $p = 0.001$, $\eta_p^2 = 0.413$). Post hoc comparisons found that concentric Glass pattern adaptation significantly reduced discriminability relative to translational ($t(7) = 3.26$, $p = 0.014$), and random ($t(7) = 3.03$, $p = 0.019$) Glass patterns. Although concentric Glass pattern adaptation reduced discriminability more than radial, the

effect was only a trend ($t(7) = 2.17, p = 0.067$). No significant effects of discriminability were found when comparing face, snow, and no adaptation conditions (All p values > 0.157).

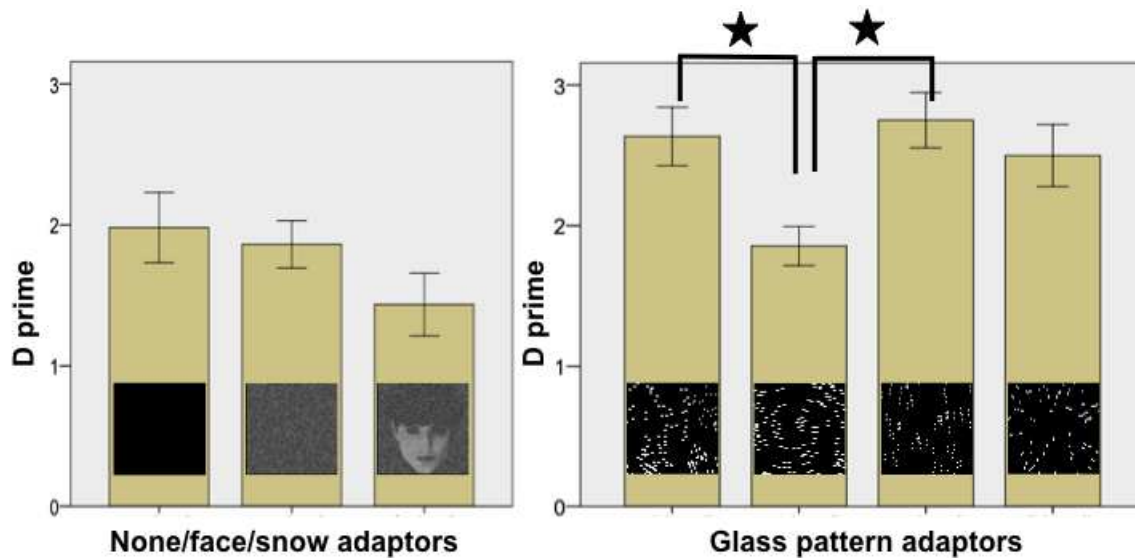
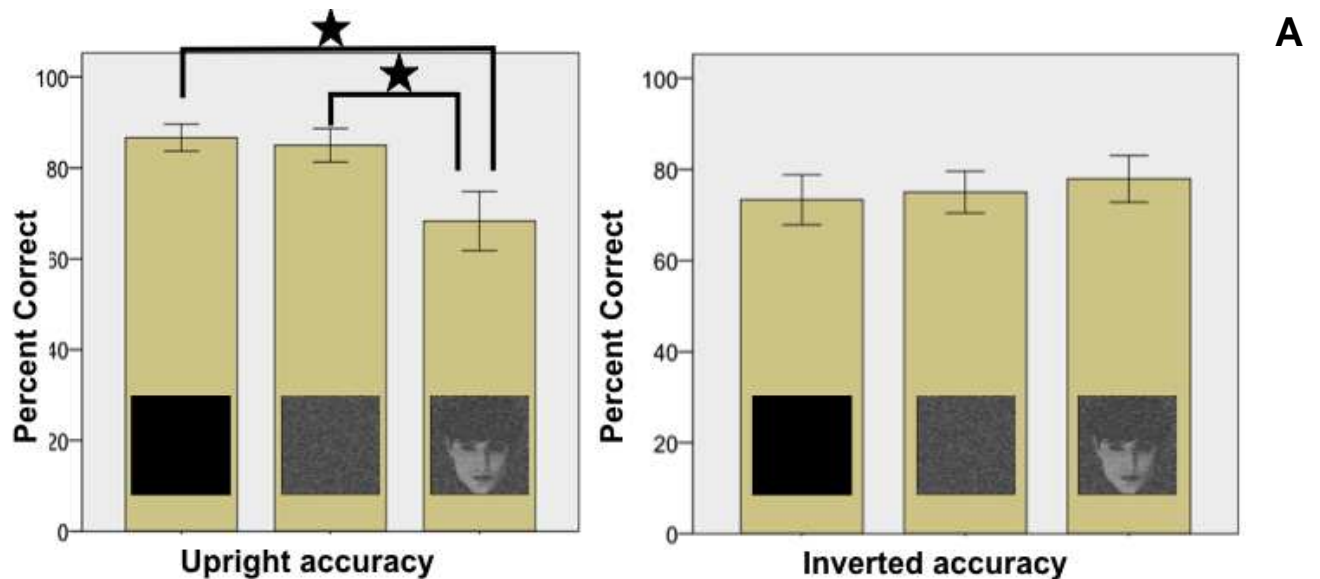


Figure 2.4 Graphs of d' plotted for the conditions in experiment 2. Pictures on the columns represent adaptation conditions. Glass patterns depicted here are shown on a black background for clarity. Error bars represent one standard error of the mean, corrected for repeated measures. Lines with a star indicate significant post-hoc comparisons ($p < 0.05$, uncorrected). From left to right, columns represent d' for: no adaptation, snow adaptation, upright face adaptation, random adaptation, concentric adaptation, translational adaptation, and radial adaptation.

Although no differences in discriminability were observed between face, snow, and no adaptation conditions, adaptation to faces significantly impaired upright face accuracy relative to snow and no adaptation (figure 2.5). The omnibus ANOVA found a significant interaction between adapting condition and target type ($F(3.02, 39.2) = 3.8, p < 0.005, \eta_p^2 = 0.352$). For adaptation to upright faces compared to no adaptor, post hoc tests showed a significant difference for upright (figure 2.5A, left; $t(7) = 2.86, p = 0.024$), but not inverted (figure 2.5A, right; $t(7) = 0.524, p = 0.616$) face accuracy. Post hoc tests comparing face adaptation to snow

adaptation showed significant effects for upright (figure 2.5A, left; $t(7) = 2.45$, $p = 0.044$), but not inverted (figure 2.5A, right; $t(7) = 0.224$, $p = 0.650$) face accuracy.

Post hoc tests for Glass patterns revealed that concentric Glass pattern adaptation significantly impaired inverted face accuracy compared to random (figure 2.5B, right; $t(7) = 2.89$, $p = 0.023$), translational (figure 2.5B, right; $t(7) = 4.65$, $p = 0.002$), and radial (figure 2.5B, right; $t(7) = 4.18$, $p = 0.004$) Glass pattern adaptation. For upright face accuracy, concentric Glass pattern adaptation was not significantly different from translational (figure 2.5B, left; $t(7) = 0.325$, $p = 0.754$) or random (figure 2.5B, left; $t(7) = 0.954$, $p = 0.274$) Glass pattern adaptation. For upright face accuracy, the post hoc test between concentric and radial Glass pattern adaptation revealed a trend (figure 2.5B, left; $t(7) = 2.32$, $p = 0.053$), such that adaptation to radial patterns may reduce upright face accuracy. However, this effect did not replicate in experiment 3.



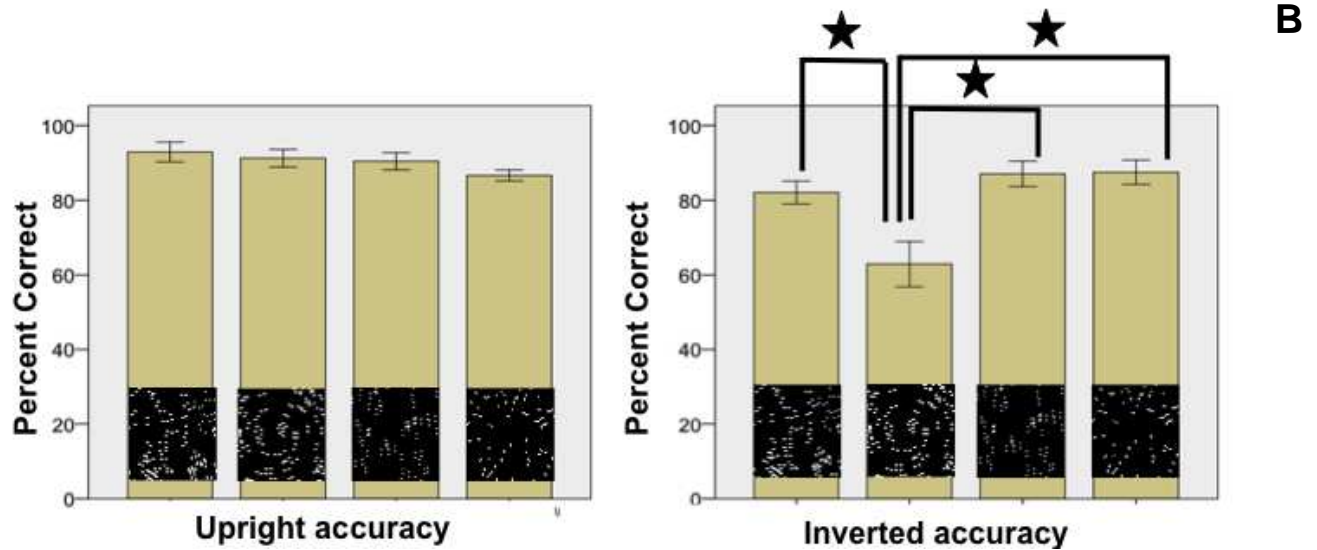


Figure 2.5 A graph of accuracy data for experiment 2. Pictures on the columns represent adaptation conditions. Glass patterns are shown as white dots on a black background for clarity (in the actual experiment the Glass patterns consisted of white dots on a mid-grey background). Error bars represent one standard error of the mean, corrected for repeated measures. Lines with a star indicate significant *post-hoc* tests ($P < 0.05$, uncorrected). (A) Face conditions. From left to right, columns represent upright face accuracy for no adaptation, snow adaptation, and upright face adaptation; inverted face accuracy for no adaptation, snow adaptation, and upright face adaptation. (B) Glass pattern conditions. From left to right, columns represent upright face accuracy for random adaptation, concentric adaptation, translational adaptation, and radial adaptation; inverted face accuracy for random adaptation, concentric adaptation, translational adaptation, and radial adaptation.

Discussion

Experiment 2 found that concentric Glass pattern adaptation reduced upright/inverted face discriminability relative to non-concentric Glass patterns. This suggests that concentric Glass pattern and face perception share a common processing mechanism. Interestingly,

accuracy measures show that concentric Glass pattern adaptation impaired inverted face accuracy, but not upright face accuracy. One possible explanation is that inverted faces are harder and take longer to process than upright faces [10]. Therefore, if the process-terminating mask had a shorter stimulus onset asynchrony, then upright face accuracy may be reduced. Alternatively, there may be differences in upright and inverted face processing, such that concentric Glass pattern and inverted, but not upright, face perception share a common processing mechanism.

Experiment 2 also found that adapting to upright faces impairs upright face perception. Intriguingly, upright face adaptation had no effect on inverted face perception. The lack of an effect on discriminability may reflect the specificity of the adaptation effect, or it may simply reflect a lack of statistical power. To our knowledge, this is the first demonstration of face adaptation impairing perception in an upright/inverted judgment. The specificity of the face adaptation effects may reflect differences in processing upright and inverted faces. As discussed in the introduction, Gilaie-Dotan et al examined tuning to faces in the fusiform face area using a fMRI visual adaptation paradigm. They found evidence suggesting that neurons in FFA are broadly tuned to inverted faces, but narrowly tuned to upright faces [11]. This difference in processing is supported by behavioral studies demonstrating differences in inverted and upright face perception [12-14] and could explain why adaptation to upright face impaired upright face accuracy only. If a difference exists between upright and inverted face processing, then inverted face adaptation should impair inverted, but not upright, face accuracy.

Experiment 3: Effects of upright and inverted face adaptation on upright/inverted face discrimination: 16 subject pilot

Introduction

Experiment 2 showed that adaptation to concentric Glass patterns impaired inverted face perception, and that upright face adaptation impaired upright face perception. However, it is unclear whether these results reflect differences in upright and inverted face processing, or if upright faces are simply easier to process than inverted faces. Experiment 3 attempted to replicate these effects in a larger number of subjects and to test whether concentric Glass pattern adaptation can impact upright face accuracy by using a process-terminating backwards mask with a shorter SOA.

Methods

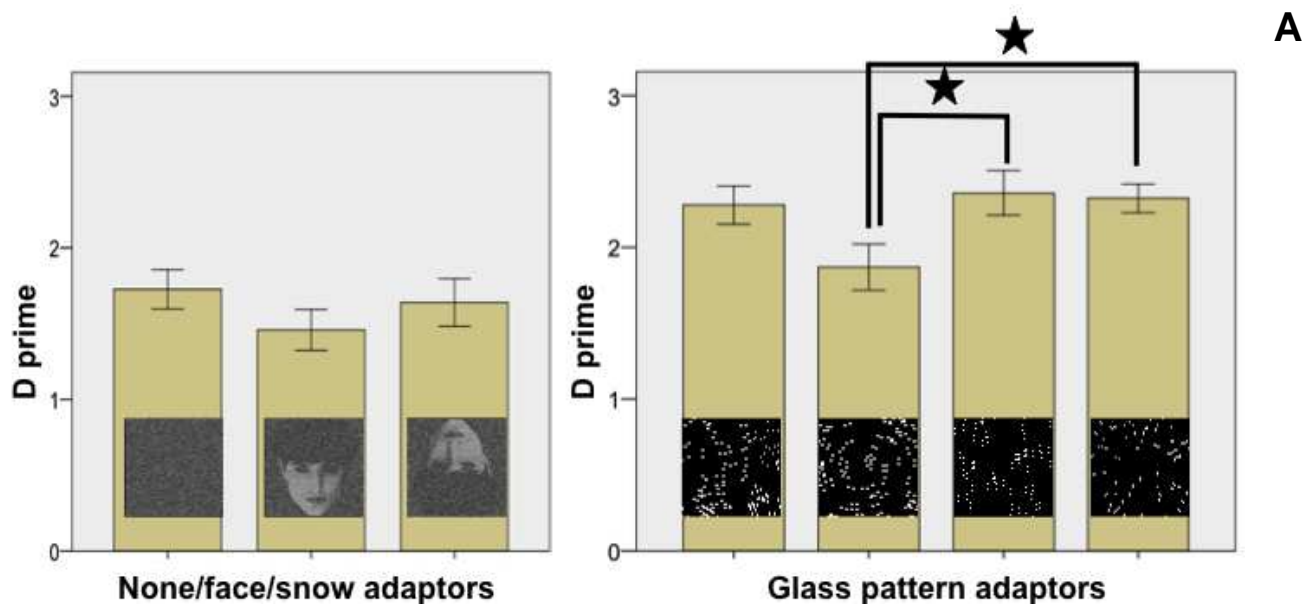
16 subjects participated in experiment 3. The design of the experiment was nearly identical to experiment 2. The no adaptation condition was replaced with an inverted face adaptation condition. For the mask, SOAs of 60ms and 80ms were used. Subjects performed the experiment in two visits, one visit using the 60ms SOA, and another using the 80ms SOA. The order of conditions and timing were counterbalanced to eliminate practice as a confound. Data for the 60 and 80ms SOAs were analyzed separately as described in experiment 2.

Results

Discriminability for the 80ms and 60ms SOA conditions are shown in figure 2.6. For the 80ms SOA, concentric Glass pattern adaptation reduced discriminability relative to other Glass patterns. Repeated measures ANOVA show a significant main effect of condition ($F(3.83, 57.5) = 8.78, p < 0.001, \eta_p^2 = 0.369$). Post-hoc comparisons show that concentric Glass

pattern adaptation reduced discriminability relative to translational ($t(15) = 2.36, p = 0.033$) and radial ($t(15) = 2.61, p = 0.020$) Glass patterns.

The 60ms SOA results (figure 2.6B) show that upright face adaptation, relative to snow, reduced discriminability, while the results for the Glass pattern conditions are convergent with the previous findings. Repeated measures ANOVA showed a significant main effect of condition ($F(6,90) = 9.17, p < 0.001, \eta_p^2 = 0.379$). Post-hoc comparisons show that upright face adaptation reduced discriminability relative to snow ($t(15) = 2.66, p = 0.018$). Concentric Glass pattern adaptation reduced discriminability relative to random ($t(15) = 2.36, p = 0.032$) and radial ($t(15) = 4.43, p < 0.001$) Glass patterns.



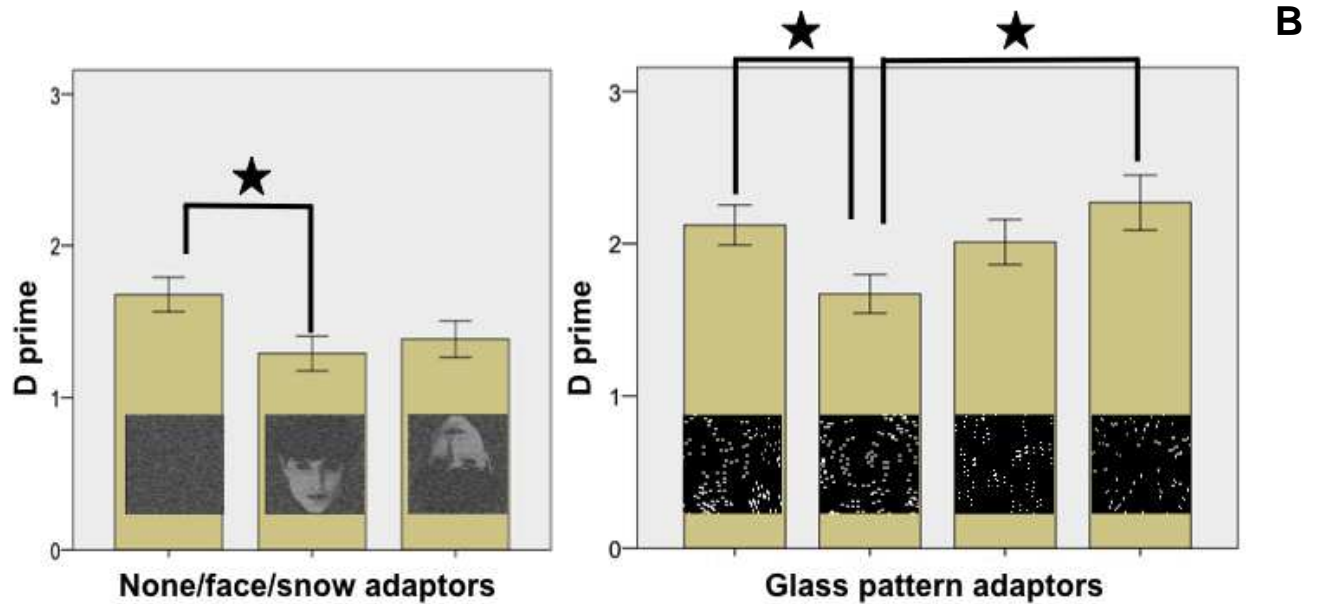
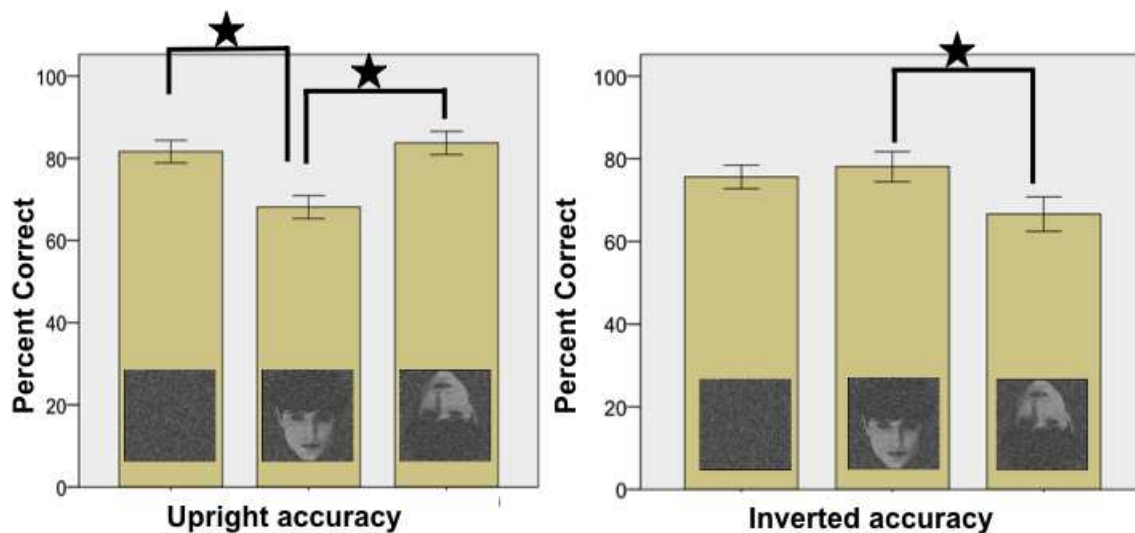


Figure 2.6 A graph of discriminability data for experiment 3. Pictures on the columns represent adaptation conditions. Error bars represent one standard error of the mean, corrected for repeated measures. Lines with a star indicate significant post-hoc comparisons ($p < 0.05$, uncorrected). From left to right, columns represent d' for: no adaptation, snow adaptation, upright face adaptation, random adaptation, concentric adaptation, translational adaptation, and radial adaptation. (A) 80ms SOA results. (B) 60ms SOA results

Accuracy data at the 80ms SOA (figure 2.7) show that upright face adaptation impairs upright face accuracy, inverted face adaptation impairs inverted face accuracy, and concentric Glass pattern adaptation impaired inverted face accuracy. The repeated measures ANOVA reveals a significant condition by target type interaction ($F(6, 90) = 4.420$, $p = 0.001$, $\eta_p^2 = 0.229$). Post-hoc comparisons for the face conditions revealed that upright face adaptation significantly impaired upright face accuracy compared to snow (figure 2.7A, left; $t(15) = 5.43$, $p < 0.001$) and inverted face (figure 2.7A, left; $t(15) = 2.21$, $p < 0.001$) adaptation. Inverted face adaptation significantly impaired inverted face accuracy compared to upright face adaptation

(figure 2.7A, right; $t(15) = 2.21$, $p = 0.043$), and a trend was observed such that inverted face adaptation impaired inverted face accuracy compared to snow adaptation (figure 2.7A, right; $t(15) = 2.04$, $p = 0.060$).

For Glass patterns, post-hoc comparisons showed that Concentric Glass pattern adaptation significantly impaired inverted face perception compared to radial (figure 2.7B, right; $t(15) = 2.33$, $p = 0.034$) and translational (figure 2.7B, right; $t(15) = 2.28$, $P = 0.038$) Glass patterns. A trend was observed for Concentric Glass pattern adaptation impairing inverted face perception compared to random Glass patterns (figure 2.7B, right; $t(15) = 1.95$, $p = 0.071$). No other trends were observed on face accuracy between different Glass pattern types (all p values > 0.132).



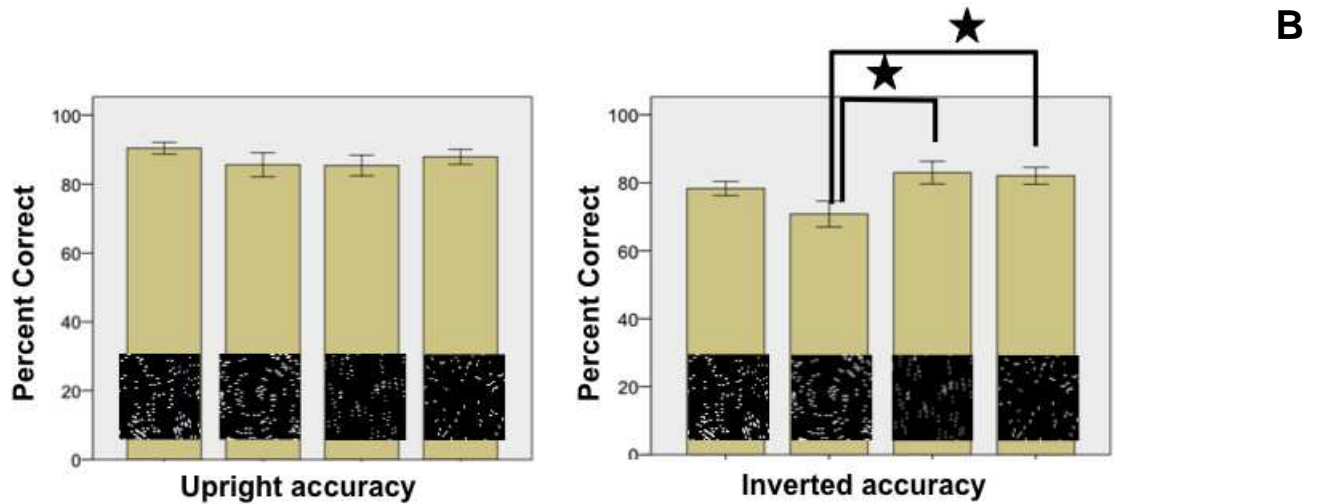
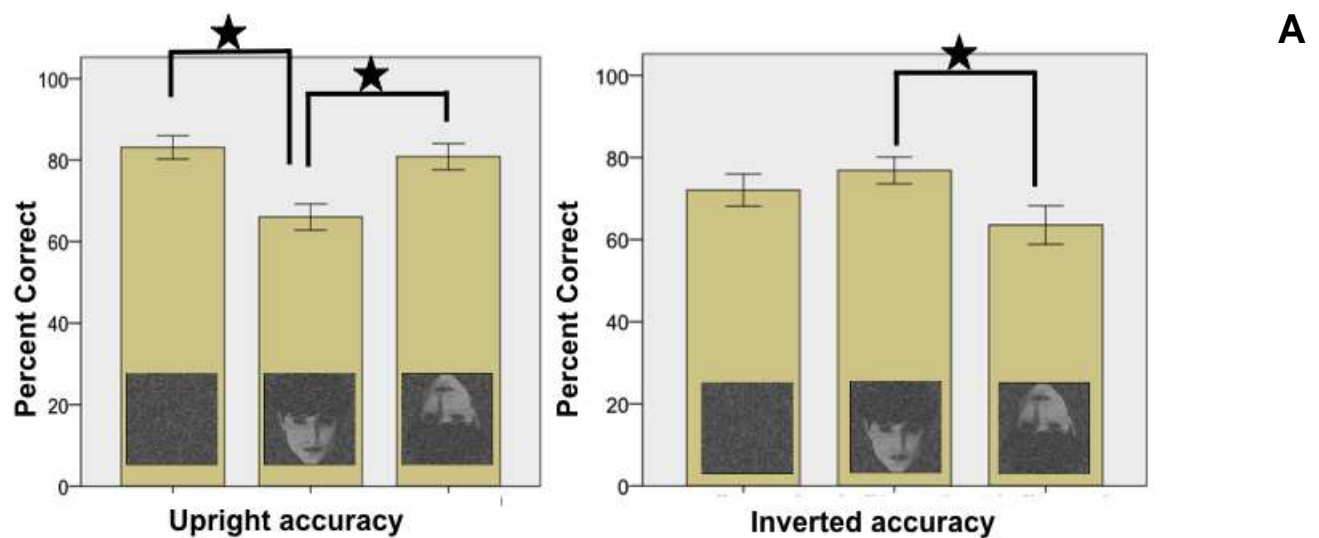


Figure 2.7 A graph of accuracy data from 80ms SOA conditions in experiment 3. Pictures on the columns represent adaptation conditions. Error bars represent one standard error of the mean, corrected for repeated measures. Lines with stars indicate significant *post-hoc* tests ($P < 0.05$, uncorrected). (A) Face conditions. From left to right, columns represent upright face accuracy for snow adaptation, upright face adaptation, and inverted face adaptation; inverted face accuracy for snow adaptation, upright face adaptation, and inverted face adaptation. (B) Glass pattern conditions. From left to right, columns represent upright face accuracy for random adaptation, concentric adaptation, translational adaptation, and radial adaptation; inverted face accuracy for random adaptation, concentric adaptation, translational adaptation, and radial adaptation.

Accuracy data at the 60ms SOA (figure 2.8) are mostly consistent with data from the 80ms SOA, but additionally show a trend, such that concentric Glass pattern adaptation may also impair upright face accuracy. For the omnibus repeated measures ANOVA (7x2), a significant interaction between adapting condition and target type was observed ($F(6, 90) = 3.78, p = 0.002, \eta_p^2 = 0.201$). Post-hoc tests for the face conditions revealed that upright face adaptation significantly impaired upright face accuracy compared to snow (figure 2.8A, left;

$t(15) = 6.05, p < 0.001$) and inverted face adaptation (figure 2.8A, left; $t(15) = 4.49, p < 0.001$). Inverted face adaptation impaired inverted face accuracy compared to upright face (figure 2.8A, right; $t(15) = 2.99, p = 0.009$) adaptation.

Post-hoc comparisons for Glass patterns revealed that concentric Glass pattern adaptation impaired inverted face perception compared to random (figure 2.8B, right; $t(15) = 2.23, p = 0.041$) and radial (figure 2.8B, right; $t(15) = 2.97, p = 0.010$), Glass pattern adaptation. A trend was observed for concentric Glass pattern adaptation impairing upright face accuracy compared to random Glass patterns (figure 2.8B, left; $t(15) = 2.06, p = 0.058$). No other significant differences in performance were found between the Glass patterns (other post-hoc comparisons: $p > 0.143$).



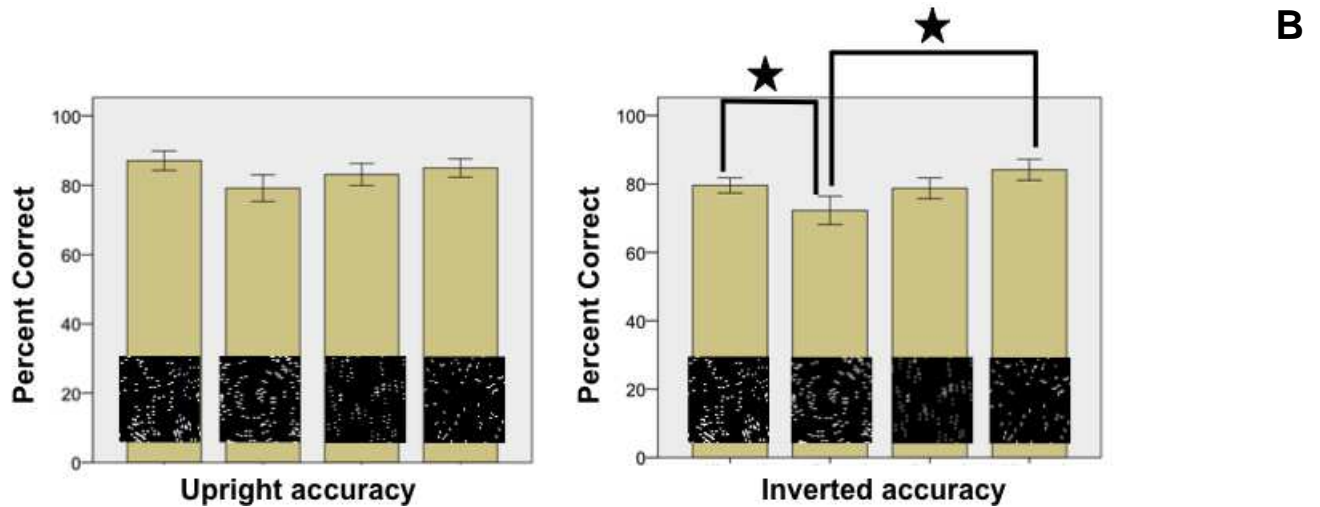


Figure 2.8 A graph of accuracy data from 60ms SOA conditions in experiment 3. Formatting is the same as in Figure 2.7

Discussion

Results from experiment 3 are consistent with the results from experiment 2. Face adaptation effects were replicated, and concentric Glass pattern adaptation reduced face discriminability. The results from the 60ms SOA experiment hint that shorter SOAs may be necessary for testing cross-adaptation between concentric Glass patterns and faces because at a 60ms (but not 80ms) SOA, concentric Glass pattern adaptation showed a trend for impairing upright face accuracy. This finding suggests that the processing mechanism affected by concentric Glass pattern adaptation is utilized for both upright and inverted face perception, and this processing mechanism operates more quickly on upright than on inverted faces. The idea that inverted and upright face perception share a common processing mechanism is supported in the literature. Although a number of studies have shown differences in inverted and upright face perception [12-14], others have shown that there are also similarities [15-19]. Participants showed the same performance for upright and inverted faces when asked to

discriminate between two faces, where the face features differ (e.g. figure 1.3) [15-19]. Visual search for upright and inverted faces produces similar search slopes [18, 19]. The relationship between reaction time and the number of items in the search array is flat for both upright and inverted face search, suggesting that some aspect of inverted and upright face processing may be the same. Therefore, our data here suggest that a common processing mechanism, involved in upright and inverted face perception, is also utilized in concentric Glass pattern perception.

Summary

Taken together, the three preliminary studies suggest that face and concentric Glass pattern perception share a common processing mechanism. Adaptation to concentric, but not translational Glass patterns impairs subsequent concentric Glass pattern adaptation. Adaptation to faces impairs subsequent upright/inverted face discriminations. Adaptation to concentric, but not non-concentric, Glass patterns impairs subsequent upright/inverted face discriminations.

The results from the pilots are consistent with previous findings in the literature. We observed stronger effects of concentric Glass pattern adaptation on inverted face accuracy than on upright face accuracy. The SOA manipulation in experiment 3 suggests the possibility that same mechanism utilized by upright and inverted face perception is affected by concentric Glass pattern perception, and that this mechanism operates more quickly for upright than inverted faces. This is consistent with the observations that people perceive upright faces more quickly than inverted faces [10], and that the processing of arrangements of features may be more important for upright than inverted face perception [12-14, 17, 20-32].

Experiments 1-3 set the stage for more precise follow-up studies. The follow-up experiments better control the luminance and contrast properties of the stimuli, and directly measure the timing of the paradigm. Manipulations of the onset of the target with respect to the offset of the adaptor can dissociate whether the effects observed in experiments 2 and 3 resulted from visual masking and not visual adaptation. The adaptation studies (experiments 4 and 5) presented in the following chapter controlled for all of these low level factors.

References

1. Clifford, C.W. and E. Weston, *Aftereffect of adaptation to Glass patterns*. Vision Res, 2005. **45**(11): p. 1355-63.
2. Ross, J. and J. Edwin Dickinson, *Effects of adaptation to Glass pattern structure and to path of optic flow*. Vision Res, 2007. **47**(16): p. 2150-5.
3. Vreven, D. and J. Berge, *Detecting structure in glass patterns: an interocular transfer study*. Perception, 2007. **36**(12): p. 1769-78.
4. Appelle, S., *Perception and discrimination as a function of stimulus orientation: the "oblique effect" in man and animals*. Psychological Bulletin, 1972. **78**(4): p. 266-78.
5. Jenkins, B., *Orientalional anisotropy in the human visual system*. Percept Psychophys, 1985. **37**(2): p. 125-34.
6. Green, D.M. and J.A. Swets, *Signal Detection Theory and Psychophysics*, 1966, New York: Wiley.
7. Aspell, J.E., J. Wattam-Bell, and O. Braddick, *Interaction of spatial and temporal integration in global form processing*. Vision Res, 2006. **46**(18): p. 2834-41.
8. Wilson, H.R. and F. Wilkinson, *Detection of global structure in Glass patterns: implications for form vision*. Vision Res, 1998. **38**(19): p. 2933-47.
9. Wig, G.S., et al., *Separable routes to human memory formation: dissociating task and material contributions in the prefrontal cortex*. J Cogn Neurosci, 2004. **16**(1): p. 139-48.
10. Yin, R.K., *Looking at upside-down faces*. Journal of Experimental Psychology, 1969. **81**(1): p. 141-145.
11. Gilaie-Dotan, S., H. Gelbard-Sagiv, and R. Malach, *Perceptual shape sensitivity to upright and inverted faces is reflected in neuronal adaptation*. Neuroimage, 2010. **50**(2): p. 383-95.
12. Thompson, P., *Margaret Thatcher: a new illusion*. Perception, 1980. **9**(4): p. 483-4.
13. Rhodes, G., S. Brake, and A.P. Atkinson, *What's lost in inverted faces?* Cognition, 1993. **47**(1): p. 25-57.
14. Tanaka, J.W. and M.J. Farah, *Parts and wholes in face recognition*. Q J Exp Psychol A, 1993. **46**(2): p. 225-45.

15. Leder, H. and V. Bruce, *When inverted faces are recognized: the role of configural information in face recognition*. Q J Exp Psychol A, 2000. **53**(2): p. 513-36.
16. Freire, A., K. Lee, and L.A. Symons, *The face-inversion effect as a deficit in the encoding of configural information: direct evidence*. Perception, 2000. **29**(2): p. 159-70.
17. Mondloch, C.J., R. Le Grand, and D. Maurer, *Configural face processing develops more slowly than featural face processing*. Perception, 2002. **31**(5): p. 553-66.
18. Hershler, O. and S. Hochstein, *At first sight: a high-level pop out effect for faces*. Vision Res, 2005. **45**(13): p. 1707-24.
19. Lewis, M. and A. Edmonds, *Searching for faces in scrambled scenes*. Visual Cognition, 2005. **12**(7): p. 1309-1336.
20. Diamond, R. and S. Carey, *Why faces are and are not special: an effect of expertise*. J Exp Psychol Gen, 1986. **115**(2): p. 107-17.
21. Young, A.W., D. Hellawell, and D.C. Hay, *Configurational information in face perception*. Perception, 1987. **16**(6): p. 747-59.
22. Lewis, M.B. and R.A. Johnston, *The Thatcher illusion as a test of configural disruption*. Perception, 1997. **26**(2): p. 225-7.
23. Gauthier, I. and M.J. Tarr, *Becoming a "Greeble" expert: exploring mechanisms for face recognition*. Vision Res, 1997. **37**(12): p. 1673-82.
24. Gauthier, I. and C.A. Nelson, *The development of face expertise*. Curr Opin Neurobiol, 2001. **11**(2): p. 219-24.
25. Maurer, D., R.L. Grand, and C.J. Mondloch, *The many faces of configural processing*. Trends Cogn Sci, 2002. **6**(6): p. 255-260.
26. Joseph, R.M. and J. Tanaka, *Holistic and part-based face recognition in children with autism*. J Child Psychol Psychiatry, 2003. **44**(4): p. 529-42.
27. Rouse, H., et al., *Do children with autism perceive second-order relational features? The case of the Thatcher illusion*. J Child Psychol Psychiatry, 2004. **45**(7): p. 1246-57.
28. Loffler, G., et al., *Configural masking of faces: evidence for high-level interactions in face perception*. Vision Res, 2005. **45**(17): p. 2287-97.
29. Boutsen, L., et al., *Comparing neural correlates of configural processing in faces and objects: an ERP study of the Thatcher illusion*. Neuroimage, 2006. **32**(1): p. 352-67.
30. Gilaie-Dotan, S. and R. Malach, *Sub-exemplar shape tuning in human face-related areas*. Cereb Cortex, 2007. **17**(2): p. 325-38.
31. Benton, C.P. and E.C. Burgess, *The direction of measured face aftereffects*. J Vis, 2008. **8**(15): p. 1 1-6.
32. Mondloch, C.J. and D. Maurer, *The effect of face orientation on holistic processing*. Perception, 2008. **37**(8): p. 1175-86.

Chapter 3: Concentric Glass pattern masking, but not adaptation, impairs upright/inverted face discrimination

Introduction

While pilot experiments 1-3 (see: Chapter 2) suggested that adaptation to concentric Glass patterns may reduce accuracy during upright/inverted face discrimination, I sought to extend our findings by using better controlled stimuli in more formal visual adaptation and masking experiments. As discussed in Chapter 1, Visual adaptation occurs when one views a stimulus, an adaptor, for a long period of time [1-3]. The viewing alters subsequent processing to create an aftereffect: a subsequently presented stimulus, the target, is perceived differently. Visual masking occurs when a stimulus, the mask, is presented either before or after the appearance of a target. The presentation of the mask limits or enhances the perception of the target by interfering with the processing of the target. Operationally, visual masking and visual adaptation can be dissociated behaviorally by examining the duration of the effects. Effects of visual masking typically last less than 150 milliseconds [4-6], while effects of visual adaptation can last more than 500 milliseconds [1]. If adaptation to concentric Glass patterns impairs face perception and vice versa, or if concentric Glass pattern masking impairs subsequent face perception, then we will have evidence that face and concentric Glass pattern perception utilize a common processor.

General Methods

Participants

18-30 year-old, right-handed participants were recruited from the local community (see: “acknowledgements”), financially compensated for their time, and consented according to procedures approved by the Washington University Human Research Protection Office. Participants had no first-degree relatives with an autism spectrum disorder or attention deficit hyperactivity disorder. Participants were screened out for any neurological deficit, strabismus, or vision not correcting to normal acuity with glasses.

Experimental procedures

Experimental setup

Participants were seated in a darkened room, 53.4 centimeters away from the center of the monitor. Participants were provided with a chin rest and head strap to minimize head movements (Headspot, Tall Option: University of Houston College of Optometry), and the monitor height was modified using an adjustable stand to ensure that each participant’s eyes were level with the center of the monitor. Participants responded to stimuli that appeared on the screen using a CMU button box (New Micros, Inc.; Dallas, TX; 1ms timing resolution).

All stimuli were presented on a 17” CRT monitor (Dell model E771A, 15.5” viewable). The monitor was controlled by a MacBook Pro laptop (Apple Computer, Inc.), and the monitor resolution was set to 1024x768 at 75 Hz. All experiments were written in MATLAB (The Mathworks, Inc. Natick, MA), using the Psychophysics Toolbox

extensions [7]. The timing of the stimulus presentation was tested using a photodiode connected to a separate Macintosh computer running PowerLab (ADInstruments, <http://www.adinstruments.com>). The luminance of the monitor and all stimuli were measured using a LS-100 photometer (Konica Minolta, <http://sensing.konicaminolta.us/>). Every possible luminance value for the display setup was measured to create a gamma lookup table to linearize luminance values. The luminance of the monitor could vary from 0 to 69 cd/m². For all experiments, the display background was set to a mean of 22 cd/m².

Stimulus design

Glass patterns

Glass patterns were also created with code written in MATLAB, using the Psychophysics Toolbox extensions. Glass patterns were constructed by randomly placing square dots, each with a length of 1.8 minutes of arc, within the extent of an imaginary ellipse. For each randomly placed dot, a second paired dot was displaced 7.3 minutes of arc from the first dot. Dot density was 33 percent for every pattern. The geometric rule governing the displacement of dots determined the global form of the Glass pattern [8]. A rotational rule defined concentric forms (figure 3.1A), a vertical displacement rule defined the translational forms (figure 3.1B), and an expansion rule defined the radial forms (figure 3.1C). For random Glass patterns (figure 3.1D) the direction of the displacement was randomly determined for each dipole while the dipole separation distance was kept constant. For our studies, we used vertical translational patterns because our piloting (data not shown) and other studies have shown that they are more salient than horizontal translational patterns [9, 10]. The dots were white dots

on a mid-gray background, and the extent of the pattern measured 12 visual degrees in length and 8 visual degrees in width.

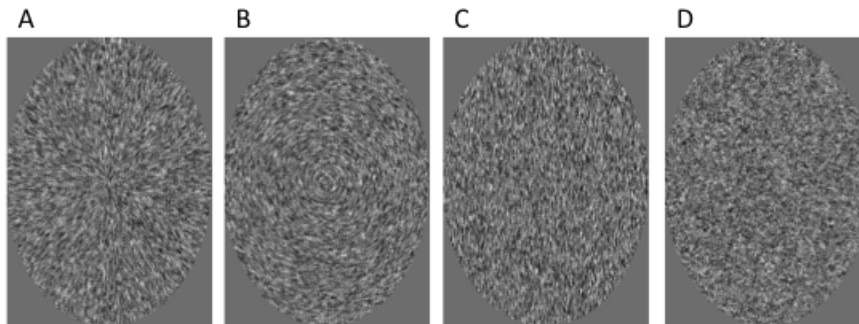


Figure 3.1. Radial (A), concentric (B), translational (C) and random (D) Glass patterns used in this study are depicted. The glass patterns shown contain both white and black dots to increase pattern visibility.

Faces

The face stimuli for experiments 4-7 came from three sets: NimStim [11], Karolinska Institute [12], and William Kelley's lab [13]. For this study, the faces were cropped to 12 visual degrees in length and 8 visual degrees in width to remove extraneous features, such as hair. Faces with eyewear or other discerning features (e.g. facial hair, moles, emotional expressions) were excluded from the final set. All faces were chosen such that the eyes for each face were located 2.5 visual degrees vertically from the center of the face. The contrast of the face was measured by calculating the root mean square of the luminance for each face (standard deviation of luminance divided by the mean luminance of all pixels in the face) [14]. All faces were scaled to equate the mean luminance for each face to 22 cd/m^2 , and normalized to equate the root mean square for all faces to 1.

Flowers

The flowers (figure 3.2A) used in experiment 4 came from the Microsoft Photo Gallery (<http://dgl.microsoft.com>). The pictures were converted to gray scale and cropped so that the dimensions of each picture matched the face stimuli (12 visual degrees in length, 8 visual degrees in height). The mean luminance and contrast of each picture was equated using the same procedure as with the face stimuli.

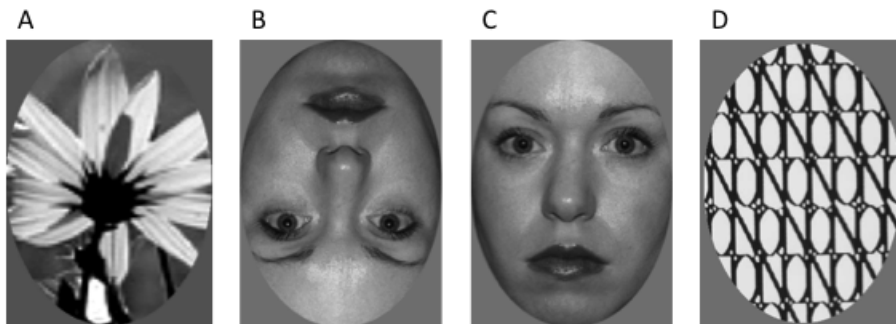


Figure 3.2. Examples of flower (A), inverted face (B), and upright face (C) adaptors used in experiment 4 are shown here. The N-O mask (D) was used as a process-terminating backward mask in experiment 5.

Staircasing procedure

To equate task difficulty across all participants, the visual salience of the targets within an experiment was determined via a staircasing procedure. Prior to each experiment, each participant performed a two interval, two alternative forced choice discrimination task, where subjects were presented with two stimuli and indicated whether the first or the second stimulus matched the pre-determined target. For example, a trial might begin with a face appearing for a short duration followed by a second face. One of these faces was upside-down and the other upright, and the participant must then indicate whether the first or second face was upright. If the participant correctly responded for four consecutive trials, the visual salience of the

target was reduced by 14 percent. If the participant made an incorrect response on a trial, the visual salience of the target was increased by 50 percent. The staircasing procedure continued until the subject showed 10 reversals, where the salience of the target either increased after being reduced or vice versa. The mean measured salience for the reversals determined the saliency of the targets in the experiment itself. This procedure has been shown to approximate 75 percent accuracy ($\sim 1.5 d'$ units) for a two alternative forced choice discrimination task [15].

Analysis

All experiments performed were one interval, two alternative forced-choice tasks, where participants indicated whether a given target belonged to one of two groups of targets: group A or group B. Measures of accuracy were derived for each target separately (see: Supplementary Materials). Discriminability was measured by d' , which is derived from signal detection theory [16]. This measure can be calculated with the following equation: $d' = Z(\text{group A targets called A/group A targets}) - Z(\text{group B targets called A/group B targets})$, where $Z(p)$ is the inverse of the cumulative Gaussian distribution. Bias is measured using beta. $\text{Beta} = Y(\text{group A targets called A/group A targets})/Y(\text{group B targets called group A/group B targets})$, where $Y(p)$ is the probability density function of the normal distribution. No adjustments were made to d' to account for differences in beta, because d' is thought to be independent of bias. In experiment 4, pattern trials were labeled as group A, and noise trials were labeled as group B. In experiment 5, upright faces were labeled as group A, and inverted faces were labeled as group B.

Experiment 4: face adaptation

Methods

30 adults (19 male/11 female; aged 25 +/- 2.7 years) participated in this experiment. A schematic of the experiment is shown in figure 3.3. Each run comprised 30 trials; 15 trials had random Glass pattern targets, termed noise, and the other 15 had pattern targets. The first trial began with an initial adaptation period of 20 seconds [17]. During the adaptation period, a different stimulus of the same category was presented 1 second for every second. After the adaptation period, a target would appear for 500 milliseconds. After hearing a tone, the participant would then respond whether the target was a pattern or noise. Every subsequent trial began with a similar 5-second adaptation period followed by the presentation of a target for 500 milliseconds. There were 12 runs, and the type of adaptor and type of target varied from run to run. The order of the runs was pseudo-randomly counterbalanced for the participants. Adaptors were random Glass patterns, flowers (figure 3.2A), upright faces (figure 3.2B), and inverted faces (figure 3.2C). Targets were concentric, radial, or translational Glass patterns. Target coherence, measured as the proportion of dipoles following the geometric rule, was determined for each subject per target type via the staircasing procedure.

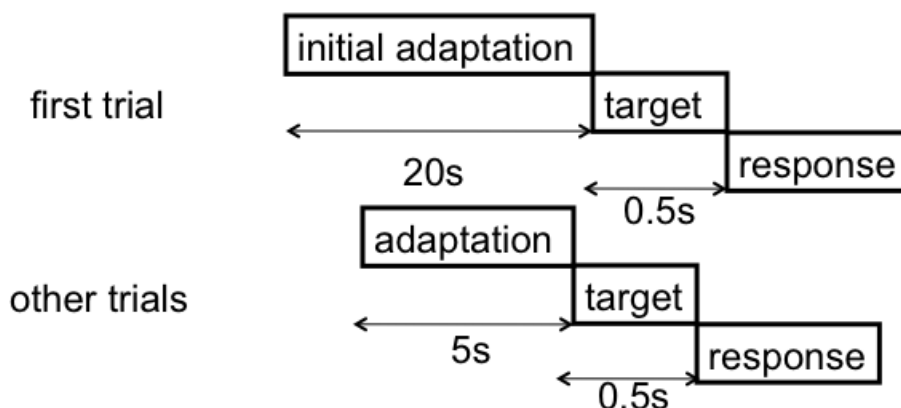


Figure 3.3. Schematic of experiment 4 paradigm. An explanation of the schematic is provided in the text.

Accuracy, d' , and beta were measured for each participant. Target by adaptor by target type (2x4x3) repeated measures ANOVA was used to test for significant adaptor-target interactions for accuracy. Adaptor by target type (4x3) repeated measures ANOVAs were used to test for significant adaptor-target interactions for d' and beta. Significant effects were examined *post-hoc* using paired t-tests. *Post-hoc* statistics are reported as uncorrected values.

Results: Adaptation to faces does not impair concentric Glass pattern discrimination

Measures of d' show that adaptation to flowers impaired radial Glass pattern discrimination, but face adaptation did not impair concentric Glass pattern discrimination (figure 3.4). An adaptor by pattern (4x3) repeated measures ANOVA revealed a significant adaptor by pattern interaction ($F(4.32, 125) = 5.786$, $p < 0.001$, $\eta_p^2 = 0.166$). A flower-specific effect of adaptation was observed for discriminating radial Glass patterns such that flower adaptors reduced d' relative to random ($t(29) = 4.4$, $p < 0.001$), inverted face ($t(29) = 3.7$, $p < 0.001$), and upright face ($t(29) = 4.6$, $p < 0.001$) adaptors. This flower-specific adaptation demonstrates that the timing parameters for the paradigm produced behavioral effects of visual adaptation and that we could generate object-to-Glass pattern cross-adaptation. A non-specific effect of adaptation was observed for discriminating translational Glass patterns such that discriminability was reduced for flower ($t(29) = 5.5$, $p < 0.001$), inverted face ($t(29) = 5.1$, $p < 0.001$), and upright face

($t(29) = 5.3, p < 0.001$) adaptors relative to random pattern adaptors. No face-specific effects of adaptation were observed on discriminability of concentric Glass patterns ($p > 0.42$).

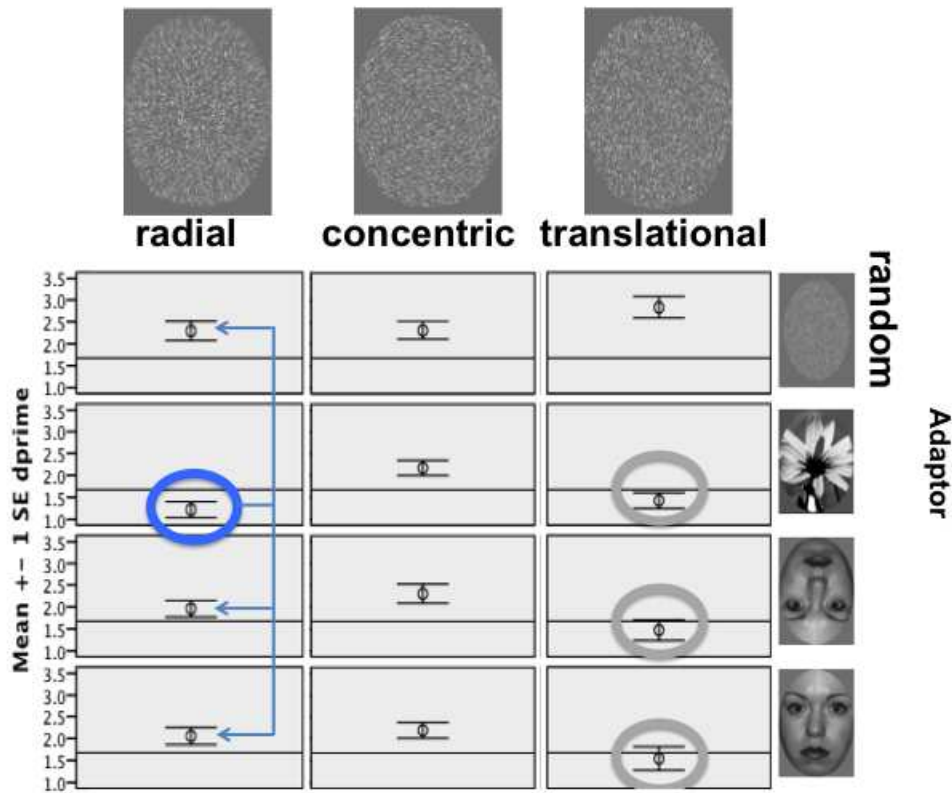


Figure 3.4. Discriminability is plotted for the 12 runs performed during experiment 4. Each column represents runs where the pattern targets were of a particular type (radial, concentric, or translational). Each row represents the type of adaptor stimulus used in each block. Flower adaptation impaired radial Glass pattern discrimination (blue circle) relative to face and random adaptation (blue lines). Flower and face adaptation impaired translational Glass pattern discrimination relative to random adaptation (grey circles). The targets shown in the figure are enlarged to make the global forms visible; the actual size of the targets is described in the General Methods section.

Face and flower adaptation affected bias for concentric Glass pattern discriminations, but no other effects were found. Measures of beta are shown in figure 3.5. An adaptor by pattern (4x3) repeated measures ANOVA revealed a significant adaptor by pattern interaction ($F(3.53, 174) = 3.1, p = 0.023, \eta_p^2 = 0.097$). *Post-hoc* pairwise comparisons show that for runs with concentric and noise targets, participants indicated that the target was noise more than concentric during random pattern adaptation relative to flower ($t(29) = 2.9, p = 0.006$), inverted face ($t(29) = 2.5, p = 0.02$), and upright face ($t(29) = 2.9, p = 0.007$) adaptors. No other effects of bias were found ($p > 0.1$).

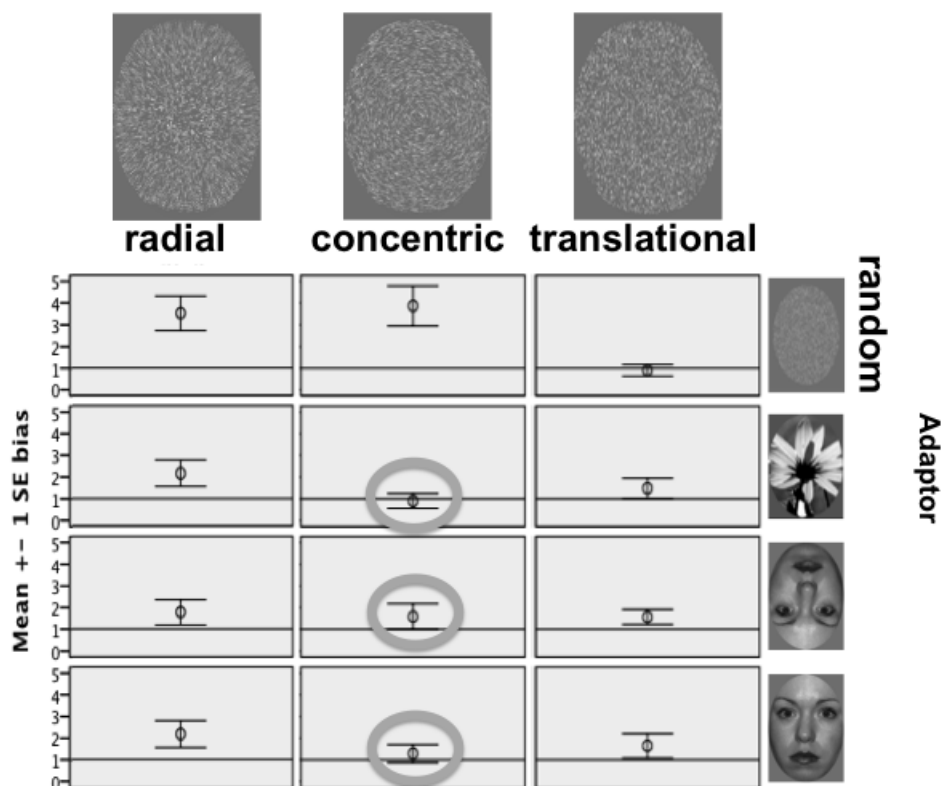


Figure 3.5. Beta estimates for experiment 4 are plotted for the 12 runs in experiment 4. The organization of the figure is the same as in the Figure 3.4.

Accuracy for pattern trials is shown in figure 3.6, and accuracy for noise trials is shown in figure 3.7. An adaptor by pattern by target (4x3x2) repeated measures ANOVA revealed a significant adaptor by pattern by target interaction ($F(6,174) = 4.403, p < 0.001, \eta_p^2 = 0.132$). Regardless of pattern type, face and flower adaptors reduced accuracy for noise trials relative to the random adaptor (All $t(29)$ values > 2.2 , all p values < 0.035). For concentric targets, accuracy increased for face (upright: $t(29) = 3.8, p = 0.001$; inverted: $t(29) = 2.6, p = 0.014$) and flower ($t(29) = -5.1, p < 0.001$) adaptors relative to the random adaptor. For radial targets, flower adaptors reduced accuracy relative to upright ($t(29) = 3.9, p = 0.001$) and inverted ($t(29) = 3.1, p = 0.004$) face adaptors. For translational targets, face (upright: $t(29) = 3.2, p = 0.003$; inverted: $t(29) = 2.7, p = 0.013$) and flower ($t(29) = 3.5, p = 0.001$) adaptors reduced accuracy relative to the random adaptor.

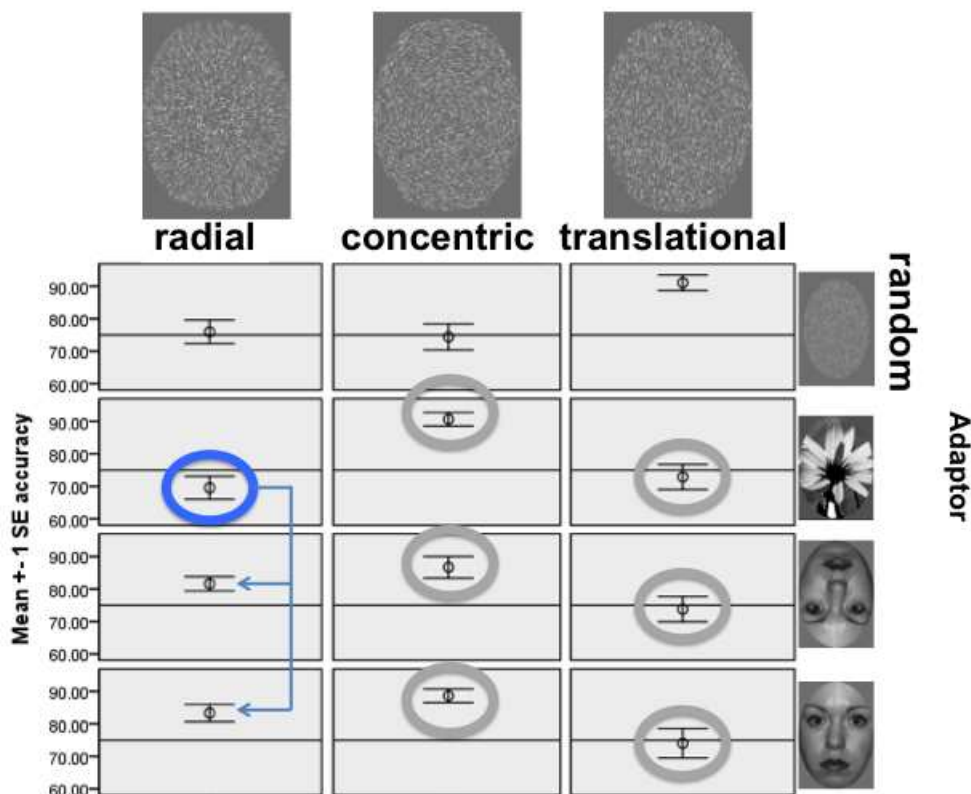


Figure 3.6. Accuracy for pattern trials from experiment 4 are plotted for the 12 runs. The organization of the figure is the same as in figure 3.4. Flower adaptation impaired radial Glass pattern accuracy (blue circle) relative to inverted and upright face adaptation (blue lines). Random adaptation impaired concentric Glass pattern accuracy relative to flower and face adaptation (middle column; grey circles). Flower and face adaptation impaired translational Glass pattern accuracy relative to random adaptation (right column: grey circles).

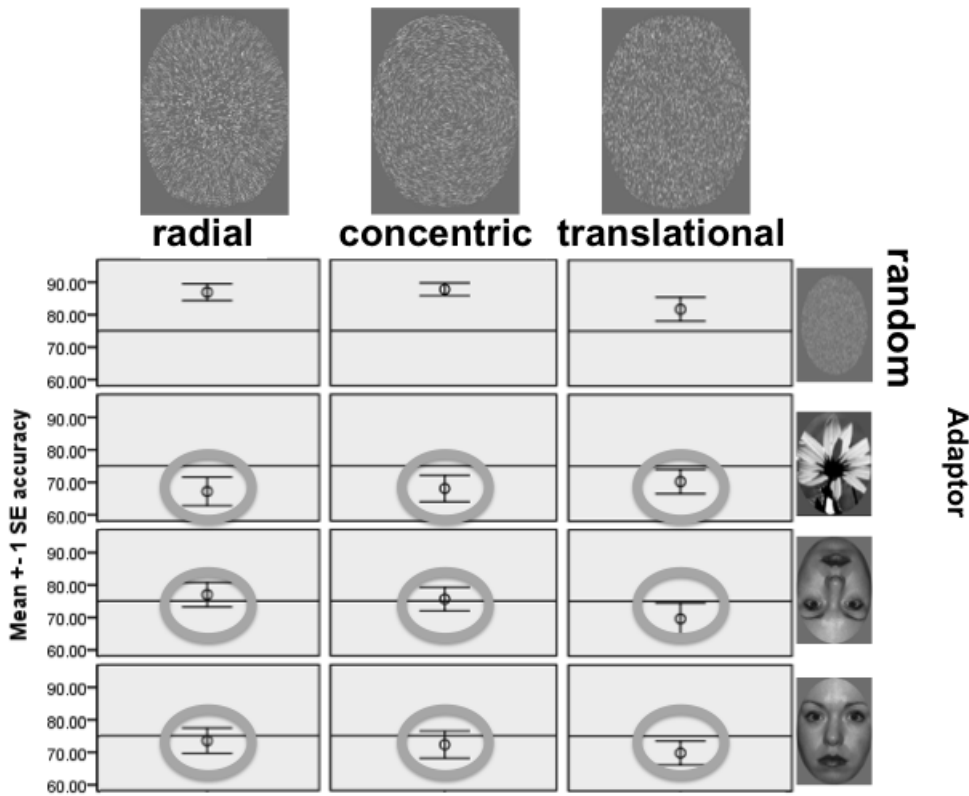


Figure 3.7. Accuracy for noise trials from experiment 4 are plotted for the 12 runs. The figure organization is the same as in figure 3.6.

Discussion

The data presented here show that adaptation to faces does not affect concentric Glass pattern discrimination. The flower-specific adaptation effects on radial Glass

pattern discrimination suggests that the paradigm employed can reveal visual adaptation effects of photographic pictures on dot patterns. Therefore, the lack of face-specific adaptation effects on concentric Glass pattern perception does not simply reflect a problem with the experimental approach or design implementation. It is possible that adaptation effects are unidirectional [18]. Therefore, experiment 5 tested whether adaptation to concentric Glass patterns impairs face discrimination.

Experiment 5: Glass pattern adaptation

Introduction

Results from Experiments 2 and 3 (see: Chapter 2), where the methods used were modified from published papers studying Glass pattern adaptation [17, 18], suggested that adaptation to concentric Glass patterns might impair upright/inverted face discrimination. However, experiments 2 and 3 also raised the possibility that the findings may be explained as visual masking effects. As described in the introduction section, effects of visual adaptation last longer than visual masking. In experiments 2 and 3, the target appeared immediately after the adaptation period, so the observed effects of adaptation could possibly be a form of visual masking. The conditions in the following experiment manipulated the onset of the target relative to the adaptation period to test whether adaptation (i.e. long duration between onset of target relative to adaptor) or masking (short duration between onset of target relative to adaptor) with concentric Glass patterns impaired subsequent upright/inverted face discrimination.

Methods

5 adults (2 male/3 female) participated in this experiment. A schematic of the experiment is shown in figure 3.8. Each run comprised 150 trials; the target for 75 trials was an upright face, and the target for the other 75 was an inverted face. Similar to experiment 4, the first trial began with a 20 second adaptation period, while the other trials began with a 5 second adaptation period. A target face was presented after the adaptation period for 13 milliseconds. At 27, 40, 67, 80, or 107 milliseconds after the onset of the target, a process terminating backward mask was presented for 300 milliseconds. The participant would then indicate whether the target face was upright or inverted. Five conditions were tested to determine whether adaptation to or masking with concentric Glass patterns impaired discrimination between upright and inverted faces (Table 3.1). The adaptors were either concentric Glass patterns or none. The backward mask was either an N-O mask that was constructed similar to the N-O mask used in previous studies [19] (figure 3.2D) or a noise mask used in experiments 2 and 3. The onset of the target face occurred either immediately (gap absent) or 500 milliseconds (gap present) after the adaptation period.

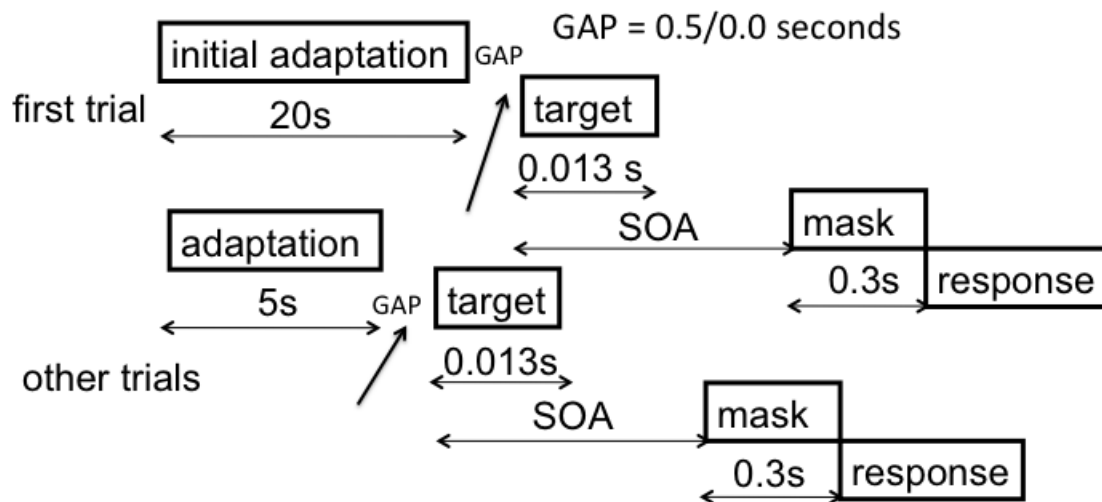


Figure 3.8. Schematic for the paradigm used in experiment 5. Explanation of the schematic is provided in the text.

condition	adaptor	gap?	backwards mask
1	none	n/a	N-O
2	concentric	absent	N-O
3	concentric	absent	N-O
4	concentric	present	N-O
5	concentric	present	noise

Table 3.1. Conditions in experiment 5 are shown here. (1) No adaptor control condition. (3) The adaptor and face stimuli used in this condition were the same as in experiments 2 and 3. (2,4,5) Adaptor and face stimuli used in these conditions were the same as in experiment 4.

Conditions one, two, four, and five utilized the stimuli depicted in the general methods section (see: stimulus design). Briefly, Glass patterns were white dots on a gray background. The faces were derived from three face sets, and were all mean luminance and contrast equated. Target faces were degraded by swapping a percentage of face pixels with pixels from a white noise stimulus. The white noise stimulus was a 12 by 8 visual degree ellipse where the intensity of each pixel within the ellipse was randomly selected from a Gaussian distribution of intensity values. The central tendency of this distribution corresponded to a luminance of 22 cd/m², and the range of intensity values was selected to match the contrast of the face. Examples of degraded faces are shown in figure 3.9. Target degradation was determined for each

subject by the staircasing procedure. For each trial in the staircasing procedure, a random Glass pattern was presented 67 milliseconds after every target as a backward process-terminating mask.

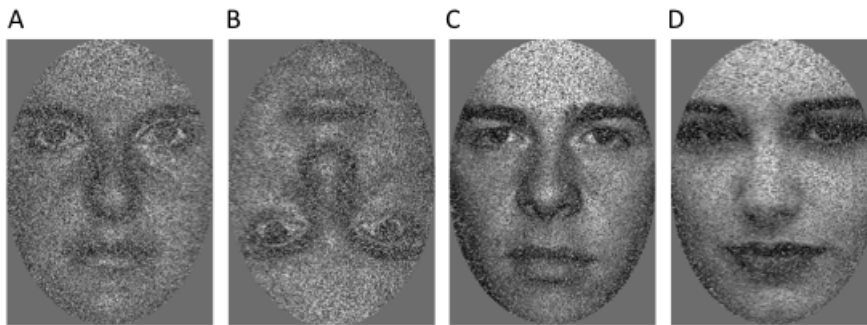


Figure 3.9. Examples of degraded faces are shown here. For experiments 5 and 6 (see: chapter 4), the median percentage of face pixels swapped for upright (A) and inverted (B) faces was 77 percent. For experiment 7 (see: chapter 4), the median percentage of face pixels swapped for male (C) and female (D) faces was 50 percent.

The third condition in this study used stimuli presented in experiments 2 and 3. Briefly, faces were either upright or inverted faces embedded in snow. The snow consisted of white noise pixels with a Gaussian distribution centered on the pixel intensity of a mid-gray background. The faces were embedded in snow to increase the difficulty of the task, as subjects were at ceiling when the faces were not embedded in snow. The snow was also used as the noise mask in condition 5. Glass patterns were constructed using MATLAB and the psychophysics toolbox. Patterns were presented as white dots on a mid-gray background. Dots measured 0.04 visual degrees (one pixel). Dipole separation was 0.12 visual degrees. Dot density was 25 percent. The stimulus

extent was square to match the stimulus extent of the faces. The mean pixel intensity of the glass patterns was approximated to the mean pixel intensity of the faces.

Accuracy, d' , and beta were determined for each participant. For accuracy, a target by stimulus onset asynchrony (SOA) by condition (2x5x5) repeated measures ANOVA was used to examine SOA-condition interactions. For d' and beta, SOA by condition (5x5) repeated measures ANOVAs were used to test for significant interactions. Significant effects of condition for specific SOAs were subsequently tested using paired t-tests. *Post-hoc* statistics are reported as uncorrected values.

Results: Concentric Glass pattern masking, but not adaptation, impairs upright/inverted face discrimination

The conditions tested show differences in discriminability but not bias. Measures of bias are depicted in figure 3.10 (top). A condition by SOA (5x5) repeated measures ANOVA shows no significant condition by SOA interaction ($F(16,64) = 0.39$, $p = 0.98$, $\eta_p^2 = 0.089$). Measures of d' are depicted in figure 3.10 (bottom). A condition by SOA (5x5) repeated measures ANOVA shows a significant condition by SOA interaction ($F(16,64) = 2$, $p = 0.023$, $\eta_p^2 = 0.338$). Because there was no effects of bias, post-hoc comparisons of performance were made on d' only.

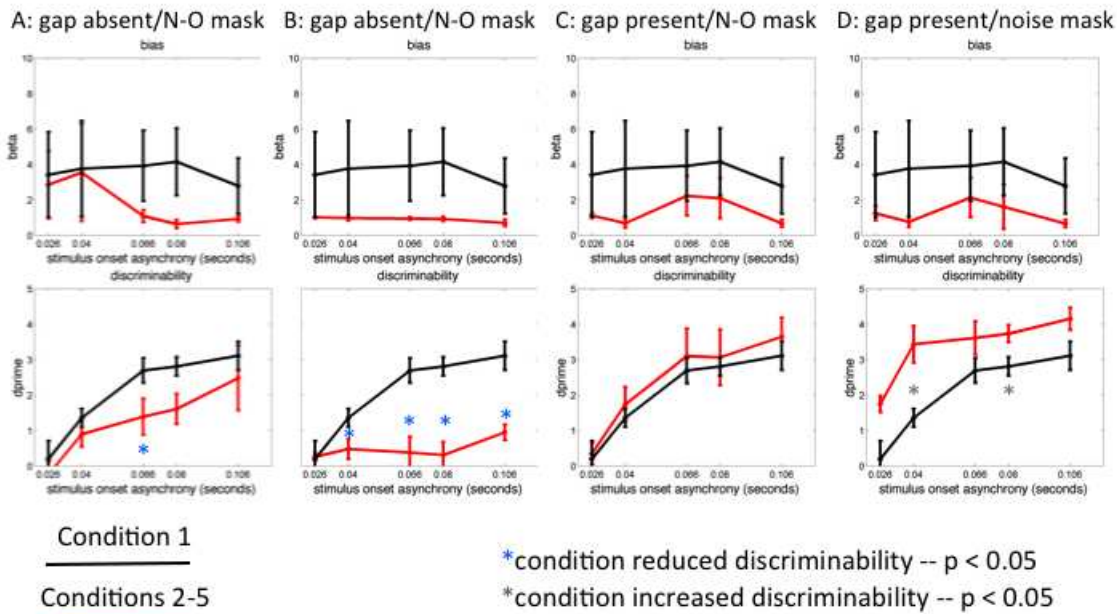


Figure 3.10 Measures of bias (top) and discriminability (bottom) for the conditions in experiment 5. The control condition (black) is compared with the non-control conditions (red): (A) condition 2, (B) condition 3, (C) condition 4, (D) condition 5.

Post-hoc comparisons show that discriminability was reduced in conditions when the gap was absent and not when the gap was present. Conditions in which the gap between adaptation and target presentation was absent (i.e. conditions 2 and 3) reduced d' at the 70 millisecond (condition 2: $t(4) = 3.5$, $p = 0.024$; condition 5: $t(4) = 6.8$, $p = 0.002$) SOA relative to the no adaptation condition. A trend was observed, such that condition 2 reduced discriminability relative to the no adaptation condition at the 40 millisecond SOA ($t(4) = 2.7$, $p = 0.054$), while condition 3 reduced discriminability relative to the no adaptation condition at the 40 ($t(4) = 2.9$, $p = 0.044$), 80 ($t(4) = 4.7$, $p =$

0.009), and 107 millisecond ($t(4) = 7.0, p = 0.002$) SOAs. Conditions where the gap was present produced no reduction in discriminability across the SOAs. Condition 4 showed no effects at all on discriminability ($p > 0.4$), while condition 5 showed increased discriminability for the 40 ($t(4) = 3.3, p = 0.031$) and 80 ($t(4) = 3.3, p = 0.031$) millisecond SOAs.

Measures of accuracy are depicted in figure 3.11. A condition by SOA by target (5x5x2) repeated measures ANOVA revealed a significant condition by SOA interaction ($F(16,64) = 2.8, p = 0.002, \eta_p^2 = 0.416$), but no condition by SOA by target interaction ($F(16,64) = 0.59, p = 0.87, \eta_p^2 = 0.13$). Because the three-way repeated measures ANOVA shows no significant effect, no post-hoc tests were conducted.

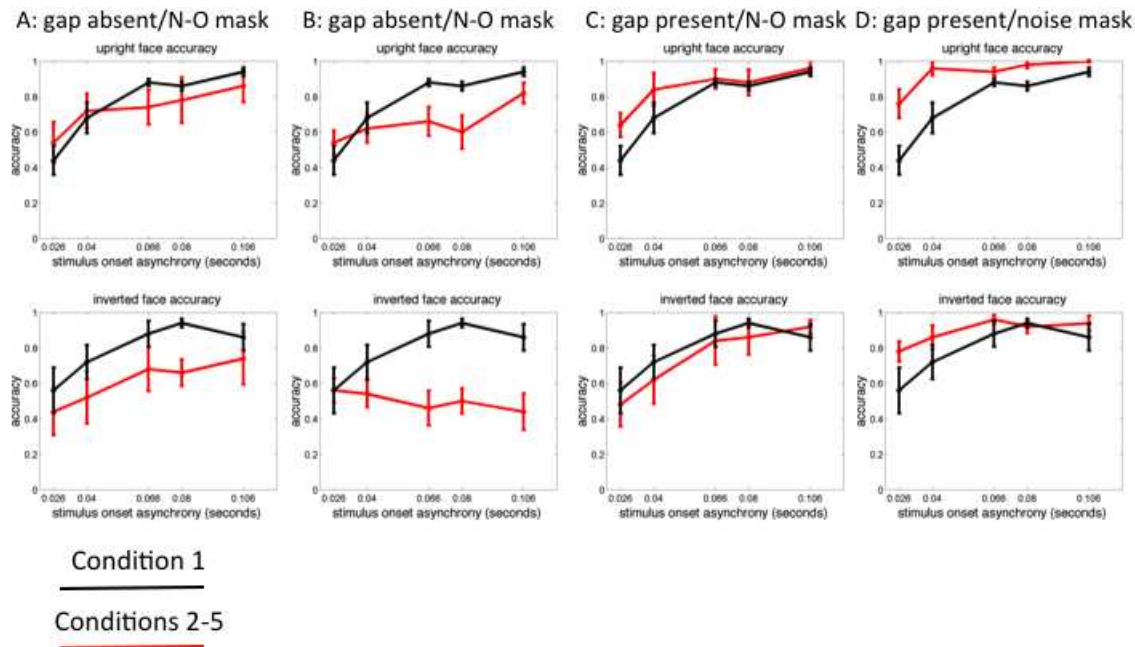


Figure 3.11. Measures of upright (top) and inverted (bottom) accuracy for the conditions in experiment 5. The control condition (black) is compared with the non-control conditions (red): (A) condition 2, (B) condition 3, (C) condition 4, (D) condition 5.

Discussion

Findings from experiment 5 suggest that concentric Glass pattern masking, but not adaptation, impairs face perception. The experiment shows that impairment only occurs when the adaptor and target are presented close together, and effects of visual masking are shorter in duration [19] than effects of adaptation, which typically last longer than 500 milliseconds [1].

General Discussion

The positive finding in the visual masking experiments, when contrasted with the negative finding for the visual adaptation experiments, reveals a behavioral phenomenon that has a potential neurophysiological interpretation. Though one should regard this interpretation as somewhat speculative, it may provide a direction for future studies, and is therefore important to include here.

One explanation for these findings is that the processing mechanism affected by visual masking may be robust to adaptation itself. Neurons instantiating this mechanism may not habituate for long periods of time. Studies have shown altered neuronal tuning curves following visual adaptation [20, 21]. This alteration may occur because these neurons habituate to the presentation of the adaptor. A review of visual masking studies suggests that masking suppresses neuronal activity, but does not cause the neurons to habituate for long periods of time [6].

Interestingly, previous studies of Glass pattern adaptation have not examined the duration of the adaptation effects; the target was presented immediately after the adaptors [17, 18, 22]. It is possible that these adaptation effects are actually visual masking effects, and therefore this processing mechanism may not be affected strongly

by visual adaptation. Future adaptation studies of Glass patterns can test this by modifying the onset of the target relative to the adaptation period. If a 500-millisecond gap between the target and adaptation period does not impair target discrimination, then the processing mechanism involved in perceiving concentric Glass patterns may not be affected by visual adaptation.

Chapter 4 describes experiments that test whether this masking effect is specific to concentric Glass patterns. In the chapter, two experiments (experiments 6 and 7) examine whether concentric, more so than radial or translational, masking impair upright/inverted and/or face gender discriminations.

References

1. Krekelberg, B., G.M. Boynton, and R.J. van Wezel, *Adaptation: from single cells to BOLD signals*. Trends Neurosci, 2006. **29**(5): p. 250-6.
2. Kohn, A., *Visual adaptation: physiology, mechanisms, and functional benefits*. J Neurophysiol, 2007. **97**(5): p. 3155-64.
3. Clifford, C.W., et al., *Visual adaptation: neural, psychological and computational aspects*. Vision Res, 2007. **47**(25): p. 3125-31.
4. Breitmeyer, B.G. and H. Ogmen, *Recent models and findings in visual backward masking: a comparison, review, and update*. Percept Psychophys, 2000. **62**(8): p. 1572-95.
5. Rolls, E.T., *Consciousness absent and present: a neurophysiological exploration*. Prog Brain Res, 2004. **144**: p. 95-106.
6. Breitmeyer, B.G., *Visual masking: past accomplishments, present status, future developments*. Adv Cogn Psychol, 2007. **3**(1-2): p. 9-20.
7. Brainard, D.H., *The Psychophysics Toolbox*. Spat Vis, 1997. **10**(4): p. 433-6.
8. Wilson, H.R. and F. Wilkinson, *Detection of global structure in Glass patterns: implications for form vision*. Vision Res, 1998. **38**(19): p. 2933-47.
9. Appelle, S., *Perception and discrimination as a function of stimulus orientation: the "oblique effect" in man and animals*. Psychological Bulletin, 1972. **78**(4): p. 266-78.
10. Jenkins, B., *Oriental anisotropy in the human visual system*. Percept Psychophys, 1985. **37**(2): p. 125-34.
11. Tottenham, N., et al., *The NimStim set of facial expressions: judgments from untrained research participants*. Psychiatry Res, 2009. **168**(3): p. 242-9.

12. Lundqvist, D., A. Flykt, and A. Ohman, *The Karolinska Directed Emotional Faces - KDEF*, 1998, Department of Clinical Neuroscience, Psychology section Karolinska Institutet.
13. Wig, G.S., et al., *Separable routes to human memory formation: dissociating task and material contributions in the prefrontal cortex*. *J Cogn Neurosci*, 2004. **16**(1): p. 139-48.
14. Oruc, I. and J.J. Barton, *Critical frequencies in the perception of letters, faces, and novel shapes: evidence for limited scale invariance for faces*. *J Vis*, 2010. **10**(12): p. 20.
15. Garcia-Perez, M.A., *Forced-choice staircases with fixed step sizes: asymptotic and small-sample properties*. *Vision Res*, 1998. **38**(12): p. 1861-81.
16. Green, D.M. and J.A. Swets, *Signal Detection Theory and Psychophysics* 1966, New York: Wiley.
17. Clifford, C.W. and E. Weston, *Aftereffect of adaptation to Glass patterns*. *Vision Res*, 2005. **45**(11): p. 1355-63.
18. Ross, J. and J. Edwin Dickinson, *Effects of adaptation to Glass pattern structure and to path of optic flow*. *Vision Res*, 2007. **47**(16): p. 2150-5.
19. Rolls, E.T., N.C. Aggelopoulos, and F. Zheng, *The receptive fields of inferior temporal cortex neurons in natural scenes*. *J Neurosci*, 2003. **23**(1): p. 339-48.
20. Carandini, M., J.A. Movshon, and D. Ferster, *Pattern adaptation and cross-orientation interactions in the primary visual cortex*. *Neuropharmacology*, 1998. **37**(4-5): p. 501-11.
21. Dragoi, V., J. Sharma, and M. Sur, *Adaptation-induced plasticity of orientation tuning in adult visual cortex*. *Neuron*, 2000. **28**(1): p. 287-98.
22. Vreven, D. and J. Berge, *Detecting structure in glass patterns: an interocular transfer study*. *Perception*, 2007. **36**(12): p. 1769-78.

Chapter 4: Sandwich masking experiments reveal pattern-specific masking for upright/inverted and gender face discrimination

Introduction

Chapter 4 reports experiments that test whether this masking effect is specific to concentric Glass patterns. In the chapter, two experiments examine whether concentric, more so than radial or translational, masking impaired upright/inverted and/or face gender discriminations. We decided to use sandwich masking experiments to extend our results because experiments 2,3, and 5 all used a backward mask to make the task more difficult. Therefore, we wanted to use both a forward and a backward mask to make the subsequent experiments harder. Additionally, a published, well-designed fMRI masking study relied on the use of sandwich masking, so our design could easily be extended to an fMRI study [1].

General Methods

Participants and experimental setup are the same as in Chapter 3. The Glass patterns used were generated as described in Chapter 3. For these experiments, half the dipoles were white and the other half black on a mid-gray background, and the extent of the pattern measured 21.5 visual degrees in length and 14.5 visual degrees in width. All Glass patterns were luminance equated to a mean luminance of 22 cd/m².

The staircasing procedure and analysis were performed as described in Chapter 3. For calculating discriminability in experiment 6, upright faces were labeled as group

A, and inverted faces were labeled as group B. For experiment 7, male faces were labeled as group A, and female faces were labeled as group B.

Experiment 6: upright inverted face discrimination

Methods

34 adults (15 male/19 female; aged 23.6 \pm 3.1 years) participated in this sandwich masking experiment, where both a forward and backward mask is presented for each target (e.g. [1]). A schematic of this experiment is provided in figure 4.1. At the start of each trial, a forward masking Glass pattern would appear for 40 milliseconds. 500 or 67 milliseconds after the onset of the mask, a target face would appear for 13 milliseconds. Vertical offset conditions were employed to prevent participants from only using the eyes or mouth to determine whether the face was upright (Figure 3.9A) or inverted (Figure 3.9B). The center of the target face could be located in the center of the screen, shifted vertically up 4.1 degrees from the center, or shifted vertically down 4.8 degrees from the center. These shifts ensured that the eyes for the upright face in the center were located in the same position as the eyes for the inverted face shifted upwards, and that the eyes for the inverted face in the center were located in the same position as the eyes for the upright face shifted downwards. 500 or 67 milliseconds after the onset of the target, a backward masking Glass pattern of same type as the first pattern would appear for 40 milliseconds. Unlike adaptation, masks affect target discrimination for a very short time. Therefore, the 500-millisecond presentation condition is a control condition where no masking is expected. The participant would then indicate whether the target face was upright or inverted. For each trial, both masks were concentric, radial, or translational Glass patterns. Target degradation was

determined for each participant using the staircasing procedure detailed for experiment 5.

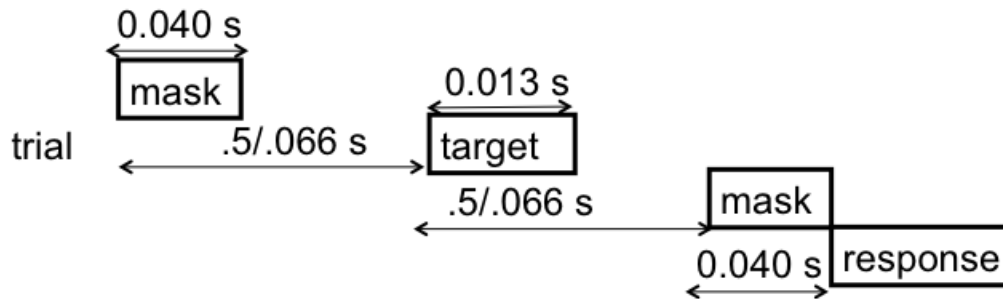


Figure 4.1. Schematic for the paradigm used in experiments 6 and 7.

Accuracy, d' , and beta were measured for each participant. *A priori*, no difference between the down and up offset conditions was predicted, and the down and up offset conditions were collapsed across each other to simplify the analysis. For accuracy, a target by SOA by offset (yes or no) by pattern (2x2x2x3) repeated measures ANOVA was used to test for significant pattern-SOA interactions. For d' and beta, SOA by offset by pattern (2x2x3) repeated measures ANOVAs were used to test for significant pattern-SOA interactions. Effects between individual conditions were evaluated with subsequent *post-hoc* t-tests. *Post-hoc* statistics are reported as uncorrected values.

Results: Concentric Glass pattern sandwich masking impairs upright/inverted face discrimination

Measures of d' show a pattern-specific effect of visual masking, such that concentric Glass patterns impaired face discrimination more than radial Glass patterns, and radial Glass patterns impaired face discrimination more than translational Glass patterns (figure 4.2). A pattern by SOA by offset repeated measures ANOVA shows a

significant pattern by SOA by offset interaction ($F(2,66) = 3.5, p = 0.033, \eta_p^2 = 0.098$).

Post-hoc comparisons show a pattern specific masking effect for central face presentations (figure 4.2A), such that concentric Glass pattern masking reduced d' at the 67 millisecond SOA more than radial ($t(33) = 3.0, p = 0.005$) or translational ($t(33) = 5.7, p < 0.001$) Glass patterns. Radial Glass pattern maskers reduced d' at the 60 millisecond SOA more than translational patterns ($t(33) = 2.2, p = 0.039$). When the face is presented offset from the center of the screen (figure 4.2B), no significant pattern by SOA interactions are observed ($F(2,66) = 0.431, p = 0.65, \eta_p^2 = 0.013$).

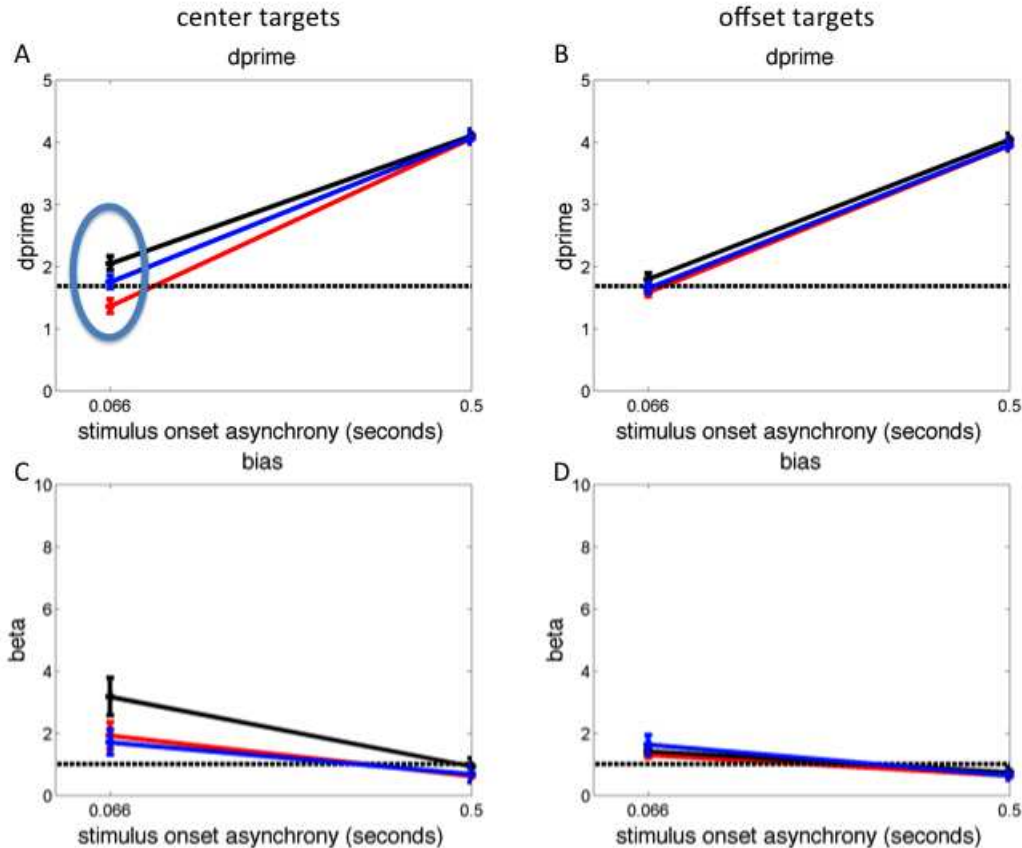


Figure 4.2. Discriminability (A) and bias measures (C) for experiment 6 are plotted for targets located in the center. Discriminability (B) and bias measures (D) for targets located offset from the center are also plotted. Lines and bars are colored to represent concentric (red), radial (blue), and translational (black) maskers. A pattern-specific effect of visual masking was found such that concentric masks

impaired discriminability more than radial masks, which impaired discriminability more than translational masks (blue ellipsoid).

There was no pattern-specific effect of masking on bias (figure 4.2C and figure 4.2D). A pattern by SOA by offset (3x2x2) repeated measures ANOVA revealed no significant pattern by SOA interaction ($F(1.7,55.8) = 1.08$, $p = 0.337$, $\eta_p^2 = 0.032$).

Pattern-specific masking effects on accuracy are shown in figure 4.3. A pattern by SOA by offset by target (3x2x2x2) repeated measures ANOVA revealed significant 3-way interactions between pattern, SOA, and target ($F(2,66) = 4.188$, $p = 0.02$, $\eta_p^2 = 0.113$), as well as between pattern, SOA, and offset ($F(2,66) = 7.2$, $p = 0.001$, $\eta_p^2 = 0.179$). Post-hoc comparisons show concentric masking effects at the 67 millisecond SOA on accuracy for upright (figure 4.3A) and both concentric and radial masking effects at the 67 millisecond SOA for inverted (figure 4.3C) face targets located in the center of the pattern. For upright face targets, concentric masking impaired accuracy more than radial ($t(33) = 3.1$, $p = 0.004$), and translational ($t(33) = 2.1$, $p = 0.046$) masking. For inverted face targets, concentric masking impaired accuracy more than radial ($t(33) = 2.1$, $p = 0.048$), and translational ($t(33) = 5.2$, $p < 0.001$) maskers. Radial masking, relative to translational masking, impaired accuracy for inverted ($t(33) = 3.7$, $p = 0.001$), but not upright ($t(33) = 0.669$, $p = 0.51$) faces. For upright face targets offset from the center (figure 4.3B), pairwise comparisons show no effects on upright face accuracy ($p < 0.72$). For inverted face targets offset from the center (figure 4.3D), concentric ($t(33) = 3.3$, $p = 0.002$) and radial ($t(33) = 2.4$, $p = 0.024$) masking reduced inverted face accuracy relative to translational masking at the 67 millisecond SOA.

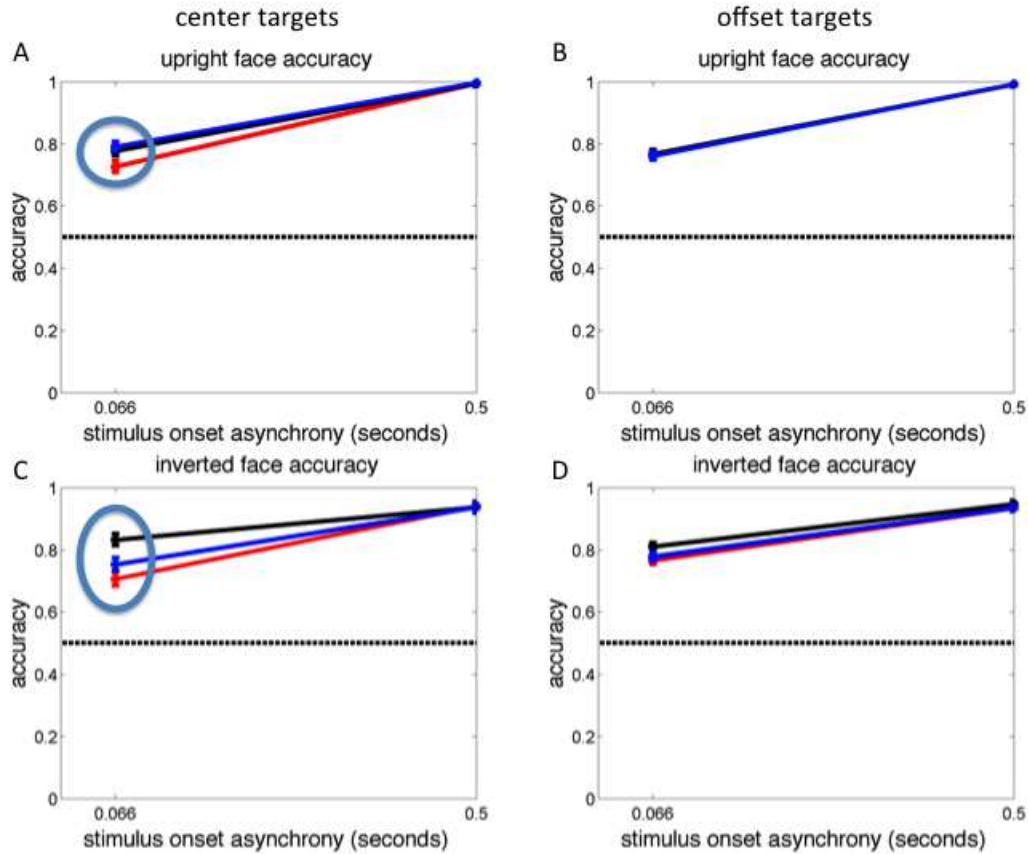


Figure 4.3. Upright (A) and inverted face accuracy (C) for experiment 6 are plotted for targets located in the center. Upright (B) and inverted face accuracy (D) for targets located offset from the center are also plotted. Lines and bars are colored to represent concentric (red), radial (blue), and translational (black) maskers. Pattern-specific masking effects were observed when the face was located in the center (blue circles).

Discussion

The results from experiment 6 show a pattern-specific masking effect; concentric Glass pattern masks impair upright/face discrimination more than radial or translational pattern masks. This evidence supports the hypothesis that concentric Glass patterns and faces share a common processor. Radial Glass patterns impaired upright/face discrimination more than translational patterns, suggesting a possible separate

interaction between radial form and face perception (see the General Discussion section for a discussion of this finding). These effects were attenuated when the faces were offset from the center of the Glass pattern, which suggests two points.

Because the offsets created positional ambiguity for the location of face features, participants may have been unable to utilize a feature-based strategy (that they might have adopted at the offset locations) for performing the task when the face was centered. The offset conditions, therefore, forced the participants to make judgments based on the arrangements of the features (i.e., whether the eyes are above or below the mouth) when the face was centered.

Additionally, the lack of any masking effect at the offset positions may suggest that the processing of arrangements of features involves more than simply processing the geometric rule, and that such processing may only affect face perception when the face is located in the center of the Glass pattern. Although concentric and radial Glass patterns are defined by a geometric rule, pieces of a Glass pattern do not represent the whole pattern. If one focuses only on the pieces of the Glass patterns, one sees arcs or sets of angled lines. However, at the center of the pattern, these arcs or lines come together to form concentric or radial shapes. Because pattern-specific masking occurs only when the faces are located at the center of the pattern, it may be the perception of the whole pattern that interacts with face perception. Future studies could manipulate the location of the center of the masking Glass pattern with respect to the face target to see where the pattern-specific masking effects are the strongest.

Experiment 7 extends our finding of form-specific Glass pattern effects on upright/inverted face judgments by testing whether concentric and radial, more so than translational, Glass patterns impair face gender discrimination.

Experiment 7: Gender Discrimination

Methods

30 adults (12 male/18 female; aged 23.4 +/-3.2 years) participated in this experiment; these adults also participated in experiment 6. Experiment 7 was similar to experiment 6 (Figure 4.1); the target faces in experiment 7 were male (Figure 3.9C) and female (Figure 3.9D) faces, and no vertical offset conditions were used. Target degradation was determined for each participant using the staircasing procedure detailed for experiment 5.

Accuracy, d' , and beta were measured for each participant. For accuracy, a target by SOA by pattern (2x2x3) repeated measures ANOVA was used to test for significant pattern-SOA interactions. For d' and beta, SOA by pattern (2x3) repeated measures ANOVAs were used to test for significant pattern-SOA interactions. Effects between individual conditions were evaluated with subsequent *post-hoc* t-tests. *Post-hoc* statistics are reported as uncorrected values.

Results: Concentric Glass pattern sandwich masking impairs gender discrimination

Consistent with the results from experiment 6, concentric Glass pattern masks reduced d' relative to radial Glass patterns, which reduced d' relative to translational masks (Figure 4.4A). A pattern by SOA (3x2) repeated measures ANOVA revealed a

significant pattern by SOA interaction ($F(2,58) = 4.5$, $p = 0.015$, $\eta_p^2 = 0.134$). *Post-hoc* comparisons show pattern-specific effects of masking at the 67 millisecond SOA, such that concentric Glass pattern masking reduced d' relative to radial ($t(29) = 3.0$, $p = 0.005$) and translational ($t(29) = 4.7$, $p < 0.001$) masking. Radial Glass pattern masking reduced d' relative to translational masking ($t(29) = 2.6$, $p = 0.015$).

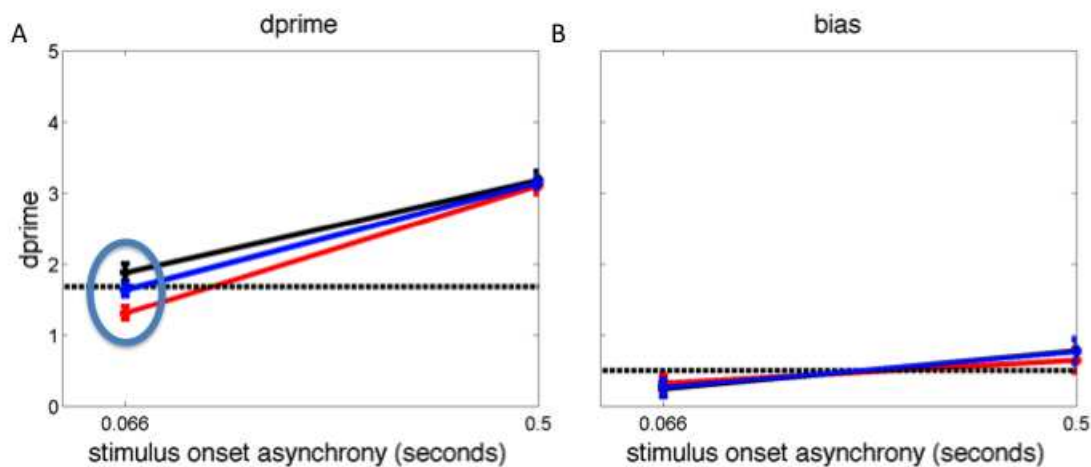


Figure 4.4. Discriminability (A), and bias (B) measures plotted for experiment 7. Lines and bars are colored to represent concentric (red), radial (blue), and translational (black) maskers. Pattern-specific masking effects were observed such that concentric masks reduced face discriminability more than radial masks, which reduced face discriminability more than translational masks (blue ellipsoid).

No effects of masking on bias were observed (Figure 4.4B). A pattern by SOA (3×2) repeated measures ANOVA shows no significant pattern by SOA interaction ($F(1.67, 48.3) = 0.572$, $p = 0.538$, $\eta_p^2 = 0.019$).

Accuracy is plotted in figure 4.5. A pattern by SOA by target ($3 \times 2 \times 2$) repeated measures ANOVA revealed a significant pattern by SOA interaction ($F(2,58) = 3.7$, $p = 0.031$, $\eta_p^2 = 0.113$), and no pattern by SOA by target interaction ($F(2,58) = 0.98$, $p =$

0.381, $\eta_p^2 = 0.033$). Because the three-way interaction was not significant, post-hoc comparisons were not conducted.

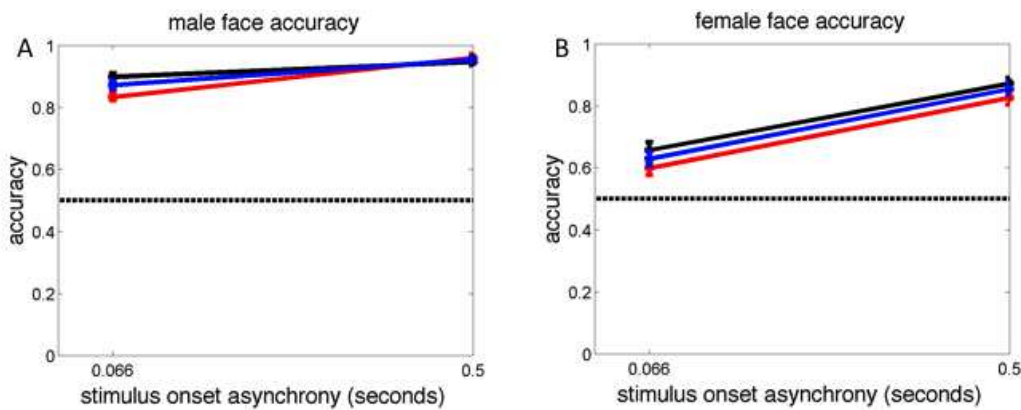


Figure 4.5. Male (A), and female (B) accuracy measures plotted for experiment 7. Lines and bars are colored to represent concentric (red), radial (blue), and translational (black) maskers.

Discussion

The results from experiment 7 provide convergent evidence for a pattern-specific masking effect on face discrimination. Since gender discrimination may be instantiated by a high-level processing mechanism, it is less likely that the pattern-specific masking effect interrupted a low-level processing mechanism. As with experiment 6, both concentric and radial masking impaired performance more than translational Glass patterns, which suggests a processing interaction between concentric and radial forms and face perception.

General Discussion

Faces are complex stimuli. Despite their complexity, humans are able to perceive and discriminate faces rapidly [2]. Studies have shown that face perception may involve processing the arrangements of the face features [3-10], and others hint at a possible

interaction between concentric Glass patterns and faces [11-18]. The observation that concentric and radial Glass pattern masks impaired performance more than translational Glass pattern masks suggests that concentric and radial Glass pattern perception are more similar to face perception than translational Glass pattern perception. The parsimonious explanation for this perceptual similarity is that face perception utilizes a processing mechanism shared by concentric and radial Glass pattern perception.

Differences between concentric, radial, and translational Glass pattern masking effects on face discrimination

The notion of a shared processor for face, concentric, and radial Glass pattern perception is consistent with findings from previous studies. Psychophysical data have shown that processing the arrangements of features is important for concentric and radial, but not translational, Glass patterns. It is easier to detect concentric and radial, but not translational Glass patterns when the whole pattern is presented [13]. While larger concentric Glass patterns are more quickly discriminated, larger translational Glass patterns are more slowly discriminated [15]. Translational maskers do not affect concentric or radial Glass pattern discrimination [19]. An fMRI study showed that regions sensitive to objects responded to concentric and radial, but not translational forms [14].

Concentric Glass pattern masking impaired face discrimination more than radial Glass pattern masking. This finding suggests that concentric Glass pattern perception may be more similar to face perception than radial Glass pattern perception. Previous visual adaptation and visual masking studies support this distinction. While one visual

adaptation study suggested that radial and concentric Glass patterns might share a common processing mechanism [20], another visual adaptation study suggested that radial and concentric Glass pattern perception use different mechanisms for processing the global form [21]. The masking study mentioned above also showed that radial Glass pattern maskers do not affect concentric Glass pattern perception [19]. The fMRI study mentioned above showed that concentric, but not radial, form presentation increases activation of visual regions involved in face processing [14], suggesting that face perception may utilize a processing mechanism shared by concentric, but not radial, Glass pattern perception. Another fMRI study demonstrated that blood-oxygen-level-dependent (BOLD) responses become increasingly selective for concentric Glass patterns for successively higher-level visual areas [17], suggesting that the high-level visual processing of radial and concentric Glass patterns may differ.

Unfortunately, the neural loci of the masking effect cannot be deduced from our behavioral results. Fortunately, the design of the behavioral studies can be easily transformed into an fMRI paradigm [1]. The following chapter explicates the experiment and its possible results.

References

1. Huang, J., M. Xiang, and Y. Cao, *Reduction in V1 activation associated with decreased visibility of a visual target*. *Neuroimage*, 2006. **31**(4): p. 1693-9.
2. Tsao, D.Y. and M.S. Livingstone, *Mechanisms of face perception*. *Annual Review of Neuroscience*, 2008. **31**: p. 411-37.
3. Thompson, P., *Margaret Thatcher: a new illusion*. *Perception*, 1980. **9**(4): p. 483-4.
4. Young, A.W., D. Hellowell, and D.C. Hay, *Configurational information in face perception*. *Perception*, 1987. **16**(6): p. 747-59.
5. Tanaka, J.W. and M.J. Farah, *Parts and wholes in face recognition*. *Q J Exp Psychol A*, 1993. **46**(2): p. 225-45.

6. Rhodes, G., S. Brake, and A.P. Atkinson, *What's lost in inverted faces?* Cognition, 1993. **47**(1): p. 25-57.
7. Lewis, M.B. and R.A. Johnston, *The Thatcher illusion as a test of configural disruption.* Perception, 1997. **26**(2): p. 225-7.
8. Maurer, D., R.L. Grand, and C.J. Mondloch, *The many faces of configural processing.* Trends Cogn Sci, 2002. **6**(6): p. 255-260.
9. Boutsen, L., et al., *Comparing neural correlates of configural processing in faces and objects: an ERP study of the Thatcher illusion.* Neuroimage, 2006. **32**(1): p. 352-67.
10. Mondloch, C.J. and D. Maurer, *The effect of face orientation on holistic processing.* Perception, 2008. **37**(8): p. 1175-86.
11. Rentschler, I., B. Treutwein, and T. Landis, *Dissociation of local and global processing in visual agnosia.* Vision Res, 1994. **34**(7): p. 963-71.
12. Wilson, H.R., F. Wilkinson, and W. Asaad, *Concentric orientation summation in human form vision.* Vision Res, 1997. **37**(17): p. 2325-30.
13. Wilson, H.R. and F. Wilkinson, *Detection of global structure in Glass patterns: implications for form vision.* Vision Res, 1998. **38**(19): p. 2933-47.
14. Wilkinson, F., et al., *An fMRI study of the selective activation of human extrastriate form vision areas by radial and concentric gratings.* Curr Biol, 2000. **10**(22): p. 1455-8.
15. Aspell, J.E., J. Wattam-Bell, and O. Braddick, *Interaction of spatial and temporal integration in global form processing.* Vision Res, 2006. **46**(18): p. 2834-41.
16. Smith, M.A., A. Kohn, and J.A. Movshon, *Glass pattern responses in macaque V2 neurons.* J Vis, 2007. **7**(3): p. 5.
17. Ostwald, D., et al., *Neural coding of global form in the human visual cortex.* J Neurophysiol, 2008. **99**(5): p. 2456-69.
18. Poirier, F.J. and H.R. Wilson, *A biologically plausible model of human shape symmetry perception.* J Vis, 2010. **10**(1).
19. Chen, C.C., *A masking analysis of glass pattern perception.* J Vis, 2009. **9**(12): p. 2211-11.
20. Clifford, C.W. and E. Weston, *Aftereffect of adaptation to Glass patterns.* Vision Res, 2005. **45**(11): p. 1355-63.
21. Ross, J. and J. Edwin Dickinson, *Effects of adaptation to Glass pattern structure and to path of optic flow.* Vision Res, 2007. **47**(16): p. 2150-5.

Chapter 5: Conclusions and Future Directions

Conclusions

Effects of visual masking suggest that concentric Glass pattern, radial Glass pattern, and face perception share a common processing mechanism

Visual masking using Glass patterns impaired performance on face discrimination tasks. The observation that concentric and radial Glass pattern masks impaired performance more than translational Glass pattern masks suggests that concentric and radial Glass pattern perception are more similar to face perception than translational Glass pattern perception. The parsimonious explanation for this perceptual similarity is that face perception utilizes a processing mechanism shared by concentric and radial Glass pattern perception.

Based on hints from the previous literature, and results from our own studies, I propose that this shared mechanism involves processing the arrangements of features. In our upright/inverted face discrimination experiment (experiment 6), pattern-specific masking effects were observed when the faces were located in the center of the screen, and a subject could not discriminate upright/inverted faces in the center by simply looking at the location of a single feature. In the offset position, where such a strategy might have been adopted, we found no pattern-specific masking effects, suggesting that the concentric and radial masks interfered with processing the arrangement of the face features and did not interfere with processing of the face features themselves. The pattern-specific masking effects observed in the gender discrimination task (experiment 7) provide further evidence that the concentric and radial masks interfered with processing the arrangement of the face features. Extraneous features that could

distinguish gender were removed, suggesting that participants relied on the arrangement of the features when discriminating male from female faces. This finding is consistent with behavioral [1-15], fMRI [16, 17], and lesion [18] studies, which all suggest that face perception is disrupted when the arrangement of the features is altered. Other behavioral studies show that concentric and radial Glass pattern perception is impaired when the arrangement of the features is restricted [19, 20]. Therefore, processing the arrangement of features is important for concentric Glass pattern, radial Glass pattern, and face perception. The putative feature-arrangement processor may be shared because fMRI evidence shows that face-sensitive regions show increased activity for concentric, but not radial, forms [21].

The results from the psychophysical studies [19, 20] of Glass pattern perception helped Poirier and Wilson develop a biologically plausible model of shape perception that involves processing the arrangements of features [22]. This model is tuned to both faces and concentric Glass patterns [22]. Briefly, the model is divided into five stages. (1) The contour information of an object is recovered using filters that encode contours. (2) Coarse, large-scale, filters that encode the center of concentric contours are used to recover the center of the object. (3) Multiple oriented filters recover local curvature information of contours relative to the center of the object. (4) The information from the first few stages is pooled to determine the shape of the object based on curvature strength. (5) This information is used to identify the axes of symmetry within an object. Each of these stages is thought to be instantiated by successively higher-level visual regions. A shared mechanism could involve any of these stages, so an fMRI visual masking paradigm could identify which regions along the visual system are affected by

concentric and radial masks when discriminating faces. The location of such regions may suggest which stages of the model may be shared, and, therefore, provide empirical insight into mechanisms involved in face perception.

Findings from the visual masking and adaptation experiments suggest that the shared mechanism may only be affected by a stimulus for a short period of time

We found that concentric and radial Glass pattern visual masking, but not visual adaptation, impaired face discrimination (experiments 4 and 5). This distinction suggests that the neurons instantiating the putatively shared processing mechanism may not habituate to the attributes of a given stimulus. As discussed in chapter one, pattern-specific masks generally reduce the visibility of a presented stimulus [23, 24], whereas in visual adaptation, one generally perceives the presented stimulus as the opposite of the adapting stimulus [25-27]. A mechanistic explanation for visual adaptation is that adaptation causes the individual neurons responsive to the target to habituate to the attributes of the adapted stimulus [26, 28]. Because we find no effects of visual adaptation, it is possible that neurons tuned to faces do not respond to concentric and radial Glass patterns and, therefore, do not habituate to the attributes of those patterns. Taken together, these findings hint at an intriguing possibility that face, concentric Glass pattern, and radial Glass pattern perception may share a common processing mechanism, and the neurons instantiating the mechanism are robust to visual adaptation.

Interestingly, previous studies of Glass pattern adaptation have not examined the duration of the adaptation effects; the target was presented immediately after the adaptors [29-31]. It is possible that these adaptation effects are actually visual masking

effects, and therefore this processing mechanism may not be affected strongly by visual adaptation. Future adaptation studies of Glass patterns can test this by modifying the onset of the target relative to the adaptation period. If adding a 500-millisecond gap between the target and adaptation period reduces the effect of the adaptor on target discrimination, then previously reported Glass pattern-Glass pattern “adaptation” effects may actually be instances of form-specific pattern masking.

Implications for clinical disorders, such as autism or prosopagnosia

The possibility of a shared mechanism between face, concentric, and radial Glass pattern perception may provide insights into clinical disorders involving face-processing deficits, such as autism or prosopagnosia. Both acquired visual agnosia [32] and acquired prosopagnosia [18] may impair concentric Glass pattern perception. People with autism have face perceptual deficits [11, 33-41] that may relate to a general deficit in processing the arrangements of features [42]. Psychophysical studies of concentric and radial Glass pattern perception in people with autism or prosopagnosia may provide insight into the nature of these processing deficits.

Implications for object recognition

The findings here do not test whether Glass pattern masking impairs non-face object discriminations, so there are several possible implications for the nature of the shared processor. One possibility is that faces, and not any other objects, engage this processor. A number of fMRI studies have shown that faces activate some visual regions that are not activated by non-face objects (for a review see: [43]), and some argue that this difference is reflected in a processing mechanism dedicated only to face perception [44, 45].

Alternatively, the shared processor may respond to both face and expertly perceived non-face objects (e.g. dogs perceived by dog experts). There is evidence that expertly perceived objects may involve some neural regions thought to be specific to face perception [46, 47]. Similar to face perception, the parts of expertly perceived non-faces are better recognized when the whole object is presented [7]. Therefore, processing feature arrangements may be important for discriminating both faces and expertly perceived non-face objects [2, 7].

It is also possible that general form perception, and therefore all object (expert or non-expert) perception, utilize this shared processor. Visual area V4, which is involved in form perception [48, 49], may instantiate such a mechanism. Psychophysical [50], computational [22], and neurophysiological [51] studies suggest that V4 may be important for concentric Glass pattern perception. A case study of a lesion in putative V4 showed disrupted form perception, and the participant could not discriminate concentric Glass patterns [32].

Summary

Although concentric Glass pattern, radial Glass pattern, and face perception may share a common processor, the nature of the processor is unclear from the visual masking studies. The processor may be important for the representation of properties of all objects. Alternatively, the processor might be important for the representation of faces, but not non-face objects (e.g. houses or cars). Identifying the neural loci of the interaction, using a functional magnetic resonance imaging (fMRI) sandwich masking paradigm [52] may help identify the neural regions instantiating this process and therefore address this question.

Future fMRI masking studies may help characterize the neural mechanism for these interactions

Introduction

A few studies have examined the effects of visual masking on the brain using fMRI [53-55]. We are intrigued by a study that used a sandwich masking fMRI paradigm [52], which motivated the design of our psychophysical study. Since our behavioral experiments (i.e. experiments 6 and 7) were successful, transitioning to an fMRI paradigm should be relatively straightforward.

An fMRI sandwich masking study is an effective approach because the results help determine whether a given region is involved in processing the mask and the target themselves, and whether this processing may be shared between the two stimuli [52]. In such a study, each trial may be placed in one of three categories: (1) single target presentation, (2) mask-no target-mask presentation (3) mask-target-mask presentation. The SOA of the stimuli for conditions 2 and 3 are either short or long per trial. The first two conditions allow one to examine whether a given region is involved in mask and/or target perception: The first presentation condition allows one to examine BOLD responses to the target itself. If the BOLD response in a given region increases for the target relative to fixation, said region may be involved in processing the target. The second presentation condition measures the BOLD response to the mask itself. An increased BOLD response for mask-mask trials relative to fixation in a region suggests that the region may be involved in processing the mask. A reduced BOLD response when the SOA between the masks is short vs long would suggest that the region is important for mask-mask interactions because in the short SOA condition, the visibility

of the mask should be reduced. The third condition allows one to test whether the activity in a given region is important for mask-target interactions, because such regions will have reduced BOLD responses for mask-target presentations when the SOA is short, relative to when the SOA is long.

Using an fMRI sandwich-masking paradigm, the proposed experiment below will attempt to identify the loci of concentric and radial masking effects on face perception. Regions important for mask-target interactions will be identified by suppressed BOLD responses in condition 3 when the SOA is short. If an interacting locus shows positive BOLD responses for conditions 1 and condition 2, then the given locus may insatiate a shared processor. Separately, the specificity of a region's activity can be determined *a priori* by using a functional localizer [56]. If regions that are more sensitive to faces than objects show mask-target interactions, then the mechanism affected by the interaction may be face-specific. If such responses are observed in regions that are equally sensitive to faces and objects, then the affected mechanism may not be specific to faces.

Methods

Stimulus design

Sandwich masking experiment

The stimuli for the sandwich masking experiment will be the same set of faces, and the same design for the Glass patterns, as in the behavioral masking gender discrimination experiment. Because different display devices produce different luminance and contrast properties, luminance and contrast will be matched in the

scanner room for the faces and the Glass patterns using the procedure detailed in chapter 3.

Functional localizers

The purpose of these functional localizers will be to identify visual cortical regions in each individual subject that may represent low (e.g. V1/V2) and high levels (e.g. FFA) of information processing for visual stimuli. The stimuli for the V1/V2 localizer (see the fMRI paradigms section) will be two black-and-white circular checkerboards that will be alternately patterned [57]. The diameter of the checkerboards will be 20 visual degrees. The stimuli for the dynamic face localizer will be a series of two-second video-clips of faces and common non-face objects [56]. The face video-clips will consist of changes in facial expression, while the object video-clips consist of changes in objects (e.g. a flickering candle). Because the particular set of movie clips may not be ideal (see: preliminary results below), a set of video-clips will be acquired and used to create the dynamic localizer. The results of the dynamic localizer will be compared to a static face localizer [21, 58], and the superior localizer will be used for the study. The stimuli for the static face localizer will comprise luminance and contrast equated photographs of faces and non-face objects.

Equipment

Stimuli will be presented using a DLP projector. The projector screen will measure 36.5 x 27.6 visual degrees, and the timing of the display will be validated using a photodiode connected to a Macintosh system running PowerLab. The subject will lie down on a bed and see the projector through a mirror. Stimulus presentation and timing

will be controlled using a Macintosh computer running MATLAB with the psychtoolbox extensions [59]. Subjects will respond to stimuli using a button box.

MR acquisition

Brain imaging data will be acquired using a Siemens TIM Trio 3T scanner with a 12-channel head coil. Both functional and structural imaging data will be acquired for each subject. For structural data, one run of high-resolution T1-weighted MPRAGE (TE=3.93 ms, TR = 1.9 s, TI = 1000 ms, flip angle = 7 degrees, 128 slices at 1x1x1 mm resolution/voxel) and one run of T2-weighted fast spin echo image (TR =4380 ms, TE = 94 ms, 1x1x4 resolution/voxel, 4mm gap between slices) data will be acquired. For functional acquisitions, a blood oxygenation level-dependent (BOLD) contrast sensitive, asymmetric spin-echo, echo-planar (T2* evolution time = 25 ms, flip angle = 90 degrees, 4x4 mm in-plane resolution/voxel) dataset will be acquired per run. Each MR frame within a dataset will be 2.5 seconds long, and will consist of 32 contiguous, 4mm-thick, axial slices centered over the hemispheric divide and parallel to the AC-PC plane. The number of frames per dataset will vary from run to run.

fMRI paradigms

Functional localizers

To delineate boundaries for low-level visual regions, (i.e. V1/V2), a flickering checkerboard blocked fMRI paradigm based on Engel et al will be used [57]. The flickering checkerboard will be presented on a mid-grey background. For each run, two wedges that comprise 1/6th of a full circle will rotate about the fixation point over the course of each 40 second block. The speed of the rotation will be one cycle per block,

and the contrast reversal rate will be 8 Hz. Each run will comprise 4 blocks, and each subject will perform 4 runs. In total, the V1/V2 localizer will last 10 minutes and 40 seconds.

We piloted a simpler version of this retinotopic localizer to demonstrate that it is possible to delineate the V1/V2 boundaries while leaving time for the other task-based studies in a single scanning session. In this version, the two wedges alternated between two positions every 20 seconds: one position was oriented along the horizontal axis (horizontal meridian), the other along the vertical axis (vertical meridian). As in the proposed localizer, each run lasted 160 seconds and 4 runs were acquired.

To delineate high-level visual regions sensitive to faces and objects, a dynamic face blocked fMRI paradigm similar to Fox et al. [56] will be used. Each run will contain 24, 20-second blocks. During half of the blocks, a fixation point will be displayed on the screen. For the other blocks, a series of two second video-clips will be shown at a rate of one clip per MR frame. In each block, all the video-clips will be of faces or objects. The subject will press a button when the same video clip plays twice in a row. Two runs of data will be acquired per subject, for a total of 16 minutes.

Fox et al. tested whether a dynamic face functional localizer improved the identification of face and object sensitive regions when compared to a static face localizer. The authors found that a dynamic face localizer consistently identified face-sensitive regions in posterior superior temporal sulcus (pSTS), inferior occipital gyrus (occipital face area: OFA), and the fusiform gyrus (fusiform face area; FFA). For a group of 16 subjects, the localizer successfully identified these face-sensitive regions 98% of

the time. By way of comparison, a static face localizer identified these face-sensitive regions only 72% of the time for the same subjects [56].

In our hands (see below) the localizer used by Fox et al. may not be ideal for isolating face and object sensitive visual cortical regions. As shown below (see: preliminary results), too much of the cortex shows greater activity for the face clips than the object clips, so delineating face-specific regions may be difficult using this particular localizer. We will acquire our own video-clips and test our dynamic localizer against a static face localizer [21] using the same timing paradigm described above. In the static face localizer, each run will contain 24, 20-second blocks. During half of the blocks a fixation point will be displayed on the screen. For the other blocks, a series of face images (for face blocks) or object images (for object blocks) will be presented for two seconds at a rate of one picture per MR frame. The subject will press a button when the same image appears twice in a row. Two runs of data will be acquired per subject, for a total of 16 minutes. Other face localizers (e.g. using scrambled faces or scrambled objects) are not considered here because they may take too long [58]. However, if neither the dynamic nor static face localizers described above are sufficient then a mini-experiment will be run to test other potential localizers.

Sandwich-masking experiment

The sandwich-masking task will be a jittered, event-related fMRI paradigm [52]. The timing of the task itself will be similar to the sandwich masking behavioral experiments. For each trial, one of three trial types will be presented: target only, mask-fixation-mask, and mask-target-mask. In the target only trial type, a target will be presented for 13 milliseconds. In the mask-fixation-mask trial type, a mask will appear

for 40 milliseconds. After a 67 or a 500 millisecond SOA, a fixation cross will be presented for 13 milliseconds. A second mask will appear after an SOA of the same duration. In the mask-target-mask trial type, a target will be presented instead of a fixation cross. Targets will be male and female faces. Masks will be concentric, radial, or translational Glass patterns, and for each trial, the same mask type will be presented before and after the target. For each trial, the subject will press one button when a presented face is male, and another when the face is female. Each subsequent trial will begin 1-3 MR frames after the previous trial.

Table 5.1 displays the different conditions in the experiment. In total, there are 13 conditions of interest in the experiment. One condition comprises target only presentations, while the other 12 are displayed in Table 5.1. Each run will contain 5 trials per condition, for a total of 65 trials. Including the MR jitter, each run will last 8.125 minutes. Six runs will be collected per subject for a total run time of 45 minutes and 45 seconds.

mask type	Condition 1	Condition 2	Condition 3	Condition 4
concentric	30 trials	30 trials	30 trials	30 trials
radial	30 trials	30 trials	30 trials	30 trials
translational	30 trials	30 trials	30 trials	30 trials

Table 5.1. Table of conditions for sandwich masking fMRI experiment, excluding the target only condition. Each mask type (concentric, radial, translational) will have four conditions associated with it. Condition 1 represents the mask-target-mask condition when the SOA is short. Condition 2 represents the mask-target-mask condition when the SOA is long. Condition 3 represents the mask-fixation-mask condition when the SOA is short. Condition 4 represents the mask-fixation-mask condition when the SOA is long. Within each cell, the number of trials across the entire

experiment is specified. Including the target only condition, 390 trials will be performed per subject.

Additional pilot experiments

For the benefit of future experimenters who may build on this proposal, other pilot experiments are described below (see: additional pilots): These two additional pilot experiments were conducted on five subjects. The first experiment was a version of the proposed experiment, where only degraded faces were presented, to test whether we may identify significant BOLD responses to very briefly presented, degraded faces relative to fixation. The second experiment was a Glass pattern discrimination experiment, where participants indicated whether a target Glass pattern was concentric, radial, or translational. The second experiment was conducted to test for significant BOLD responses to Glass patterns relative to fixation, and significant differences in BOLD responses between different Glass pattern types.

fMRI analysis

General preprocessing steps

BOLD data from each subject will be pre-processed to remove noise and artifacts [60]. An anatomical average of each subject's cross-aligned BOLD data will be registered to his/her MP-RAGE. Spatial normalization will be performed using a 12-parameter affine warping of the individual MP-RAGE images to an atlas-representative target as described previously [61]. To measure the accuracy of atlas transformations, Eta (η) values will be derived from the correlation of similarity between the atlas and the

morphed MP-RAGE images. η^2 is the measure of variance in the source image that is accounted for by variance in the target image.

Visual cortical regions of interest (ROIs) will be defined via the functional localizers

Functional MRI data from the retinotopic localizer will be analyzed via Fourier analysis [57]. Briefly, the BOLD time course at each voxel will be derived. For a given voxel, the phase and amplitude of the BOLD time course at the stimulus frequency is extracted using a discrete Fourier transform. The response phase of a given voxel at the stimulus frequency measures the signal delay with respect to neural activity. From the signal delay, it is possible to infer the retinotopic location for the receptive field of a given voxel.

The preliminary results below used a simplified version of the retinotopic paradigm to delineate V1/V2. The data were analyzed via a general linear model. For the GLM the model was convolved with a Boynton function, and a contrast of the subtraction between magnitude estimates for vertical meridian blocks minus horizontal meridian blocks. A one sample t-test against 0 was performed on the magnitude estimates across all trials to determine whether the estimate at each voxel is statistically significant. Because the magnitude estimates derived from the GLM reflect the subtraction of the vertical meridian block estimates minus the horizontal meridian block estimates, the peak positive t-score indicates the putative location of the vertical meridian, and the peak negative t-score indicates the putative location of the horizontal meridian.

The dynamic and static face localizers will be analyzed via a general linear model (GLM) for each individual subject. For the GLM, the model will be convolved with a

Boynton function, and magnitude estimates per trial will be extracted for face blocks, object blocks, and a contrast of the subtraction between magnitude estimates for face blocks minus object blocks. As in the retinotopy localizer, the magnitude estimates derived for face and object blocks are relative to the baseline (i.e. the fixation blocks in this paradigm). For example, an estimate of 0 at a given voxel for a given face block would indicate that the BOLD response of the voxel during the given face block is the same as it is during fixation. Therefore, a one-sample t-test against 0 will be performed on the magnitude estimates across all trials to determine whether the estimate at each voxel is statistically significant. A piloted version of the dynamic face localizer is described in the preliminary results section.

For these ROIs, fMRI time courses from the sandwich masking experiment will be examined

Functional MRI data will be analyzed via a general linear model (GLM) with an in-house software package [62, 63]. No assumptions about the shape of the signal will be made. Instead, the signal will be examined for 7 successive MR frames to examine the entire hemodynamic response. The GLM calculates estimates of the hemodynamic response based on a model derived from the task. Its estimates will be run through a condition by time ANOVA to determine significant differences within the estimates. A main effect of time informs whether a deviation in BOLD is significantly greater than (activation) or less than (deactivation) baseline. An interaction between condition and time will inform whether the estimates are significantly different between conditions. Time courses will be extracted from individually defined ROIs from the functional localizers. A main effect of time (7-levels) repeated measures ANOVA will be performed on the target condition per ROI. Separate condition by time (4 x 7) repeated measures

ANOVAs, which exclude the target-only condition, will be performed per mask type on the time courses for each ROI.

Significant condition by time course interactions will be broken down via two planned comparisons using pairwise t-tests at the peak of the hemodynamic response. An example of the time courses that may be observed is shown in Figure 5.1. If a given region shows increased activity for the target-only trials, then the region is responsive to the target itself (Figure 5.1A). Mask-fixation-mask tests whether a given region responds to the mask itself. Mask-fixation-mask long, compared to short, SOAs tests whether the region may be important for mask-mask interactions (Figure 5.1B) because the short SOA will impair the visibility of the first mask. Mask-target-mask long, compared to short, SOAs tests whether the region is important for mask-target interactions (Figure 5.1C). Such a finding would suggest that the region may instantiate a shared mechanism, because the short SOA will impair target visibility while the long SOA does not.

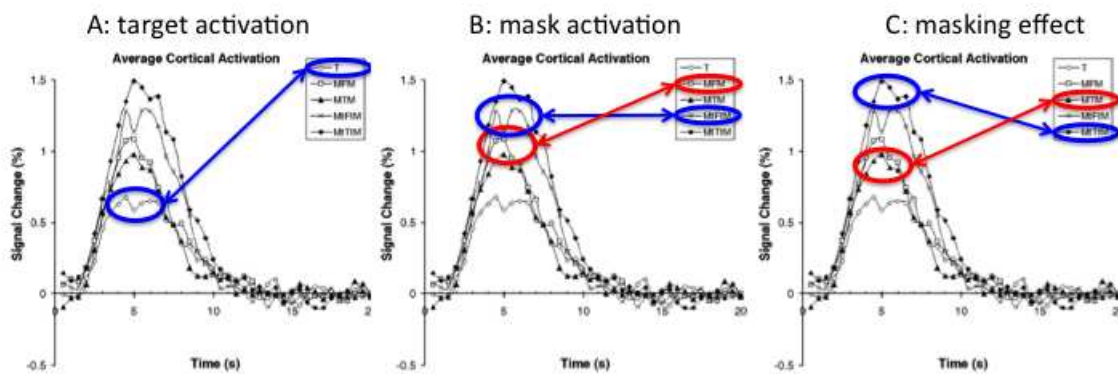


Figure 5.1. Illustrative data for a sandwich masking experiment were reproduced from Huang et al [52] figure 3. Each plot contains the same time courses for target-only presentations (T), mask-target-mask presentations with long (MtTtM) and short (MTM) SOAs, and mask-fixation-mask presentations for long (MtFtM) and short (MFM) SOAs. (A) Increases in the target only

condition (blue circles) would suggest that the region is responsive to the target itself. (B) If the BOLD signal in a region increases for mask-fixation-mask trials, and if the MtFtM (blue circles) BOLD response is greater than the MFM (red circles) BOLD response, then when the mask masks itself, the region's activity is suppressed. (C) Regions where the BOLD response is greater for MtTtM (blue circles) than MTM (red circles) trials would indicate a region whose responses to the target are suppressed by the mask.

Preliminary Results

Functional localizers can define ROIs in low- and high-level visual cortical regions per subject

Retinotopy localizer will delineate V1 and V2 regions

Preliminary results for an individual subject are overlaid on a cortical flat map (Figure 5.2). As described in the methods, this map was generated from a GLM analysis of the simplified retinotopic localizer. Boundaries for V1 and V2 are determined based on retinotopic organization. The dorsal boundary between V1 and V2 represents the lower vertical meridian. The ventral boundary between V1 and V2 represents the upper vertical meridian. The dorsal and ventral boundaries of V2 represent the horizontal meridian.

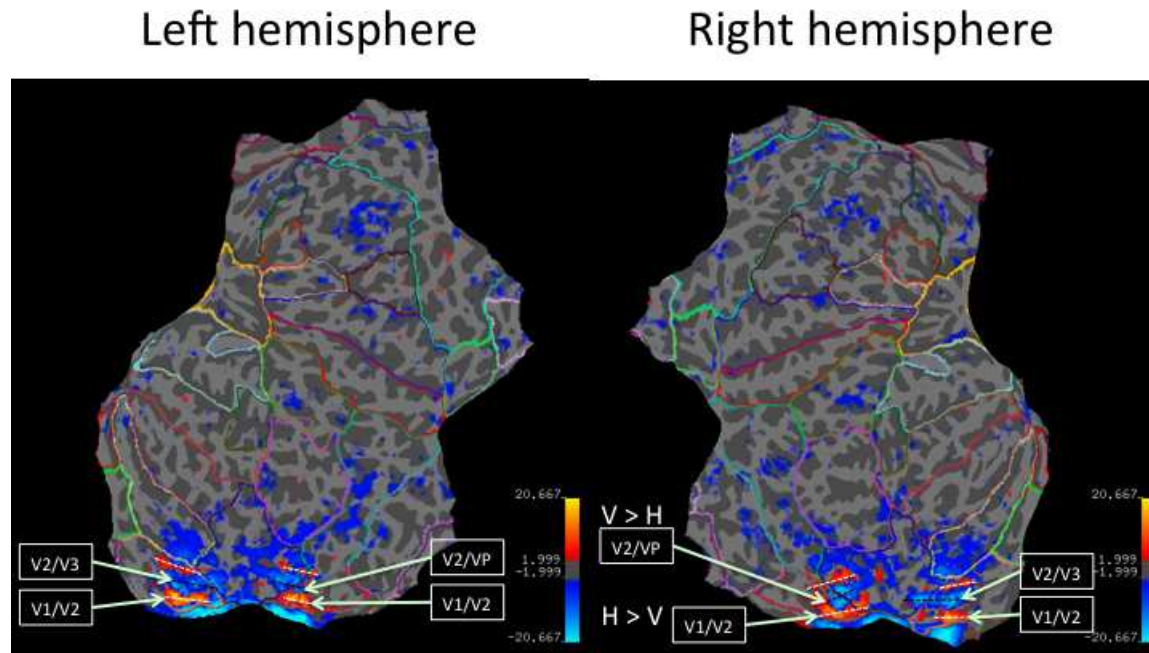


Figure 5.2. T-score statistical map produced from the retinotopic localizer as visualized on a flattened cortical representation. The map is oriented posterior-anterior from bottom to top, where the bottom of the map reflects the calcarine fissure. The lateral edges of the map (e.g. the right side of the right hemisphere and the left side of the left hemisphere) represent the most dorsal portions of cortex. The colored grid lines represent gyral and sulcal boundaries. More yellow regions respond the strongest to the vertical meridian (denoted by white-dashed lines), while bright blue regions respond the strongest to the horizontal meridian (denoted by black-dashed lines). On this map, the anterior V1/V2 boundaries are the first orange lines from the bottom, while the anterior V2 boundaries are represented by the second set of orange lines from the bottom.

Dynamic localizer identify face-sensitive and object-sensitive visual regions

Preliminary results for an individual subject are shown in Figure 5.3. The dynamic face localizer may consistently reveal several visual regions that show greater BOLD

responses for faces relative to objects in the fusiform gyrus, superior temporal sulcus, and inferior occipital gyrus.

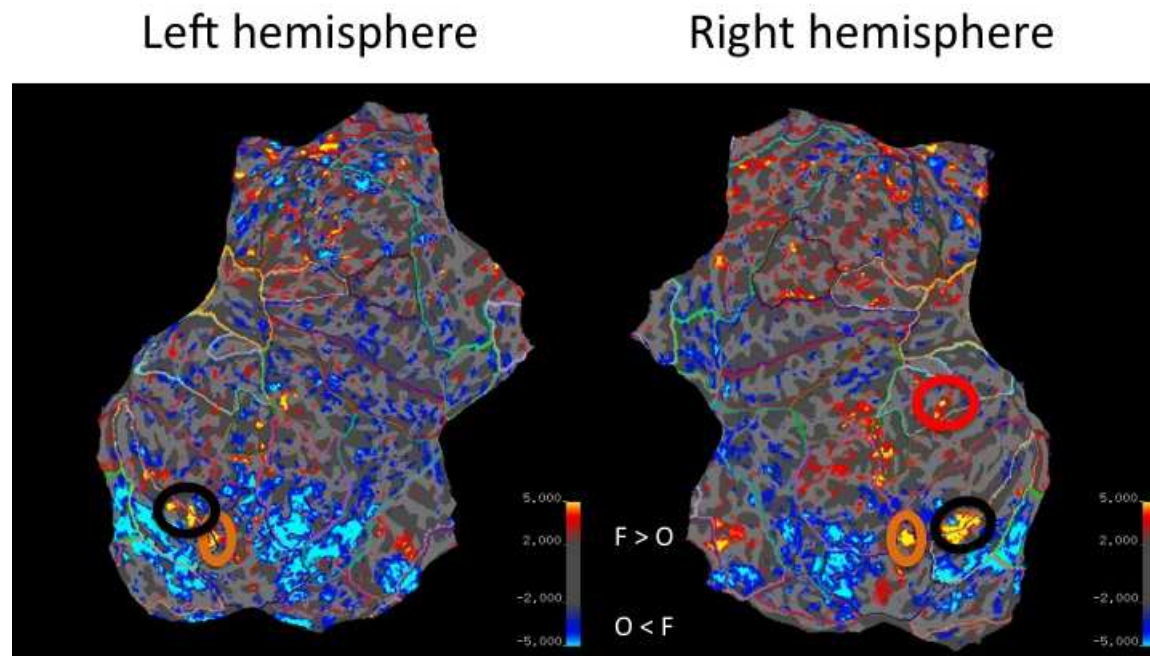


Figure 5.3. T-score statistical map from the dynamic localizer overlaid on a flattened cortical representation. The orientation of the flattened cortex is the same as in Figure 5.2. Red-orange colors represent regions with greater face than object activity, while blue colors represent regions with greater object than face activity. Face sensitive regions can be identified in: bilateral inferior occipital face gyrus (circled in orange), bilateral fusiform gyrus (circled in black), and right superior temporal sulcus (circled in red).

Expected Results

Time courses in face-sensitive visual cortical regions may reveal interactions between concentric Glass pattern and face processing

Per subject, time courses will be extracted from face-sensitive ROIs defined in the functional localizers (Figure 5.4) and analyzed with a condition by time repeated

measures ANOVA. Target presentations will show significant BOLD responses because the region is responsive to faces. For concentric Glass pattern masks, face-sensitive regions will be sensitive to concentric Glass pattern presentation (Figure 5.4A), consistent with previous findings [21]. A significant condition by time interaction will be observed in face-sensitive regions. Planned pairwise comparisons will reveal significantly larger BOLD responses for mask-fixation-mask presentations with long, relative to short, SOAs, suggesting that the region is important for mask-mask interactions. Mask-target-mask presentations will show significantly larger BOLD responses when the SOA is long, relative to short SOAs, suggesting that the region's activity is suppressed when concentric masks impair the ability to discriminate face targets.

Face sensitive regions may not be sensitive to radial and translational Glass patterns, and no effect of masking will be observed on the BOLD signal (Figure 5.4B and Figure 5.4C). No significant condition by time interaction will be observed in face sensitive regions for these conditions. Planned pairwise comparisons will show no significant differences.

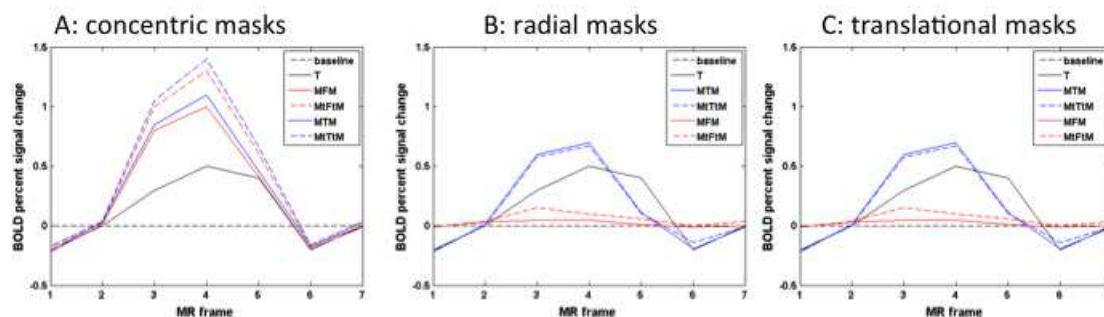


Figure 5.4. Time course plots for the different masking conditions in a putative face-sensitive region. From left to right, each chart plots time courses for (A) concentric, (B) radial, and (C)

translational masking conditions. The black dotted line represents the baseline of 0 for illustrative purposes. The black solid line (T) represents the target-only condition. The blue lines represent the mask-target-mask presentations for short (solid line: MTM) and long (dotted line: MtTtM) SOA conditions. The red lines represent the mask-fixation-mask presentations for short (solid line: MFM) and long (dotted line: MtFtM) SOA conditions. Comparisons are discussed in the main text.

Time courses in mid-level visual cortical regions may reveal interactions between concentric Glass pattern, radial Glass pattern and face processing

Time courses for the mid-level ROIs (Figure 5.5) will reveal that mid-level visual regions are sensitive to faces and concentric and radial Glass patterns. Both concentric and radial masking will suppress the BOLD signal in these regions. Target presentations will show significant BOLD responses in a given mid-level region, because many visual stimuli increase BOLD responses in mid-level visual regions [21, 51]. For concentric (Figure 5.5A) and radial (Figure 5.5B) Glass pattern masks, a significant condition by time interaction will be observed. Planned comparisons will reveal greater BOLD responses for mask-fixation-mask presentations with long SOAs, than short SOAs, suggesting that the region is important for both concentric and radial Glass pattern mask-mask interactions. Mask-target-mask presentations will show greater BOLD responses when the SOA is long and not short, indicating that the mask effectively suppressed activity related to the target in mid-level regions.

For translational Glass pattern masks (Figure 5.5C), mid-level regions will not be sensitive to the pattern, and no effect of masking will be observed. A significant condition by time interaction will be observed because increases in the BOLD signal will be observed when both the target and mask are presented, but increases in the BOLD

signal will not be observed when only the mask is presented. Planned comparisons will show no mask-mask interactions and no mask-target interactions.

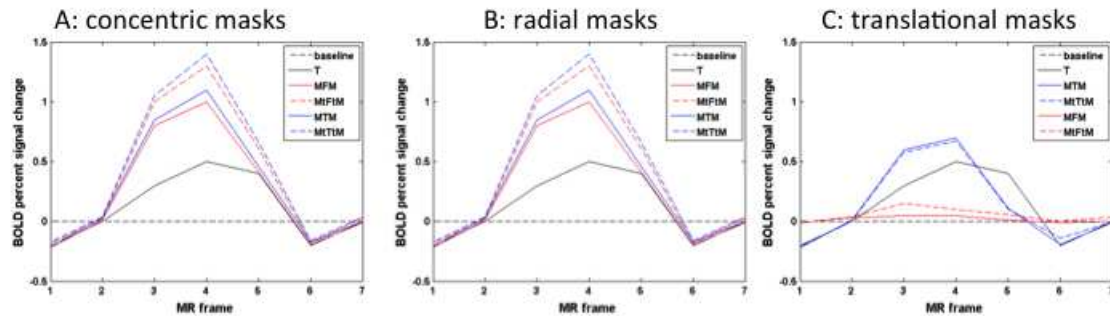


Figure 5.5. Time courses plots for a putative mid-level visual region. The presentation of the figure is the same as in Figure 5.3.

Time courses in low-level visual cortical regions may reveal interactions between translational Glass pattern and face processing

Time courses for the low-level ROIs (Figure 5.6) will reveal that all Glass pattern masks suppress the BOLD response in these regions, because activity in low-level visual regions represents the elements of the Glass pattern (i.e. local orientation of specific dipoles), but does not discriminate between different Glass pattern global forms. Target presentations will show significant BOLD responses in low-level regions because activity in low-level visual regions generally increases when a visual stimulus is presented, regardless of the global form, whereas successively higher-levels of the visual system may only show responses to specific forms [21]. For concentric (Figure 5.6A), radial (Figure 5.6B), and translational Glass pattern masks (Figure 5.6C), a significant condition by time interaction will be observed. For all masks, planned comparisons will show greater BOLD responses for long, relative to short, SOA mask-

fixation-mask presentations, and mask-target-mask presentations will show greater BOLD responses when the SOA is long.

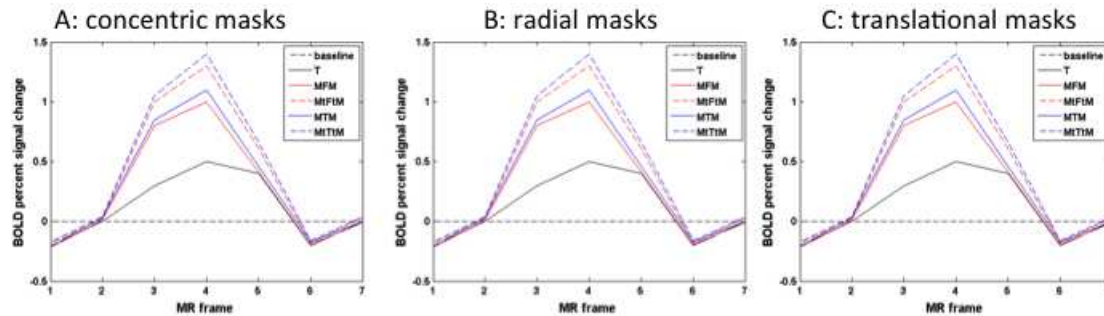


Figure 5.6. Time course plots for a putative low-level visual region show a masking effect that is not specific to any pattern. The presentation of the figure is the same as in figure 5.5.

Additional pilots

Because the proposed experiment above involves presenting faces that are degraded and briefly presented (see: Chapter 3 methods for the details), we wanted to ensure that degraded and briefly presented faces could generate BOLD responses in higher-level visual regions, such as the fusiform face area (FFA), in individual subjects. Such a result would demonstrate that we could produce robust high-level responses to faces in our proposed experiment. Therefore, we piloted a version of this experiment in 5 subjects, where only the targets are presented. In this version, the target was either an upright or inverted face and subjects had to indicate whether the target was upright or inverted. Faces were degraded as described in Chapter 3 (figure 3.9A and figure 3.9B). We used a general linear model approach to derive estimates for upright face and inverted face trials, as described in the methods section. The results for a representative subject show that significant BOLD responses for both upright (figure

5.7A) and inverted face trials (figure 5.7B), relative to fixation, occur in the fusiform gyrus. Such results suggest that higher-level visual regions will show greater BOLD responses for the target relative to fixation in the proposed study.

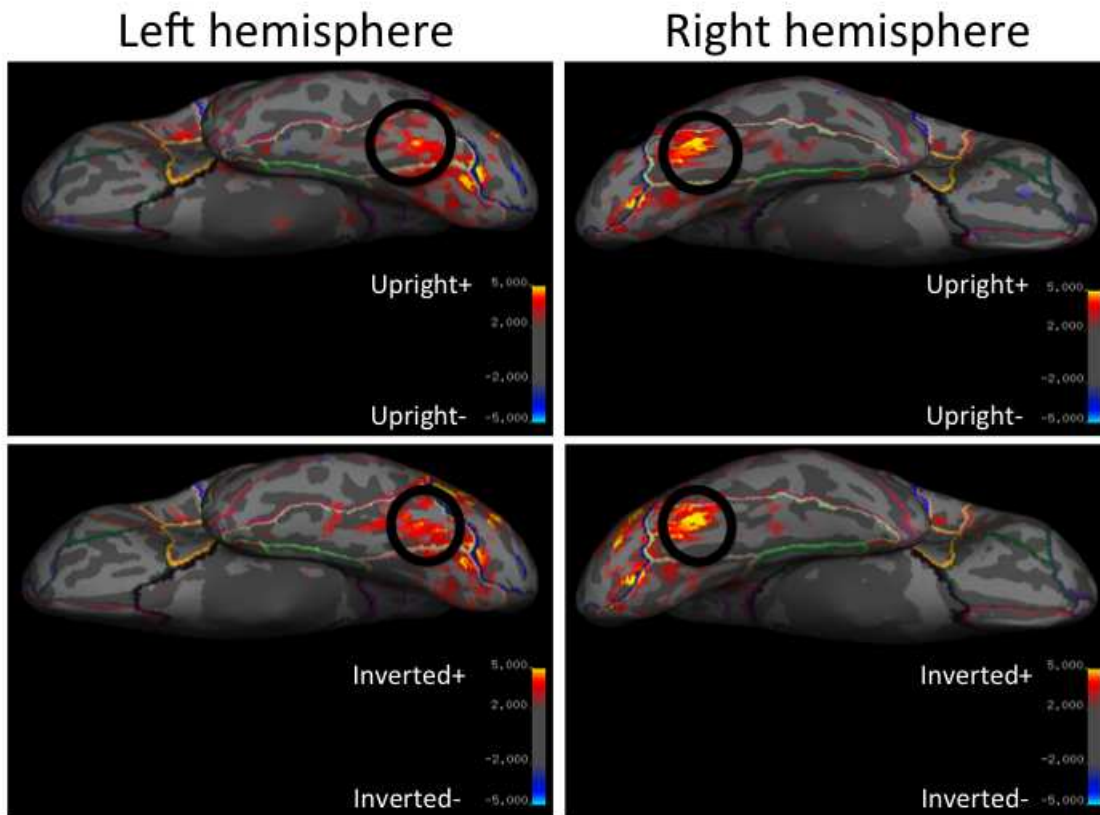


Figure 5.7. Statistical maps from degraded faces task for a single representative subject overlaid on the subject's native cortical surface. The inferior view of the surface is shown to highlight the fusiform gyrus (tan lines denote the boundaries). (A) left hemisphere view of the statistical maps for upright faces relative to fixation (top) and inverted faces relative to fixation (bottom). The posterior portion of the fusiform gyrus shows significant BOLD responses for both upright and inverted faces (black circles). (B). Right hemisphere view of the statistical maps for upright faces relative to fixation (top) and inverted faces relative to fixation (bottom). As in the left hemisphere, the right hemisphere fusiform gyrus shows significant BOLD responses for both upright and inverted faces (black circles).

To test whether BOLD responses in higher-level regions would be sensitive to specific types of Glass patterns (i.e. concentric and/or radial, but not translational), the same five subjects participated in a Glass pattern discrimination task. For each trial a Glass pattern would be presented for 500 milliseconds, and the subject would indicate whether the Glass pattern was concentric, radial, or translational. In the five-subject group, we found robust BOLD responses to the Glass patterns relative to fixation, but we found no significant differences in BOLD responses between the Glass pattern types (data not shown). It is unclear why, but the most parsimonious explanation for these findings is that we were underpowered to detect differences in the BOLD signal between global and local Glass pattern types. Additionally, by asking the subjects to discriminate between Glass pattern types, we may have changed how the subjects were processing the different Glass pattern types, and in turn, this may have affected BOLD responses in higher-level visual regions to all the Glass patterns. Future piloting using the proposed experiment may provide a solution to both problems. Glass patterns in the proposed experiment are passively viewed because they are masks and not targets, and additional data may provide sufficient power to show significant differences in BOLD responses to different Glass pattern types.

Discussion

Differences in BOLD responses across Glass pattern mask conditions would suggest differences in the shared mechanisms between the Glass pattern types and faces. We predict concentric, and not non-concentric, Glass pattern masking will suppress BOLD activity in face-selective regions. Because said regions are most sensitive to concentric Glass patterns and faces, this interaction would suggest that

face-selective regions instantiate a mechanism involved in concentric and face perception. This is consistent with the findings from a previous study that demonstrated regions with face-specific activity also show significant activity for concentric, but not radial forms [21], and behavioral studies that suggest concentric and radial Glass patterns are processed differently [29, 66]. Therefore, our experiment would be a direct test for whether concentric Glass patterns, radial Glass patterns, and faces all share a common processing mechanism.

Radial and concentric Glass pattern masking may both suppress BOLD activity in mid-level visual regions. This would suggest that radial and concentric Glass patterns and faces share a mechanism at the level of these regions. Taken together with the findings for face-sensitive regions, it would suggest that two mechanisms involved in face perception would be utilized by Glass pattern perception. One mechanism may be specific to faces and concentric Glass patterns, while the other may be more related to general form perception. Such a finding would be consistent with the similarities in concentric and radial Glass pattern perception, where the arrangement of the features are important for perceiving the global form [19, 20], and the respective differences found in fMRI [51, 65] and visual psychophysics studies [29, 66]. The shared process may relate to the fourth stage of the computational model, where the local information is pooled to determine the shape of an object [22].

All Glass pattern masks will suppress BOLD activity in low-level regions. Therefore, the fact that low-level regions will respond to both translational Glass patterns and faces would not suggest a shared mechanism between translational Glass patterns and faces, because low-level visual region activity does not relate to the Glass

pattern global form [51]. The lack of specific findings for translational Glass patterns would be consistent with neurophysiological [21, 64] and psychophysical [19, 20, 50] studies that suggest translational Glass pattern perception does not require processing a global form.

Pitfalls

Efficacy of the functional localizers

It may be possible that the functional localizers are unable to reliably identify low-, mid-, and high-level visual regions for each individual subject in the time allowed with reasonable (a) scanning session(s). Fortunately, the fMRI masking paradigm, itself, can be used to test whether potentially suppressed regions are responsive to faces and Glass patterns themselves [52]. As discussed in the results section, significant BOLD responses to target-only presentations would indicate that a given region is sensitive to faces, while significant BOLD responses to mask-only presentations would indicate that a given region is sensitive to the Glass pattern mask.

Masking effects on lower-level regions may limit the interpretation of results from higher-level regions

It is possible that BOLD responses in higher-level regions will also reveal translational Glass pattern-masking effects. Such a finding would limit the ability to interpret concentric and radial masking effects from higher-level regions. In such a case, it will remain possible that the entirety of the translational masking effect reflects interactions at low-level processes. Because the activity from the low-level visual regions serves as input into higher-level visual regions, the suppression of activity in the low-level regions may result in reduced activity in the higher-level visual regions. This

concept is known as “inheritance” [25]. Because higher-level visual regions contain neurons with larger receptive field sizes than lower-level visual regions, one way to test whether translational masking effects are inherited is to examine the spatial transfer of the masking effect. By placing the target face in locations where the target and Glass pattern mask overlap for higher-level, but not lower-level, cell receptive fields, one should reduce the impact of masking on low-level, but not high-level, visual regions. If translational Glass pattern masking effects are inherited from low-level visual regions, then the effect of translational masking would be reduced. If concentric and radial Glass pattern masking effects are instantiated in higher-level regions, then concentric and radial masking effects would not be reduced.

Conclusion

The fMRI experiment here can provide a rich set of data that better characterizes the masking effects observed in the behavioral studies. Low-, mid-, and high-level visual regions can be delineated using functional localizers. For each region, the sandwich-masking paradigm can determine whether it is face-sensitive, Glass pattern-sensitive, or instantiates a shared mechanism for faces and Glass patterns. We expect to see concentric masking effects for face sensitive regions only, concentric and radial masking effects for mid-level general regions, and a non-specific masking effect for low-level regions. Such a set of findings would identify the neural regions affected by Glass pattern masking, and provide further evidence that faces and concentric Glass patterns share a common processing mechanism.

References

1. Thompson, P., *Margaret Thatcher: a new illusion*. Perception, 1980. **9**(4): p. 483-4.
2. Diamond, R. and S. Carey, *Why faces are and are not special: an effect of expertise*. J Exp Psychol Gen, 1986. **115**(2): p. 107-17.
3. Young, A.W., D. Hellawell, and D.C. Hay, *Configurational information in face perception*. Perception, 1987. **16**(6): p. 747-59.
4. Tanaka, J.W. and M.J. Farah, *Parts and wholes in face recognition*. Q J Exp Psychol A, 1993. **46**(2): p. 225-45.
5. Rhodes, G., S. Brake, and A.P. Atkinson, *What's lost in inverted faces?* Cognition, 1993. **47**(1): p. 25-57.
6. Lewis, M.B. and R.A. Johnston, *The Thatcher illusion as a test of configural disruption*. Perception, 1997. **26**(2): p. 225-7.
7. Gauthier, I. and M.J. Tarr, *Becoming a "Greeble" expert: exploring mechanisms for face recognition*. Vision Res, 1997. **37**(12): p. 1673-82.
8. Gauthier, I. and C.A. Nelson, *The development of face expertise*. Curr Opin Neurobiol, 2001. **11**(2): p. 219-24.
9. Mondloch, C.J., R. Le Grand, and D. Maurer, *Configural face processing develops more slowly than featural face processing*. Perception, 2002. **31**(5): p. 553-66.
10. Maurer, D., R.L. Grand, and C.J. Mondloch, *The many faces of configural processing*. Trends Cogn Sci, 2002. **6**(6): p. 255-260.
11. Joseph, R.M. and J. Tanaka, *Holistic and part-based face recognition in children with autism*. J Child Psychol Psychiatry, 2003. **44**(4): p. 529-42.
12. Rouse, H., et al., *Do children with autism perceive second-order relational features? The case of the Thatcher illusion*. J Child Psychol Psychiatry, 2004. **45**(7): p. 1246-57.
13. Boutsen, L., et al., *Comparing neural correlates of configural processing in faces and objects: an ERP study of the Thatcher illusion*. Neuroimage, 2006. **32**(1): p. 352-67.
14. Benton, C.P. and E.C. Burgess, *The direction of measured face aftereffects*. J Vis, 2008. **8**(15): p. 1 1-6.
15. Mondloch, C.J. and D. Maurer, *The effect of face orientation on holistic processing*. Perception, 2008. **37**(8): p. 1175-86.
16. Loffler, G., et al., *Configural masking of faces: evidence for high-level interactions in face perception*. Vision Res, 2005. **45**(17): p. 2287-97.
17. Gilaie-Dotan, S. and R. Malach, *Sub-exemplar shape tuning in human face-related areas*. Cereb Cortex, 2007. **17**(2): p. 325-38.
18. Rentschler, I., B. Treutwein, and T. Landis, *Dissociation of local and global processing in visual agnosia*. Vision Res, 1994. **34**(7): p. 963-71.
19. Wilson, H.R. and F. Wilkinson, *Detection of global structure in Glass patterns: implications for form vision*. Vision Res, 1998. **38**(19): p. 2933-47.
20. Wilson, H.R., F. Wilkinson, and W. Asaad, *Concentric orientation summation in human form vision*. Vision Res, 1997. **37**(17): p. 2325-30.
21. Wilkinson, F., et al., *An fMRI study of the selective activation of human extrastriate form vision areas by radial and concentric gratings*. Curr Biol, 2000. **10**(22): p. 1455-8.

22. Poirier, F.J. and H.R. Wilson, *A biologically plausible model of human shape symmetry perception*. J Vis, 2010. **10**(1).
23. Rolls, E.T., *Consciousness absent and present: a neurophysiological exploration*. Prog Brain Res, 2004. **144**: p. 95-106.
24. Breitmeyer, B.G., *Visual masking: past accomplishments, present status, future developments*. Adv Cogn Psychol, 2007. **3**(1-2): p. 9-20.
25. Krekelberg, B., G.M. Boynton, and R.J. van Wezel, *Adaptation: from single cells to BOLD signals*. Trends Neurosci, 2006. **29**(5): p. 250-6.
26. Kohn, A., *Visual adaptation: physiology, mechanisms, and functional benefits*. J Neurophysiol, 2007. **97**(5): p. 3155-64.
27. Clifford, C.W., et al., *Visual adaptation: neural, psychological and computational aspects*. Vision Res, 2007. **47**(25): p. 3125-31.
28. Packer, O.S., et al., *Blue-yellow opponency in primate S cone photoreceptors*. J Neurosci, 2010. **30**(2): p. 568-72.
29. Ross, J. and J. Edwin Dickinson, *Effects of adaptation to Glass pattern structure and to path of optic flow*. Vision Res, 2007. **47**(16): p. 2150-5.
30. Clifford, C.W. and E. Weston, *Aftereffect of adaptation to Glass patterns*. Vision Res, 2005. **45**(11): p. 1355-63.
31. Vreven, D. and J. Berge, *Detecting structure in glass patterns: an interocular transfer study*. Perception, 2007. **36**(12): p. 1769-78.
32. Gallant, J.L., R.E. Shoup, and J.A. Mazer, *A human extrastriate area functionally homologous to macaque V4*. Neuron, 2000. **27**(2): p. 227-35.
33. Gauthier, I., C. Klaiman, and R.T. Schultz, *Face composite effects reveal abnormal face processing in Autism spectrum disorders*. Vision Res, 2009. **49**(4): p. 470-8.
34. van Kooten, I.A., et al., *Neurons in the fusiform gyrus are fewer and smaller in autism*. Brain, 2008. **131**(Pt 4): p. 987-99.
35. Scherf, K.S., et al., *Atypical development of face and greeble recognition in autism*. J Child Psychol Psychiatry, 2008. **49**(8): p. 838-47.
36. Klin, A. and W. Jones, *Altered face scanning and impaired recognition of biological motion in a 15-month-old infant with autism*. Dev Sci, 2008. **11**(1): p. 40-6.
37. Spezio, M.L., et al., *Abnormal use of facial information in high-functioning autism*. J Autism Dev Disord, 2007. **37**(5): p. 929-39.
38. Rutherford, M.D., K.A. Clements, and A.B. Sekuler, *Differences in discrimination of eye and mouth displacement in autism spectrum disorders*. Vision Res, 2007. **47**(15): p. 2099-110.
39. Pellicano, E., et al., *Abnormal adaptive face-coding mechanisms in children with autism spectrum disorder*. Curr Biol, 2007. **17**(17): p. 1508-12.
40. Hadjikhani, N., et al., *Activation of the fusiform gyrus when individuals with autism spectrum disorder view faces*. Neuroimage, 2004. **22**(3): p. 1141-50.
41. Teunisse, J.P. and B. de Gelder, *Face processing in adolescents with autistic disorder: the inversion and composite effects*. Brain Cogn, 2003. **52**(3): p. 285-94.
42. Behrmann, M., C. Thomas, and K. Humphreys, *Seeing it differently: visual processing in autism*. Trends Cogn Sci, 2006. **10**(6): p. 258-64.

43. Tsao, D.Y. and M.S. Livingstone, *Mechanisms of face perception*. Annual Review of Neuroscience, 2008. **31**: p. 411-37.
44. Kanwisher, N., *Functional specificity in the human brain: a window into the functional architecture of the mind*. Proc Natl Acad Sci U S A, 2010. **107**(25): p. 11163-70.
45. Kanwisher, N., *Domain specificity in face perception*. Nature Neuroscience, 2000. **3**(8): p. 759-763.
46. Gauthier, I., et al., *Activation of the middle fusiform 'face area' increases with expertise in recognizing novel objects*. Nat Neurosci, 1999. **2**(6): p. 568-73.
47. Tarr, M.J. and I. Gauthier, *FFA: A flexible fusiform area for subordinate-level visual processing automatized by expertise*. Nature Neuroscience, 2000. **3**(8): p. 764-769.
48. Kobatake, E. and K. Tanaka, *Neuronal selectivities to complex object features in the ventral visual pathway of the macaque cerebral cortex*. J Neurophysiol, 1994. **71**(3): p. 856-67.
49. Hegde, J. and D.C. Van Essen, *A comparative study of shape representation in macaque visual areas v2 and v4*. Cerebral Cortex, 2007. **17**(5): p. 1100-16.
50. Aspell, J.E., J. Wattam-Bell, and O. Braddick, *Interaction of spatial and temporal integration in global form processing*. Vision Res, 2006. **46**(18): p. 2834-41.
51. Ostwald, D., et al., *Neural coding of global form in the human visual cortex*. J Neurophysiol, 2008. **99**(5): p. 2456-69.
52. Huang, J., M. Xiang, and Y. Cao, *Reduction in V1 activation associated with decreased visibility of a visual target*. Neuroimage, 2006. **31**(4): p. 1693-9.
53. Rodriguez, V., et al., *Absence of face-specific cortical activity in the complete absence of awareness: converging evidence from functional magnetic resonance imaging and event-related potentials*. J Cogn Neurosci, 2012. **24**(2): p. 396-415.
54. Kim, M.J., et al., *Behind the mask: the influence of mask-type on amygdala response to fearful faces*. Soc Cogn Affect Neurosci, 2010. **5**(4): p. 363-8.
55. Morris, J.P., K.A. Pelphrey, and G. McCarthy, *Face processing without awareness in the right fusiform gyrus*. Neuropsychologia, 2007. **45**(13): p. 3087-91.
56. Fox, C.J., G. Iaria, and J.J. Barton, *Defining the face processing network: optimization of the functional localizer in fMRI*. Hum Brain Mapp, 2009. **30**(5): p. 1637-51.
57. Engel, S.A., G.H. Glover, and B.A. Wandell, *Retinotopic organization in human visual cortex and the spatial precision of functional MRI*. Cereb Cortex, 1997. **7**(2): p. 181-92.
58. Kanwisher, N., J. McDermott, and M.M. Chun, *The fusiform face area: a module in human extrastriate cortex specialized for face perception*. J Neurosci, 1997. **17**(11): p. 4302-11.
59. Brainard, D.H., *The Psychophysics Toolbox*. Spat Vis, 1997. **10**(4): p. 433-6.
60. Miezin, F.M., et al., *Characterizing the hemodynamic response: Effects of presentation rate, sampling procedure, and the possibility of ordering brain activity based on relative timing*. NeuroImage, 2000. **11**: p. 735-759.

61. Snyder, A.Z., *Difference image vs. ratio image error function forms in PET-PET realignment*, in *Quantification of Brain Function Using PET*, R. Myer, et al., Editors. 1996, Academic Press: San Diego, CA. p. 131-137.
62. Ollinger, J.M., M. Corbetta, and G.L. Shulman, *Separating processes within a trial in event-related functional MRI II. Analysis*. Neuroimage, 2001. **13**(1): p. 218-229.
63. Ollinger, J.M., G.L. Shulman, and M. Corbetta, *Separating processes within a trial in event-related functional MRI I. The method*. Neuroimage, 2001. **13**(1): p. 210-217.
64. Smith, M.A., A. Kohn, and J.A. Movshon, *Glass pattern responses in macaque V2 neurons*. J Vis, 2007. **7**(3): p. 5.
65. Mannion, D.J., J.S. McDonald, and C.W. Clifford, *The influence of global form on local orientation anisotropies in human visual cortex*. Neuroimage, 2010. **52**(2): p. 600-5.
66. Chen, C.C., *A masking analysis of glass pattern perception*. J Vis, 2009. **9**(12): p. 221-11.

Appendix: The hemodynamic response in simplex autism

Although my dissertation focused on face perception in typical adults, I was initially interested in testing whether and how face perception is altered in autism. However, in reading the literature (for a review see: {Tsao, 2008 #8603}) on face perception, it became clear that the intermediate mechanisms involved in face perception were poorly understood. In order to understand better how people with autism perceive faces, I examined mechanisms underlying face processing in typical populations. At the same time, my work on autism examined the structural and functional differences of the brains of children with autism relative to typical children. The autism project culminated in a structural autism paper that is in work, a functional connectivity MRI paper also in work, and a task-evoked functional MRI paper, where we tested whether the hemodynamic response is normal in autism. The task-evoked functional MRI paper has been published and is reprinted in full in this appendix.

The citation is: **Feczko E**, Miezin FM, Constantino JN, Schlaggar BL, Petersen SE, Pruetz JR Jr. 2012. The hemodynamic response in children with Simplex Autism. *Dev Cogn Neurosci*. 2(4):396-408.

Abstract

Background: Numerous functional magnetic resonance imaging (fMRI) studies of the brain-bases of autism have demonstrated altered cortical responses in subjects with autism, relative to typical subjects, during a variety of tasks. These differences may reflect altered neuronal responses or altered hemodynamic response. This study searches for evidence of hemodynamic response differences by using a simple visual

stimulus and elementary motor actions, which should elicit similar neuronal responses in patients and controls.

Methods: We acquired fMRI data from two groups of 16 children, a typical group and a group with Simplex Autism, during a simple visuomotor paradigm previously used to assess this question in other cross-group comparisons. A general linear model estimated the blood-oxygen-level-dependent (BOLD) signal time course, and repeated-measures analysis of variance tested for potential cross-group differences in the BOLD signal.

Results: The hemodynamic response in Simplex Autism is similar to that found in typical children. Although the sample size was small for a secondary analysis, medication appeared to have no effect on the hemodynamic response within the Simplex Autism group.

Conclusions: When fMRI studies show BOLD response differences between autistic and typical subjects, these results likely reflect between-group differences in neural activity and not an altered hemodynamic response.

1. Introduction

Fluctuations in the blood-oxygen-level-dependent (BOLD) signal have been shown to couple tightly with neural activity (Logothetis, et al. 2001). Thus, functional Magnetic Resonance Imaging (fMRI) and functional connectivity MRI (fcMRI) can be used as indirect measures of neural activity. However, atypical subjects, such as children with ASD (Autistic Spectrum Disorders), may have a quantitatively different

relationship between the blood-oxygen-level-dependent (BOLD) signal, which is measured by fMRI, and neuronal responses, i.e. different neurovascular coupling.

This is important because recent fMRI studies (e.g., (Mostofsky, et al. 2009; Muller, et al. 2003)) have shown differences in the BOLD signal for motor, parietal, cerebellar, and prefrontal cortical regions of the brain during complex visuomotor tasks. Further, recent fcMRI studies have reported under-connectivity between anterior and posterior regions of the brain (e.g., (Cherkassky, et al. 2006)); aberrant connectivity in frontal, parietal, and occipital regions of the brain (e.g.,(Noonan, et al. 2009)); and reduced long range functional connection between regions of the brain comprising the default-mode network (e.g.,(Kennedy and Courchesne 2008; Monk, et al. 2009; Weng, et al. 2010)).

fMRI and fcMRI comparisons of ASD and typical subjects typically assume a hemodynamic response time course that, independent of differences in neural activity, is the same between ASD and typical subjects (e.g., (Gomot, et al. 2008; Kaiser, et al. 2010)). However, little data exist to show that the hemodynamic response is generally similar between people with and without ASD. In order to interpret properly the current autism fMRI literature, it is important to demonstrate that the basic hemodynamic response is similar between ASD and typical cohorts at typical sample sizes. A key first step would be to examine the hemodynamic response of people with and without ASD during a simple task, where the demands of the task are not likely to be affected by an ASD diagnosis (Church, et al. 2011, Church et al in press; Harris, et al. 2011). The value of this step is predicated on the assumption that the two cohorts would perform

the task the same way and have similar neuronal activity that could then be measured by fMRI. The limitations to this assumption are discussed in the Discussion section.

We compared the temporal dynamics of the BOLD signal between children with and without Simplex Autism (defined below) during a simple visuomotor task (Miezin, et al. 2000) in which we would expect no significant differences in the underlying neural activity. The same paradigm has been used to test the hypothesis that typical adults and children have the same fundamental relationship between neural activity and the BOLD signal (Kang, et al. 2003). If similar BOLD time courses are observed in multiple vascular distributions when the task is sufficiently simple that neuronal processing is expected to be equivalent in autistic and control children, then differences in BOLD time courses that are observed in fMRI autism studies of similar sample sizes more likely reflect differences in neural activity than differences in the hemodynamic response.

2. Materials and Methods

2.1 Participants

Simplex Autism refers to well-characterized ASD individuals with no affected first-degree relatives. Sixteen typical and 16 Simplex Autism children (ages 9 -14 years) were recruited using a variety of means, including recruitment from the local community through flyers and advertisements, and through other research collaborations.

Demographics are shown in Table 1. Subjects were screened out for a history of focal neurological deficit, strabismus, or vision not corrected to normal acuity with glasses. All subjects (typical and ASD) had no first-degree relatives with an ASD. In addition, typical children could not have any first-degree relatives with Attention-Deficit/Hyperactivity

Disorder (ADHD). Simplex Autism participants had 1) community MD or PhD clinical diagnoses of Autistic Disorder, Asperger's Disorder, or Pervasive Developmental Disorder Not Otherwise Specified (PDD-NOS), and 2) consensus research ASD diagnoses as measured by the Autism Diagnostic Observation Schedule (Lord, et al. 2000) and Autism Diagnostic Interview Revised (Lord, et al. 1994). Five typical and two Simplex Autism subjects were assessed in previous studies using the Wechsler Intelligence Scale for Children (WISC-IV). The other children were assessed using the Wechsler Abbreviated Scale of Intelligence (WASI). All children performed the vocabulary subtest of the corresponding assessment, and all but one typical child performed the block design subtest of the corresponding assessment. Informed consent and assent were obtained using procedures approved by the Washington University Human Research Protection Office.

[Insert Table 1]

2.2 MRI protocols

MRI data were acquired using a Siemens 3T Trio scanner (Erlangen, Germany) with standard 12-channel head coil. An iMac Macintosh computer (Apple, Cupertino, CA) running Psyscope X software (Cohen, et al. 1993) was used to control the stimulus display. Responses were recorded using a fiberoptic key-press device held in the subject's hands. An LCD projector was used to project stimuli onto a screen at the head of the bore. Subjects viewed the stimuli through a mirror attached to the head coil.

High-resolution structural images were acquired using a sagittal MP-RAGE T1 weighted sequence (TE=3.08ms, TR = 2.4s, TI = 1000ms, flip angle = 8°, 176 slices at 1 mm isotropic resolution/voxel). Functional images were acquired using a BOLD contrast

sensitive, gradient echo, echo-planar sequence (TE= 27ms, flip angle = 90°, 4x4x4 mm isotropic resolution/voxel). MR acquisition was 2.5 seconds/frame and consisted of 32 contiguous, axial slices, centered on the hemispheric divide and parallel to the AC-PC plane. The first four frames in each run were discarded to allow stabilization of longitudinal magnetization. Each functional run lasted approximately three minutes (72 frames). Four runs were acquired per subject.

2.3 Behavioral paradigm

The task, a jittered event-related design known to generate highly reproducible activation in sensorimotor and visual cortex for both adults and children, has been described in detail previously (Kang, et al. 2003; Miezin, et al. 2000). Briefly, subjects pressed a button at the onset and offset of a visual stimulus presented for 1.26 seconds. The visual stimulus was a radial counterphase-flickering checkerboard subtending ~11° of the visual field surrounding the fovea. Right and left index fingers were used for onset and offset respectively. Approximately 30 stimulus presentations appeared per 72-frame run. Accuracy, measured as a percentage of onset and offset omissions, and median reaction time (RT) per subject were evaluated using two-sample two-tailed t-tests.

2.4 fMRI data analysis

BOLD data from each subject were pre-processed to remove noise and artifacts (Kang, et al. 2003; Miezin, et al. 2000). Head motion per BOLD run was quantified using total root mean square (RMS) linear and angular displacement measures. For the main analysis, and in order to match the amount of head movement between the two cohorts, two of the four runs per subject were chosen, so that average total RMS head

movement was not significantly different between the two groups. The total RMS is derived from measurements in six directions relative to the first frame acquired across each run. We attempted to match best this total RMS between each typical and each ASD subject. As a result, we did not control for the order of the runs. Results were primarily analyzed from these motion-matched, selected pairs of runs. In addition, as a secondary analysis, results from each individual run and the combined set of four BOLD runs regardless of motion difference across groups were analyzed.

An anatomical average of each subject's cross-aligned BOLD data was registered to his/her MP-RAGE. Spatial normalization was performed using a 12-parameter affine warping of the individual MP-RAGE images to an atlas-representative target as described previously (Kang, et al. 2003; Snyder 1996). The atlas-representative target itself was constructed by 12-parameter affine co-registration of a group of MP-RAGE images representing two groups of 13 young children (ages 7-9) and 12 young adults (ages 21-30). To measure the accuracy of atlas transformations, Eta (η) values were derived from the correlation of similarity between the atlas and the morphed MP-RAGE images (Snyder 1996). η^2 is the measure of variance in the source image that is accounted for by variance in the target image (Kang, et al. 2003).

To investigate putative differences in the shape of the BOLD time course in Simplex Autism, no assumptions were made about its underlying shape. Preprocessed data were smoothed using a 2 mm full-width half-max kernel, and analyzed using an implementation of the general linear model (GLM). Both a constant offset and a linear trend terms were included in the GLM for each BOLD run. Seven time points (1 TR / MR frame = 2.5s apart) for each stimulus trial were modeled in the GLM. Significant

differences between the two cohorts were tested using a voxelwise group by time course (2 groups x 7 MR frames), sphericity corrected, repeated measures ANOVA (Kang, et al. 2003; Miezin, et al. 2000), which accounts for correlations in the design (Ollinger, et al. 2001a; Ollinger, et al. 2001b). The statistical maps were corrected for multiple comparisons using the Monte Carlo method (to achieve significance with $P < 0.05$, 24 contiguous voxels with a Z score > 3.5 are needed) (Kang, et al. 2003; McAvoy, et al. 2001). In-house software, (FIDL), was used to perform these analyses. Activated regions were identified in the statistical map generated from the main effect of time course. Effects of diagnosis were examined using the group by time course interaction statistical map. The group by time course interaction measures shape differences between the BOLD signals from the two cohorts. As alluded to above, five additional group by time repeated measures ANOVAs were performed to confirm the lack of a significant group by time interaction: one ANOVA combining all four runs per subject, and one ANOVA for each individual run per subject.

To assess potential differences further, ROIs were delineated from the main effect of time course map via a peak-finding algorithm as described elsewhere (Kang, et al. 2003; Miezin, et al. 2000). Time courses, averaged over the activated voxels, were derived per ROI and subject. Time courses for each ROI were entered into a group by time repeated measures ANOVA for subsequent analysis.

3. Results

Behavioral performance was examined in terms of both accuracy and RT. No differences in onset ($T_{30} = 1.197$, $P = 0.241$) and offset ($T_{17.057} = -1.630$, $P = 0.121$) RTs were observed between Simplex Autism and typical cohorts. No significant differences

were found between Simplex Autism and typical cohorts for onset and offset omissions (all $P > 0.09$). Omissions and incorrect responses represented less than 6% of all trials per subject.

3.1 Primary analysis: two runs per subject matched for differences in motion between Simplex Autism and typical cohorts

For the primary analysis, where two runs per subject were chosen in order to control for head movement, no significant differences in head movement were observed between the Simplex Autism and typical children ($T_{30} = 0.482$, $P = 0.633$). Mean RMS values for each group were under 1 mm (0.57 mm for Simplex Autism, 0.51 mm for typical). Mean η^2 values were similar between Simplex Autism (0.9902) and typical (0.9909) groups, and means were not statistically different ($T_{21.98} = 1.734$, $P = .097$).

After correcting for multiple comparisons, the voxelwise ANOVA revealed significant main effects of time course (Figure 1a, top), but no group by time course interactions (Figure 1a, bottom). A subset of participants (12 Simplex Autism and 12 typical participants), matched for both motion ($P = 0.33$) and full-scale IQ (Simplex Autism FSIQ = 111 +/- 8, typical FSIQ = 113 +/- 9, $P = 0.53$), were also examined to ensure that IQ differences did not mask any group by time interactions. Matching for IQ revealed no Monte-Carlo corrected significant group by time course interactions (Figure 1b, bottom).

[Insert Figure 1a]

[Insert Figure 1b]

Using a peak-finding algorithm, 67 ROIs were found that showed significant time courses in the main effect analysis. Of these 67 ROIs, 19 were chosen to sample varying vascular distributions. Average time courses were computed for the 19 delineated ROIs for Simplex Autism and typical cohorts. Figure 2 shows time courses for regions fed by anterior and middle cerebral arteries. Figure 3 shows time courses for regions fed by the perforating branches from the posterior cerebral artery. Figure 4 shows time courses for regions fed by the posterior cerebral artery. Figure 5 shows time courses for regions fed by the superior cerebellar artery. The individual time courses were entered into group by time repeated measures ANOVAs for subsequent analyses (Table 2: motion matched subjects; Table 3: motion and IQ matched). No significant diagnosis by time course interaction effects were found (all P values > 0.1).

[Insert Figure 2]

[Insert Figure 3]

[Insert Figure 4]

[Insert Figure 5]

[Insert Tables 2 & 3]

The Simplex Autism cohort was then split into two groups, those subjects that had been on one or more specific class of medications and those subjects not taking these medications. Each group has 8 subjects. The medications include stimulants, anti-psychotics, and selective serotonin reuptake inhibitors (SSRIs). The 19 main effect ROIs were entered into group (medicated / not) by time course repeated measures ANOVAs, and no significant effects were observed (all P values > 0.1).

3.2. Examination of group by time interactions found in the primary analysis at a liberal threshold

For further assessment, the time course X diagnosis interaction map was examined at an extremely liberal, uncorrected threshold of $Z > 1.9$. Two ROIs in visual cortex were chosen from the statistical Z map for this liberal time course X group interaction image (Figure 6). Time courses were extracted from these ROIs and analyzed for group by time interactions using a time course by group repeated measures ANOVA (Table 4). One ROI shows a significant group by time interaction (Figure 6, top); the other region shows a group by time interaction trend (Figure 6, bottom).

[Insert Table 4]

[Insert Figure 6]

3.3. Secondary analyses: All four runs combined per subject, and each run per subject

To help ensure that the lack of observed differences were not due to the selection of specific runs, all four runs acquired per subject were concatenated and analyzed using a diagnosis by time (2x7) repeated measures voxelwise ANOVA. After correcting for multiple comparisons, the voxelwise ANOVA revealed significant main effects of time course (Figure 7, top), and a small group by time course interaction (Figure 7, bottom). The region showing a significant interaction overlaps with the region showing an uncorrected interaction in the motion-controlled analysis.

[Insert Figure 7]

We also ran a group by time course (2x7) repeated measures ANOVA for each of the four runs the subjects performed. Because a single run contains fewer trials, the estimates derived from each subject's GLM are weaker, and the ability to detect significant differences is limited. Therefore, the main effect and interaction images from each run were binarized at a threshold of $Z > 1.9$ and summed into a conjunction image. As shown in the main effect conjunction image, all 19 regions of interest show consistent significant activation for each of the four runs (Figure 8, top). However, the group by time interaction conjunction image shows a consistent activation for a region in right visual cortex, which is the same region identified in the other secondary analyses (Figure 8, bottom).

[Insert Figure 8]

Regardless of whether two motion-matched runs, all four runs, or a conjunction of each individual run is analyzed, the only observed difference between Simplex Autism and typical cohorts is located in a very small portion of right visual cortex. Other regions from multiple vascular distributions show no differences in the hemodynamic response between Simplex Autism and typical cohorts.

4. Discussion

Through this study of BOLD time courses, we found that the hemodynamic response appears comparable between Simplex Autism and typical cohorts. Head motion can potentially induce artifacts in fMRI data, which can create false positive and false negative observations. When head motion was best matched between the two groups, no significant group effects were found. When groups were IQ and motion matched, no significant group by time interactions in the BOLD response were observed.

Comparisons of medicated to non-medicated Simplex Autism subjects revealed no significant differences in BOLD activity. It should be noted that this observation is limited due to very small numbers in each cell. It is also possible that different medications could have differing or opposing effects on the hemodynamic response. Nevertheless, the data acquired show no evidence that the combined effect of medications commonly used in people with ASD impacts the hemodynamic response in this sample.

The present study represents a first step in testing whether the hemodynamic response in autism is distinguishable from typically developing children. By using a task sufficiently simple that we can assume that the two groups are performing the task similarly (Church, et al. in press; Harris, et al. 2011), demonstrable differences in BOLD response could be interpreted as evidence for an altered hemodynamic response in autism. As stated above, our approach yielded no compelling evidence for Simplex Autism versus control differences in the shape of the task-evoked BOLD signal, in multiple comparisons-corrected analyses of motion-matched BOLD runs. There are several limitations, discussed immediately below.

When head motion was ignored or statistical thresholding was relaxed far below what we would consider appropriate in reporting an “fMRI effect”, a small region located in right visual cortex appears to be significantly different between Simplex Autism and typical cohorts. One could argue that this difference may represent an altered hemodynamic response localized exclusively to a small portion of right visual cortex. However, it is possible that the difference observed in right visual cortex may relate to an unmeasured behavior. Visual fixation was only qualitatively assessed, and because people with autism may have trouble with oculomotor control (Goldberg, et al. 2000; Goldberg, et al. 2002; Luna, et al. 2007; Minshew, et al. 1999) and fixating a point (Mahone, et al. 2006; Pruett, et al. 2011), it is possible that small differences in visual fixation may have led to some small differences in visual cortical activity. Because lurking variables can potentially confound the interpretation of fMRI data, it is important to be cautious in estimating the statistical significance of an effect, in interpreting a

single finding, and in rigorously examining the quality of the data (Church, et al. in press).

The data presented here only directly pertain to neural processing resources that are engaged in this particular task. Combined electrophysiological and fMRI recordings from mice have shown that different neurons, even within the same brain region (Enager, et al. 2009), differ in their neurovascular coupling (Devonshire, et al. 2012; Sloan, et al. 2010). Therefore, it is possible that driving other populations of neurons might show differentials in fMRI responses.

Our claim, that the hemodynamic response is not altered in autism, is an operational claim, for our data do not measure neural activity directly. One interpretation of this operational claim is that the neurovascular coupling is comparable between autistic and typical cohorts. However, it is theoretically possible that some combination of altered neural activity and altered neurovascular coupling could negate each other, leaving no observed differences in BOLD activity in multiple vascular distributions. Combining MEG and/or EEG with fMRI acquisition might directly address this possibility, by providing convergent electrophysiological data that can dissociate effects of neural activity from effects of neurovascular coupling.

Because these limitations assume that both neural activity and neurovascular coupling are altered in autism, these limitations would seem to be more troubling if robust BOLD response differences were observed between the two groups. However, the data presented here show scant evidence of any meaningful difference in the hemodynamic response in ASD at these sample sizes for neural populations that are responsive to this task. A lack of significant group by time course interactions does not

indicate that the hemodynamic response is completely “normal” in Simplex Autism. However, it is encouraging to see that the hemodynamic response appears comparable in multiple vascular distributions during a simple straightforward task. This finding is important for autism fMRI / fcMRI research because it indicates that, for studies of a similar sample size, when strong autism versus control differences are seen with BOLD contrast in the regions investigated in this study, the observation is more likely not attributable to differential neurovascular coupling, but reflects differences in underlying neural activity.

Acknowledgements

This work was supported by a grant from the Simons Foundation Autism Research Initiative (“Brain Circuitry in Simplex Autism,” Steve Petersen – PI). John Pruett’s effort was supported by K12 EY16336. We thank Sarah Hoertel, for coordinating recruitment, scheduling, and assessments of the subjects. We also thank Kelly McVey for help with recruitment, scheduling, assessing, and scanning subjects. We thank Jen Simmons, Anna Abbacchi, Teddi Gray and others from the Constantino lab for assessing and/or recruiting subjects. We would also like to thank Dan Marcus and his lab for database support.

Financial Disclosures

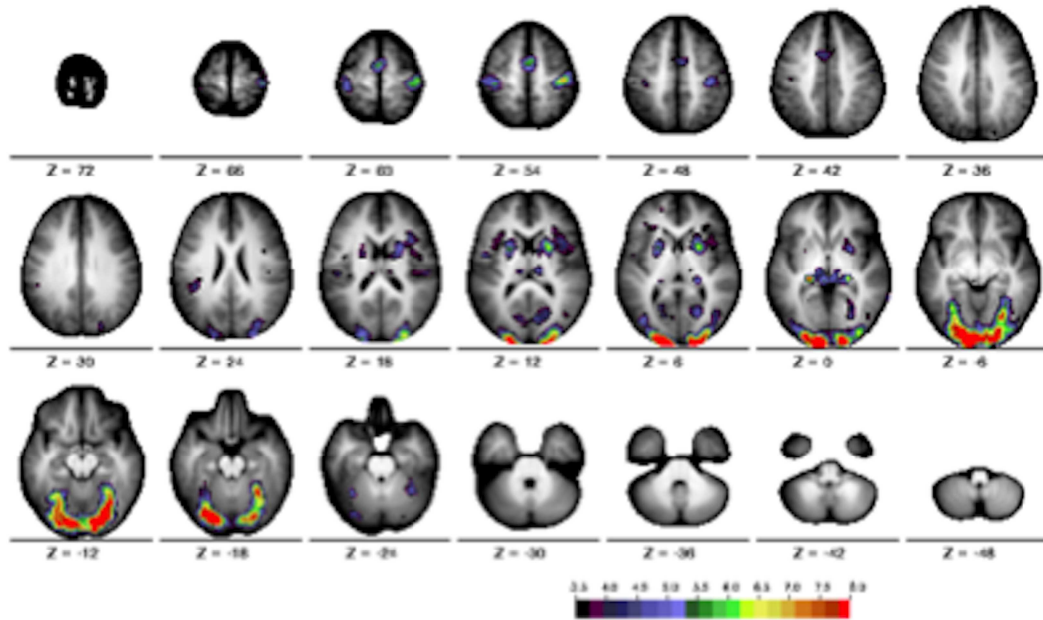
Eric Feczko reports no biomedical financial interest or potential conflicts of interest. Fran Miezin reports no biomedical financial interest or potential conflicts of interest. Dr. Schlaggar reports no biomedical financial interest or potential conflicts of interest. Dr. Constantino receives royalties on the Social Responsiveness Scale, which is published and distributed by Western Psychological Services. Dr. Petersen reports no biomedical financial interest or potential conflicts of interest. Dr. Pruett reports no biomedical financial interest or potential conflicts of interest.

References

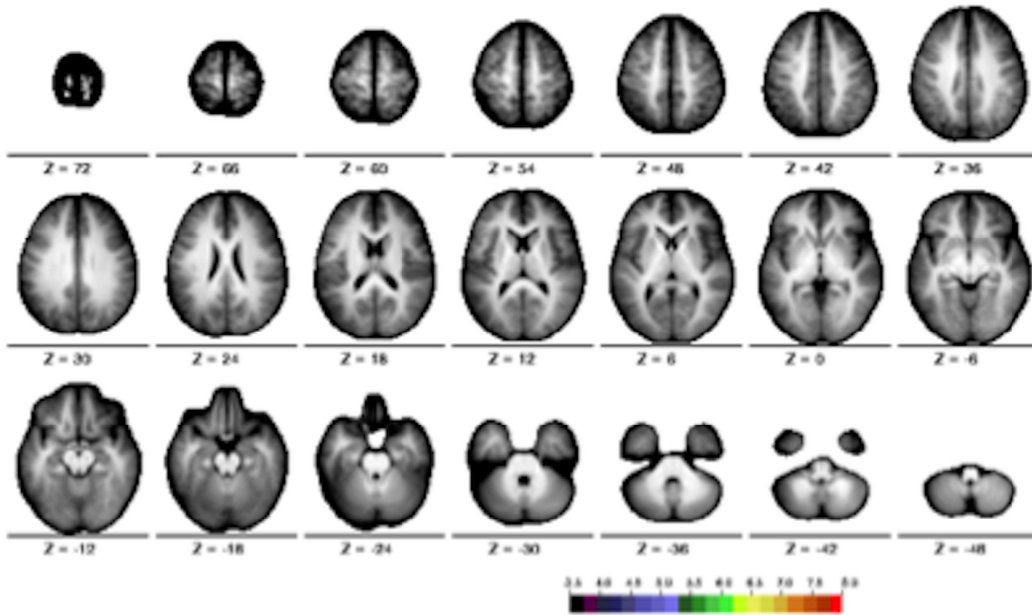
- Cherkassky VL, Kana RK, Keller TA, Just MA. 2006. Functional connectivity in a baseline resting-state network in autism. *Neuroreport* 17(16):1687-90.
- Church JA, Petersen SE, Schlaggar BL. in press. Comment on “The physiology of developmental changes in BOLD functional imaging signals” by Harris, Reynell, and Attwell. *Developmental Cognitive Neuroscience*.
- Cohen JD, MacWhinney B, Flatt M, Provost J. 1993. PsyScope: A new graphic interactive environment for designing psychology experiments. *Behavioral Research Methods, Instruments, and Computers* 25(2):257-271.
- Devonshire IM, Papadakis NG, Port M, Berwick J, Kennerley AJ, Mayhew JE, Overton PG. 2012. Neurovascular coupling is brain region-dependent. *Neuroimage* 59(3):1997-2006.
- Enager P, Piilgaard H, Offenhauser N, Kocharyan A, Fernandes P, Hamel E, Lauritzen M. 2009. Pathway-specific variations in neurovascular and neurometabolic coupling in rat primary somatosensory cortex. *J Cereb Blood Flow Metab* 29(5):976-86.
- Goldberg MC, Landa R, Lasker A, Cooper L, Zee DS. 2000. Evidence of normal cerebellar control of the vestibulo-ocular reflex (VOR) in children with high-functioning autism. *J Autism Dev Disord* 30(6):519-24.
- Goldberg MC, Lasker AG, Zee DS, Garth E, Tien A, Landa RJ. 2002. Deficits in the initiation of eye movements in the absence of a visual target in adolescents with high functioning autism. *Neuropsychologia* 40(12):2039-49.
- Gomot M, Belmonte MK, Bullmore ET, Bernard FA, Baron-Cohen S. 2008. Brain hyper-reactivity to auditory novel targets in children with high-functioning autism. *Brain* 131(Pt 9):2479-88.
- Harris JJ, Reynell C, Attwell D. 2011. The physiology of developmental changes in BOLD functional imaging signals. *Dev Cogn Neurosci* 1(3):199-216.
- Kaiser MD, Hudac CM, Shultz S, Lee SM, Cheung C, Berken AM, Deen B, Pitskel NB, Sugrue DR, Voos AC and others. 2010. Neural signatures of autism. *Proc Natl Acad Sci U S A* 107(49):21223-8.
- Kang HC, Burgund ED, Lugar HM, Petersen SE, Schlaggar BL. 2003. DUPLICATE-Comparison of functional activation foci in children and adults using a common stereotactic space. *Neuroimage* 19(1):16-28.
- Kennedy DP, Courchesne E. 2008. The intrinsic functional organization of the brain is altered in autism. *Neuroimage* 39(4):1877-85.
- Logothetis NK, Pauls J, Augath M, Trinath T, Oeltermann A. 2001. Neurophysiological investigation of the basis of the fMRI signal. *Nature* 412:150-7.
- Lord C, Risi S, Lambrecht L, Cook EH, Jr., Leventhal BL, DiLavore PC, Pickles A, Rutter M. 2000. The autism diagnostic observation schedule-generic: a standard measure of social and communication deficits associated with the spectrum of autism. *J Autism Dev Disord* 30(3):205-23.
- Lord C, Rutter M, Le Couteur A. 1994. Autism Diagnostic Interview-Revised: a revised version of a diagnostic interview for caregivers of individuals with possible pervasive developmental disorders. *J Autism Dev Disord* 24(5):659-85.

- Luna B, Doll SK, Hegedus SJ, Minshew NJ, Sweeney JA. 2007. Maturation of executive function in autism. *Biol Psychiatry* 61(4):474-81.
- Mahone EM, Powell SK, Loftis CW, Goldberg MC, Denckla MB, Mostofsky SH. 2006. Motor persistence and inhibition in autism and ADHD. *J Int Neuropsychol Soc* 12(5):622-31.
- McAvoy MP, Ollinger JM, Buckner RL. 2001. Cluster size thresholds for assessment of significant activation in fMRI. *NeuroImage* 13(6 - 2):S198.
- Miezin FM, Maccotta L, Ollinger JM, Petersen SE, Buckner RL. 2000. Characterizing the hemodynamic response: Effects of presentation rate, sampling procedure, and the possibility of ordering brain activity based on relative timing. *NeuroImage* 11:735-759.
- Minshew NJ, Luna B, Sweeney JA. 1999. Oculomotor evidence for neocortical systems but not cerebellar dysfunction in autism. *Neurology* 52(5):917-22.
- Monk CS, Peltier SJ, Wiggins JL, Weng SJ, Carrasco M, Risi S, Lord C. 2009. Abnormalities of intrinsic functional connectivity in autism spectrum disorders. *Neuroimage* 47(2):764-72.
- Mostofsky SH, Powell SK, Simmonds DJ, Goldberg MC, Caffo B, Pekar JJ. 2009. Decreased connectivity and cerebellar activity in autism during motor task performance. *Brain* 132(Pt 9):2413-25.
- Muller RA, Kleinhans N, Kemmotsu N, Pierce K, Courchesne E. 2003. Abnormal variability and distribution of functional maps in autism: an FMRI study of visuomotor learning. *Am J Psychiatry* 160(10):1847-62.
- Noonan SK, Haist F, Muller RA. 2009. Aberrant functional connectivity in autism: evidence from low-frequency BOLD signal fluctuations. *Brain Res* 1262:48-63.
- Ollinger JM, Corbetta M, Shulman GL. 2001a. Separating processes within a trial in event-related functional MRI II. Analysis. *Neuroimage* 13(1):218-229.
- Ollinger JM, Shulman GL, Corbetta M. 2001b. Separating processes within a trial in event-related functional MRI I. The method. *Neuroimage* 13(1):210-217.
- Pruett JR, Jr., Lamacchia A, Hoertel S, Squire E, McVey K, Todd RD, Constantino JN, Petersen SE. 2011. Social and non-social cueing of visuospatial attention in autism and typical development. *J Autism Dev Disord* 41(6):715-731.
- Sloan HL, Austin VC, Blamire AM, Schnupp JW, Lowe AS, Allers KA, Matthews PM, Sibson NR. 2010. Regional differences in neurovascular coupling in rat brain as determined by fMRI and electrophysiology. *Neuroimage* 53(2):399-411.
- Snyder AZ. 1996. Difference image vs. ratio image error function forms in PET-PET realignment. In: Myer R, Cunningham VJ, Bailey DL, Jones T, editors. *Quantification of Brain Function Using PET*. San Diego, CA: Academic Press. p 131-137.
- Weng SJ, Wiggins JL, Peltier SJ, Carrasco M, Risi S, Lord C, Monk CS. 2010. Alterations of resting state functional connectivity in the default network in adolescents with autism spectrum disorders. *Brain Res* 1313:202-14.

Table and Figure Legends



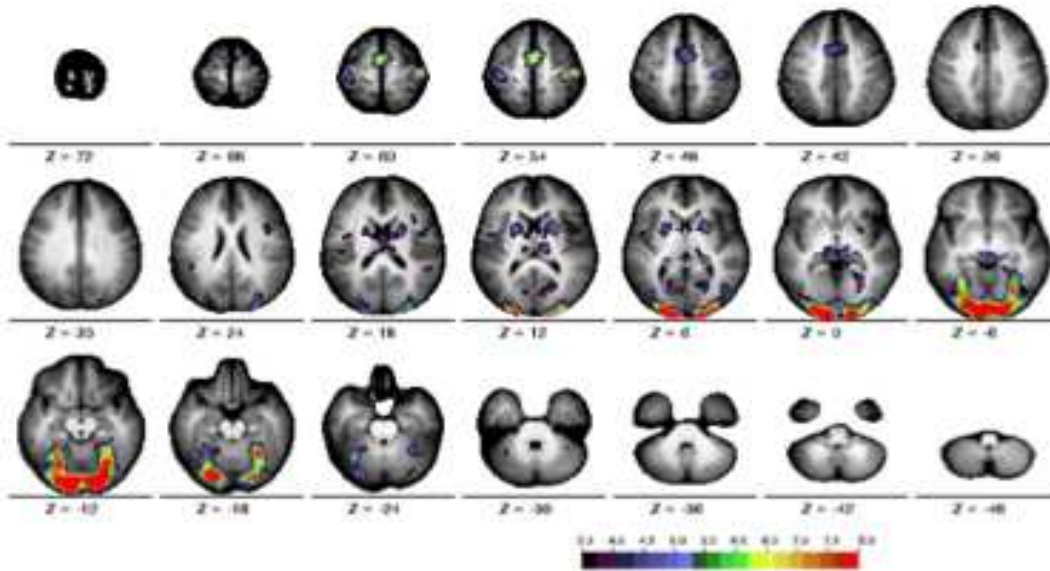
Main effect of time Z-score map



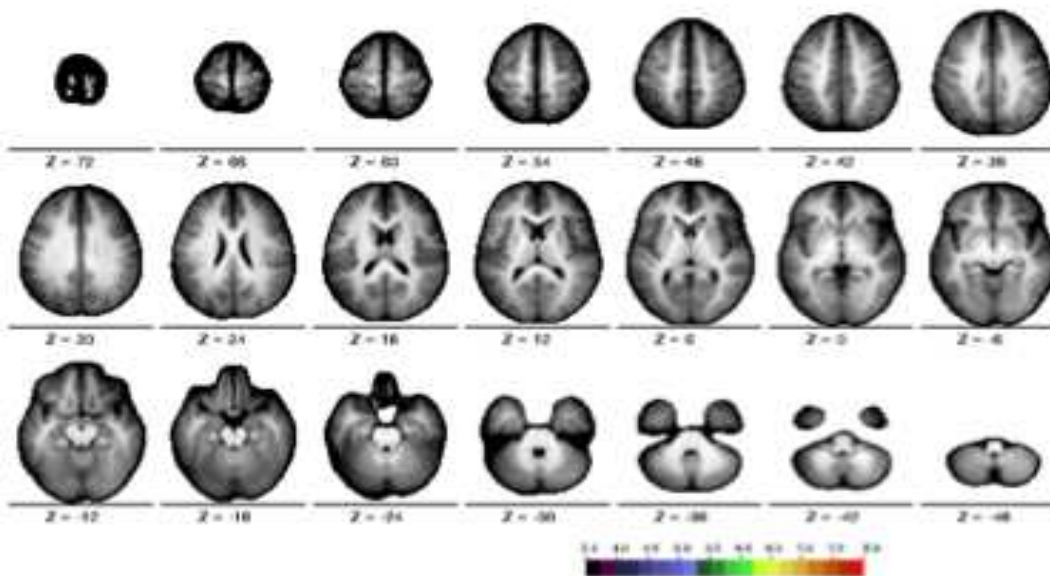
Group by time interaction Z-score map

Figure 1a. Statistical maps for the motion matched scans across the two groups (cohorts). The images show the Z score maps for the main effect of time course (top)

and the interaction of time course by group (bottom). The statistical maps are corrected for multiple comparisons using the Monte Carlo method. The colors on the map represent Z scores from 3.5 (black) to 8 (red).



Main effect of time Z-score map



Group by time interaction Z-score map

Figure 1b. Statistical maps for motion and IQ matched scans across the two groups (cohorts). The images show the Z score maps for the main effect of time course (top) and the interaction of time course by group (bottom). The statistical maps are corrected for multiple comparisons using the Monte Carlo method. The colors on the map represent Z scores from 3.5 (black) to 8 (red).

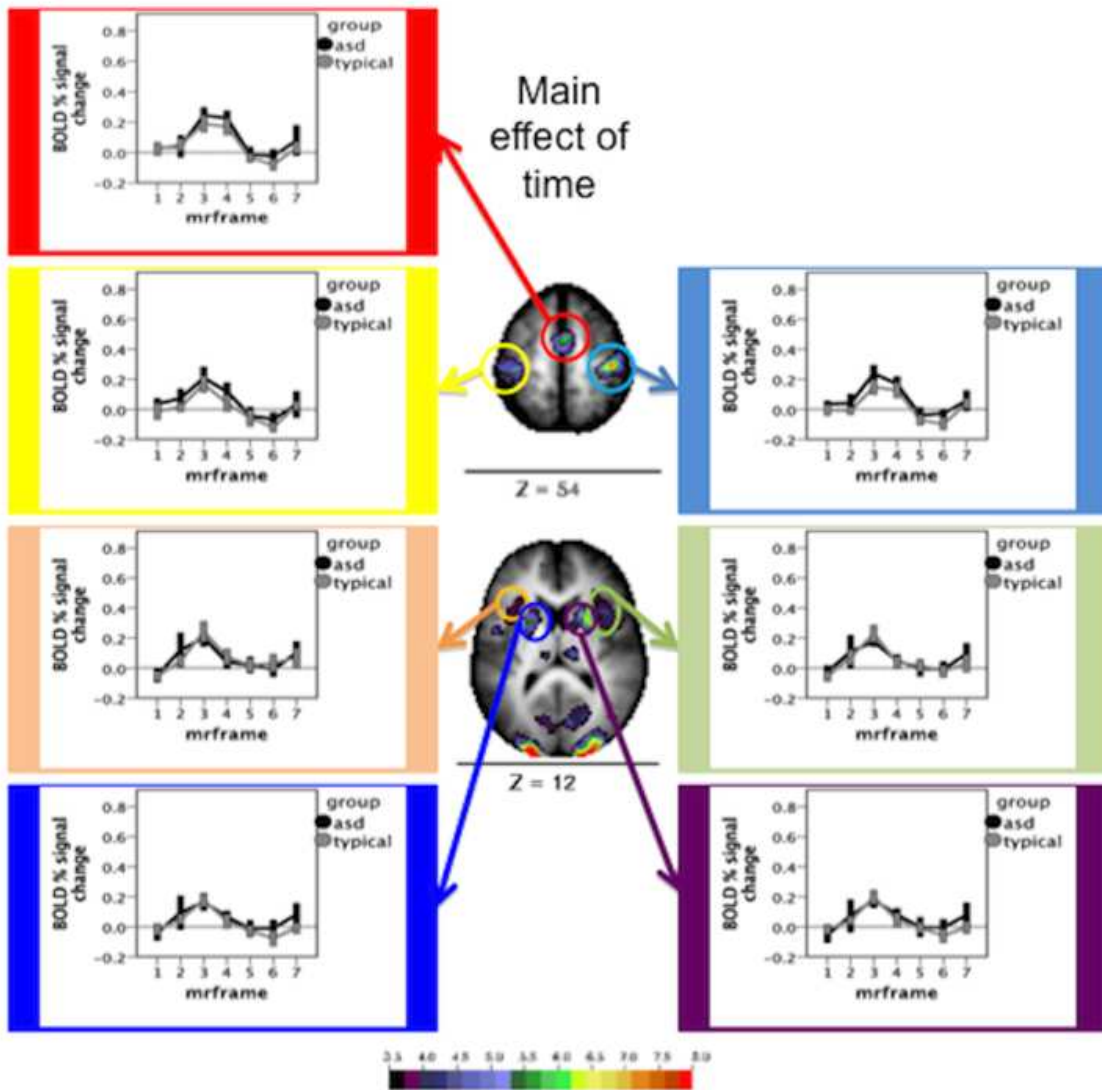


Figure 2. Time courses and Monte Carlo corrected statistical Z-map for regions served by the anterior cerebral and middle cerebral arteries. The map depicts the Z statistics derived from the main effect of time course. The mean time courses for Simplex Autism

(dark) and typical (light) cohorts are depicted for each of the chosen ROIs. Error bars represent 1 standard error of the mean. Color bar ranges from black ($Z = 3.5$) to red ($Z = 8$).

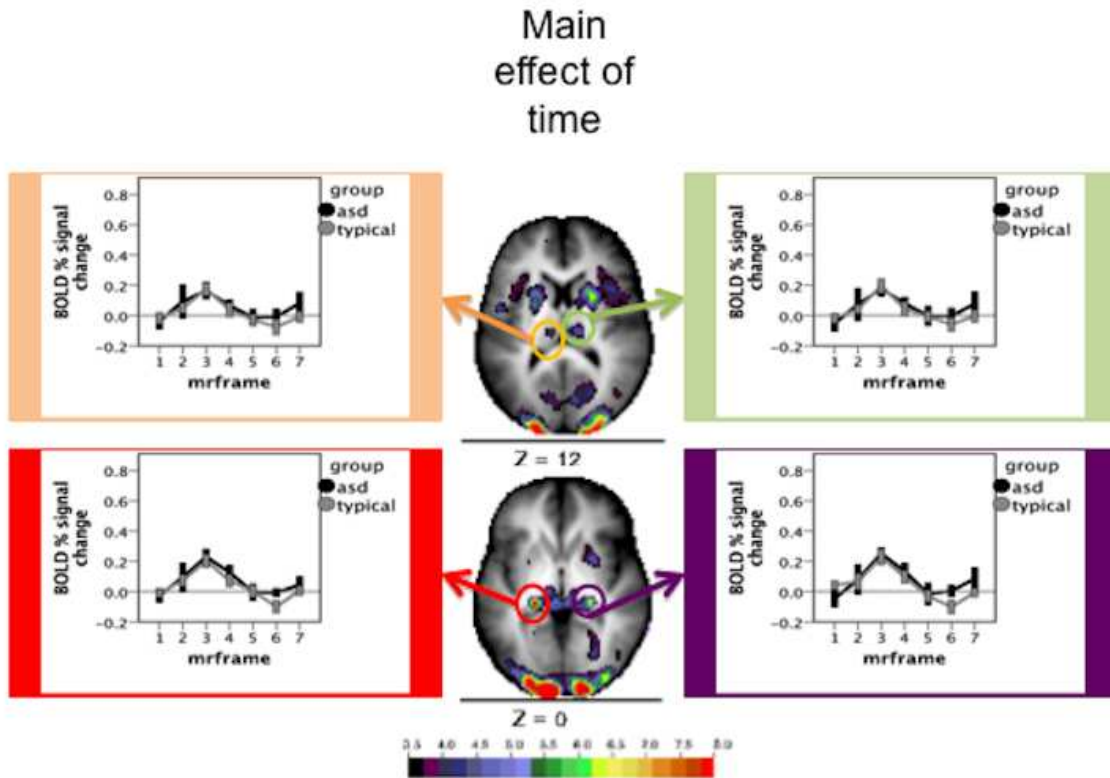


Figure 3. Time courses and Monte Carlo corrected statistical Z-map for regions served by the perforating branches from the posterior cerebral artery. The map depicts the Z statistics derived from the main effect of time course. The mean time courses for Simplex Autism (dark) and typical (light) cohorts are depicted for each of the chosen ROIs. Error bars represent 1 standard error of the mean. Color bar ranges from black ($Z = 3.5$) to red ($Z = 8$).

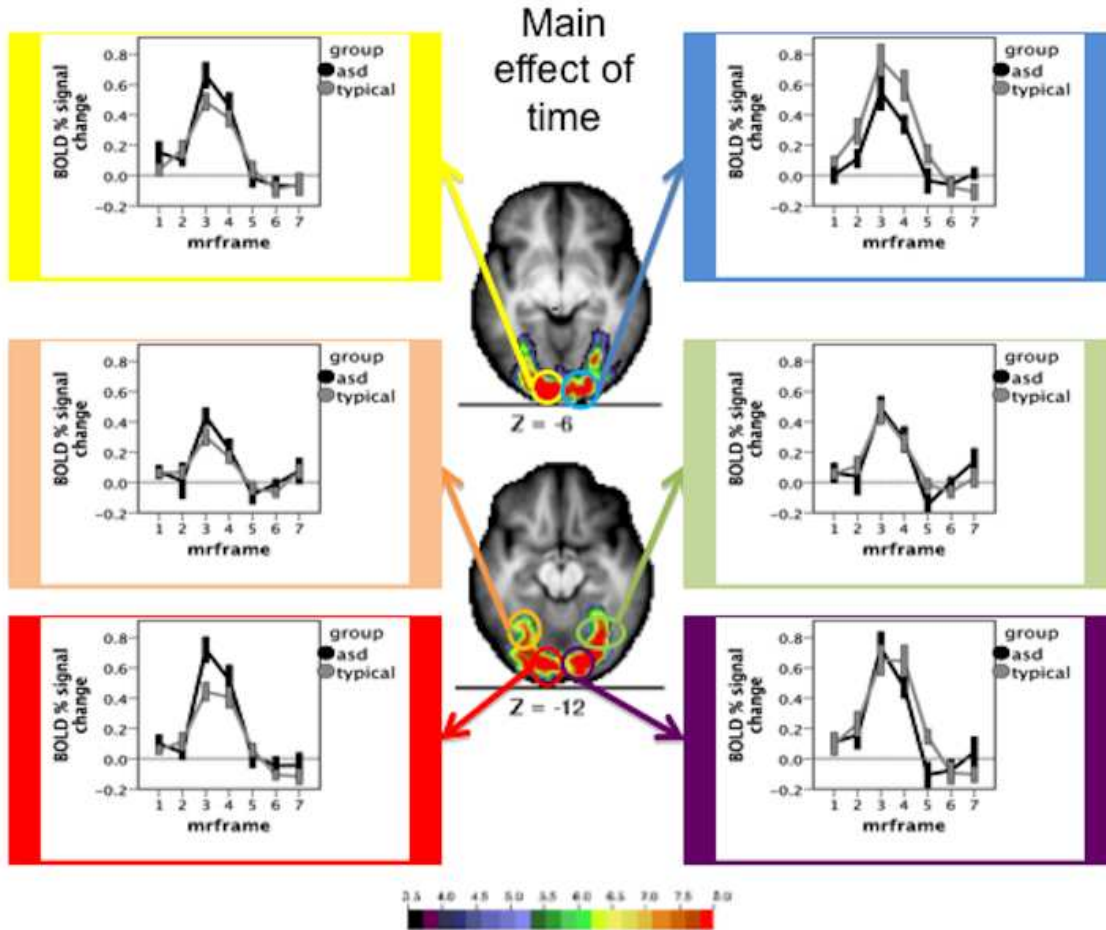


Figure 4. Time courses and Monte Carlo corrected statistical Z-map for regions served by the posterior cerebral artery. The map depicts the Z statistics derived from the main effect of time course. The mean time courses for Simplex Autism (dark) and typical (light) cohorts are depicted for each of the chosen ROIs. Error bars represent 1 standard error of the mean. Color bar ranges from black ($Z = 3.5$) to red ($Z = 8$).

Main
effect of
time

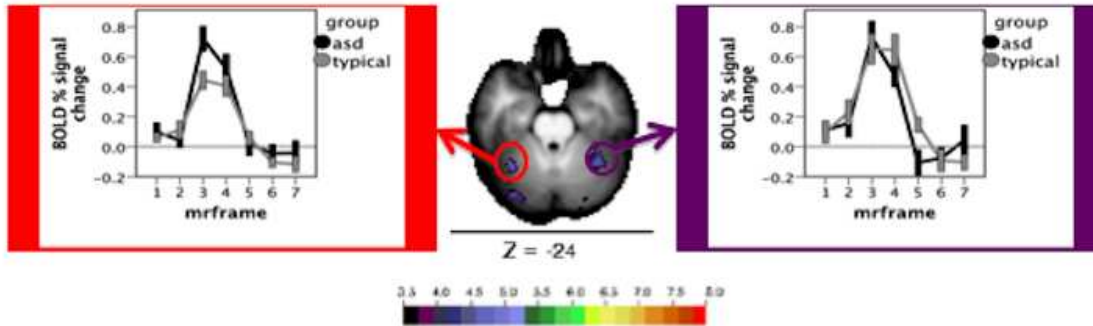


Figure 5. Time courses and Monte Carlo corrected statistical Z-map for regions served by the superior cerebellar artery. The map depicts the Z statistics derived from the main effect of time course. The mean time courses for Simplex Autism (dark) and typical (light) cohorts are depicted for each of the chosen ROIs. Error bars represent 1 standard error of the mean. Color bar ranges from black ($Z = 3.5$) to red ($Z = 8$).

Time X group interaction

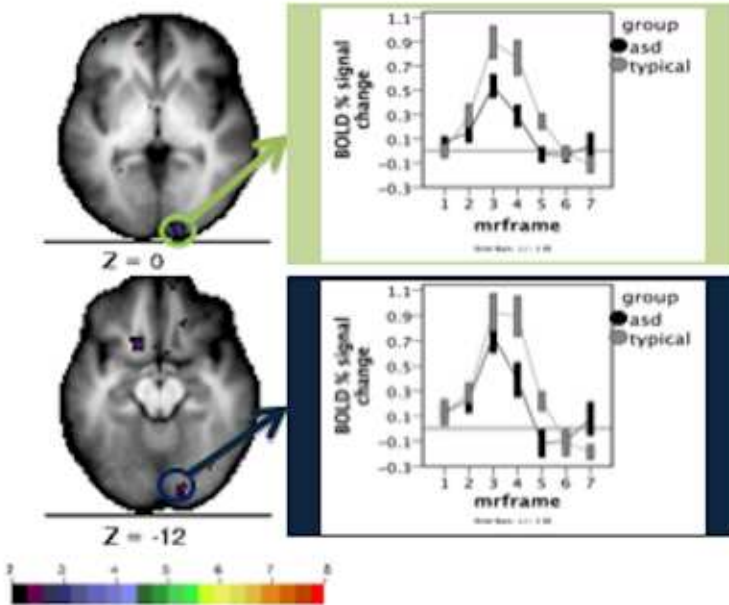
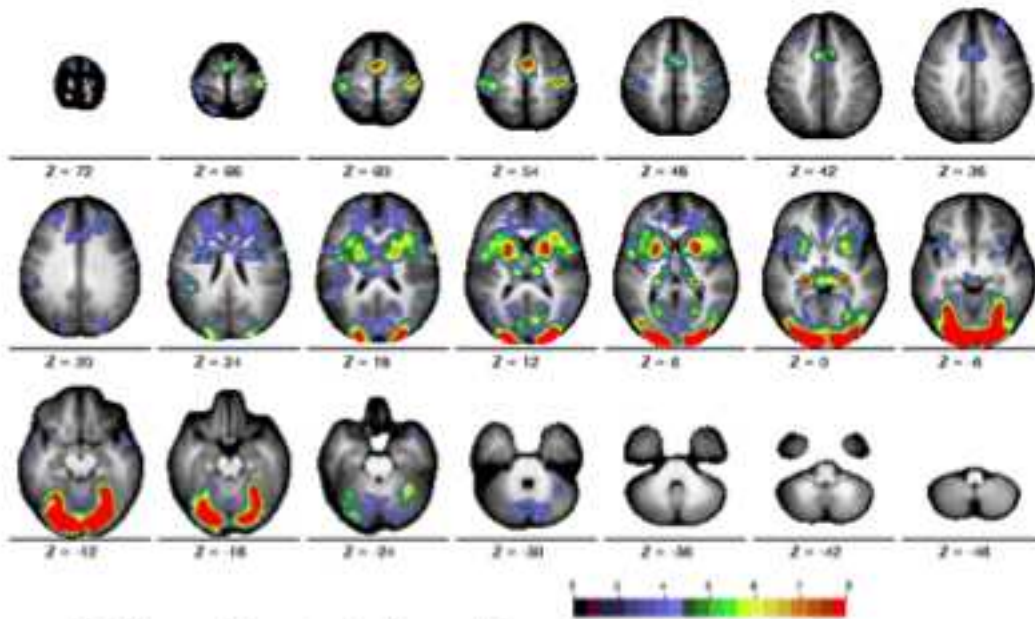
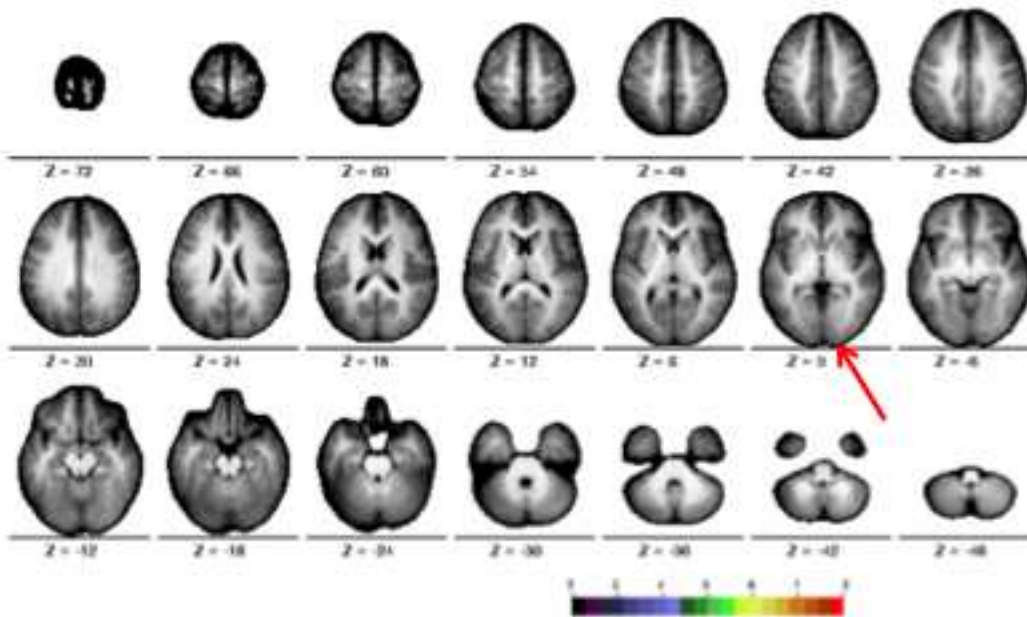


Figure 6. Time courses and statistical Z map for time course X group interaction using a quality control low Z value threshold. The map depicts the uncorrected Z values derived from the time course X group interaction. The mean time course for Simplex Autism (dark) and typical (light) cohorts are depicted for each of the chosen ROIs. Error bars represent 1 standard error of the mean. Color bar ranges from black ($Z = 2$) to red ($Z = 8$).



Main effect of time Z-score map



Group by time interaction Z-score map

Figure 7. Statistical maps for the analysis of all four runs per subject. The Monte Carlo corrected statistical Z-score maps were derived from the main effect of time course (top) and group by time course interaction (bottom). Color bar ranges from black ($Z = 2$) to red ($Z = 8$).

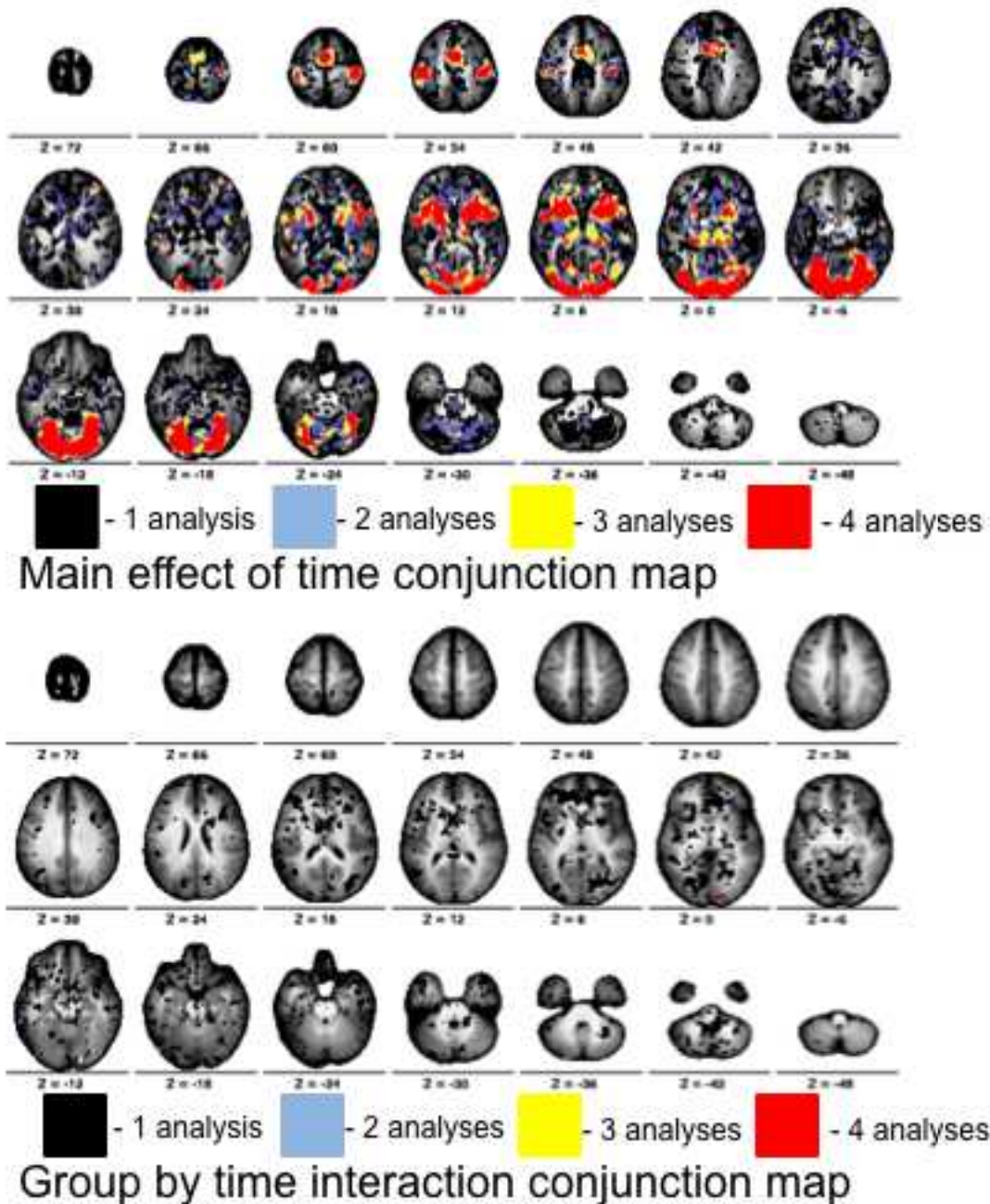


Figure 8. Conjunction maps for the four analyses of each run per subject. The main effect of time and group by time interaction Z-score maps produced from each run were thresholded at a very liberal Z value ($Z > 1.9$) and summed. Summing the binarized maps produced a single conjunction map for the main effect of time (top) and interaction (bottom). Values on the map represent the number of analyses (1-4) which showed

significant effects at a $Z > 1.9$. Color bar ranges from black (one analysis) to red (four analyses).

Table 1	Demographics	
	Simplex Autism Subjects	Typical Subjects
Male/female	13m/3f	13m/3f
Age	11.9 ± 1.89	12.6 ± 1.80
IQ	104.9 ± 12.97	115.7 ± 10.64
Vocabulary scaled score	10.25 ± 3.26	13.00 ± 2.37
Block design scaled score	10.88 ± 3.05	12.23 ± 2.12
SRS	102 ± 21.7	17.8 ± 9.56
Medicated/ Un-medicated	8/8	0/16

Table 1. Demographics of participants included in the fMRI study. Psychotropic medications included selective serotonin reuptake inhibitors, psychostimulants, and antipsychotic medications. Independent samples T-tests were conducted to determine whether the groups were significantly different on age, intelligence quotient (IQ), the vocabulary and block design scaled scores, and the Social Responsiveness Scale (SRS), a quantitative measure of autistic traits. While age was not significantly different between Simplex Autism and typical cohorts ($P = 0.28$), IQ was significantly greater for the typical than the Simplex Autism cohort ($P = 0.016$). SRS was significantly greater for the Simplex Autism than the typical cohort ($P < 0.0001$). The vocabulary ($P = 0.019$) but not block design ($P = 0.15$) subscale score was significantly greater in the typical cohort. One typical subject did not perform the block design subtest, and was not included in the T-test comparison.

Time course X group repeated measures ANOVAs							
Region	X	Y	Z	Df	F	P	Partial eta ²
right motor	39	-23	55	3.86, 115.76	0.18	0.94	0.006
SMA	-1	-4	57	3.85, 115.53	0.17	0.95	0.005
left motor	-38	-28	59	3.75, 112.48	0.14	0.96	0.005
right insula	40	8	10	3.80, 114.09	0.35	0.83	0.012
left insula	-38	8	11	3.86, 115.65	0.36	0.83	0.012
right putamen	23	4	9	3.44, 103.31	0.56	0.67	0.018
left putamen	-22	3	9	3.16, 94.78	0.28	0.85	0.009
right thalamus	12	-22	11	3.81, 114.28	0.45	0.76	0.015
left thalamus	-9	-23	12	3.58, 107.50	0.43	0.76	0.014
right LGN	19	-33	1	3.93, 117.89	1.08	0.37	0.035
left LGN	-20	-31	0	3.78, 113.51	0.46	0.75	0.015
right fusiform	28	-71	-10	3.94, 118.27	0.80	0.52	0.026
left fusiform	-27	-65	-11	3.69, 110.74	0.68	0.60	0.022
right visual	19	-87	-12	3.99, 119.71	1.52	0.20	0.048
left visual	-23	-88	-12	3.75, 112.51	1.77	0.14	0.056
right visual	15	-96	-5	3.59, 107.59	2	0.11	0.063
left visual	-13	-91	-9	3.98, 119.52	1.09	0.37	0.035
right cerebellum	36	-51	-25	3.57, 107.17	0.98	0.42	0.032
left cerebellum	-32	-53	-20	3.93, 117.99	0.59	0.67	0.019

Table 2. The results from the ROI time course by group repeated measures ANOVAs performed on the selected main-effect ROIs. X, Y, and Z coordinates correspond to the Talairach standard space. Degrees of freedom, F, P, and partial eta squared values are listed for the interaction of group diagnosis and time course.

Timecourse X group repeated measures ANOVAs: IQ matched							
Region	X	Y	Z	Df	F	P	Partial eta ²
right motor	39	-23	55	3.72, 81.9	0.57	0.67	0.025
SMA	-1	-4	57	3.82, 84.1	0.5	0.81	0.022
left motor	-38	-28	59	3.05, 67.18	0.74	0.53	0.033
right insula	40	8	10	3.28, 72.14	0.82	0.5	0.036
left insula	-38	8	11	3.3, 72.49	0.79	0.52	0.035
right putamen	23	4	9	2.96, 65.07	0.86	0.46	0.038
left putamen	-22	3	9	2.75, 60.42	0.63	0.59	0.028
right thalamus	12	-22	11	6, 132	0.29	0.94	0.013
left thalamus	-9	-23	12	4.14, 91.08	0.17	0.96	0.008
right LGN	19	-33	1	6, 132	1.03	0.41	0.045
left LGN	-20	-31	0	4.49, 98.68	1.08	0.37	0.047
right fusiform	28	-71	-10	4.04, 88.94	1.41	0.24	0.06
left fusiform	-27	-65	-11	4.05, 89.09	2.11	0.085	0.088
right visual	19	-87	-12	6, 132	1.54	0.17	0.065
left visual	-23	-88	-12	3.86, 84.76	1.75	0.15	0.074
right visual	15	-96	-5	3.94, 86.65	1.49	0.21	0.063
left visual	-13	-91	-9	3.89, 85.67	1.68	0.17	0.071
right cerebellum	36	-51	-25	6, 132	1.43	0.21	0.061
left cerebellum	-32	-53	-20	3.66, 80.62	0.93	0.45	0.041

Table 3. The results from the ROI time course by group repeated measures ANOVAs performed on the selected main-effect ROIs, for the IQ matched groups. X, Y, and Z coordinates correspond to the Talairach standard space. Degrees of freedom, F, P, and partial eta squared values are listed for the interaction of group diagnosis and time course.

TABLE 4 QC Analyses: Interactions at uncorrected significance							
Region	X	Y	Z	Df	F	P	Partial eta ²
right visual	15	-97	0	3.19,95.73	4.3	0.006	0.13
right visual	15	-91	-11	2.36,70.68	2.8	0.06	0.085

Table 4. The results from the ROI time course by group repeated measures ANOVA using the quality control low Z value threshold. These ROIs were extracted by using a peak-finding algorithm (described in the methods section), where all voxels had a $Z > 1.9$. Given X, Y, and Z coordinates correspond to the Talairach standard space. Degrees of freedom, F, and P, observed power, and partial eta squared values are depicted for the interaction of group diagnosis and time course.